Dissertation

submitted to the

Combined Faculties for the Natural Sciences and for Mathematics

of the Ruperto-Carola University of Heidelberg, Germany

for the degree of

Doctor of Natural Sciences

Presented by

Yueh-Tso Tsai

Born in: Tainan City, Taiwan

Oral examination:

Analysis of Rab42 and Rab40c as novel regulators
of secretory membrane trafficking

Referees: Prof. Dr. Walter Nickel
Dr. Vytaute Starkuviene

List of publication:

Serva A, Knapp B, **Tsai YT**, Claas C, Lisauskas T, Matula P, Harder N, Kaderali L, Rohr K, Erfle H, Eils R, Braga V, Starkuviene V. miR-17-5p regulates endocytic trafficking through targeting TBC1D2/Armus. PLoS One 2012;7(12):e52555.

List of presentation:

1. International Joint Meeting of the German Society for Cell Biology (DGZ) and the German Society for Developmental Biology (GfE), 20.-23. March 2013 Heidelberg, Germany

   Tsai YT, Lisauskas T, Claas C, Knapp B, Reusing S, Kaderali L, Erfle H, Goud B, Starkuviene V. "Comparative knock-down and knock-in screens of Rab GTPases identifies Rab40c as a novel regulator of biosynthetic trafficking"

2. International symposium for PhD students on protein trafficking in health and disease, 26.-28. May 2010 Hamburg, Germany

   Tsai YT, Claas C, Beil N, Beneke J, Knapp B, Langlotz M, Wegehingel S, Erfle H, Kaderali L, Nickel W, Pepperkok R, Starkuviene V. "Fluorescence microscopy-based assay to study the transport of GPI-anchored proteins"

Tables and figures

Supplementary tables and figures

Abbreviation

Abbreviation	
C-terminal	carboxy terminal
ER	endoplasmic reticulum
et al.	*et altera*
FACS	fluorescence activated cell sorting
GPI	glycosylphosphatidylinositol
GPI-APs	GPI-anchored proteins
HRP	horseradish peroxidase
N-terminal	amino-terminal
PC I	type I procollagen
PM	plasma membrane
PtdIns	phosphatidylinositol
PVDF	polyvinylidene fluoride
s.e.m.	standard error of the mean
SDS-PAGE	sodium dodecyl sulfate polyacrylamide gel electrophoresis
SRP	signal recognition particle
TGN	trans-Golgi network
VSVG	vesicular stomatitis virus glycoprotein

Amino acids

Abbreviation	Abbreviation	Amino acid
A	Ala	Alanine
C	Cys	Cysteine
D	Asp	Aspartate
E	Glu	Glutamate
F	Phe	Phenylalaine
G	Gly	Glycine
H	His	Histidine
I	Ile	Isoleucine
L	Leu	Leucine
M	Met	Methionine
N	Asn	Asparagine
P	Pro	Proline
Q	Gln	Glutamine
R	Arg	Arginine
S	Ser	Serine
T	Thr	Threonine
V	Val	Valine
W	Trp	Tryptophan
Y	Tyr	Tyrosine

Abstract

Secretory membrane trafficking is essential for the homeostasis of most cellular organelles and mediating the secretion of a variety of cargo proteins, including digestive enzymes, hormones, growth factors, antibodies, extracellular matrix proteins and many other proteins. Small GTPases, particularly Rab and Arf GTPases, have been shown to play key roles in regulating the transport of secretory cargo proteins. Nevertheless, the biological role of each individual small GTPase is not fully elucidated yet.

To address that, I performed microscopy-based RNAi screening to identify small GTPases that are involved in the biosynthetic transport of a secretory cargo protein ts-O45-G. From RNAi screen in HeLa cells, I identified 18 potential regulators, with 14 of them not associated with this cellular function before.

One of the hits was chosen for further characterization. Rab42 is an interesting hit in that it has not been characterized and the retroposed transcript of Rab42 is expressed in HeLa cells. After having designed specific siRNAs only targeting Rab42, it is shown that specific down-regulation of Rab42 inhibited secretion of ts-O45-G from the ER to the PM. Moreover, I showed that RNAi-mediated inhibition of ts-O45-G transport can be rescued by over-expressing a siRNA-resistant form of Rab42. By invesitigating more closely which particular stage of ts-O45-G secretion is affected, I have identified that trafficking from the TGN to the PM is affected in a more pronounced manner. Immunofluorescence analysis showed that over-expressed Rab42 localized preferentially to the cytoplasm and PM, and, to a lesser extent, to the intracellular punctual structures, which are in close proximity to perinuclear region.

During my thesis work, yet another interesting and poorly characterized Rab, Rab40c, was identified as a novel regulator for PC I secretion from our

RNAi screens in NIH3T3 fibroblasts. Down-regulation of Rab40c inhibited secretion of PC I and ts-O45-G in NIH3T3 fibroblasts, albeit it had no consistent effect on ts-O45-G secretion in HeLa cells. I showed that PC I secretion is blocked in the early secretory pathway in NIH3T3 fibroblasts depleted for Rab40c. In addition, I observed cell type-specific localization of Rab40c by comparing the localization of Rab40c in NIH3T3 fibroblasts and HeLa cells. In NIH3T3 fibroblasts FLAG-tagged Rab40c localized to the Golgi complex, whereas in HeLa cells FLAG-tagged Rab40c localized to perinuclear tubulovesicular structures and cytoplasmic structures. Furthermore, Rab40c is an interesting Rab GTPase in that it contains a GTPase domain and a SOCS-box domain. By immunofluorescence analysis, it has been shown that SOCS-box domain is crucial for the localization of Rab40c at the Golgi complex. Taken together, my thesis work has identified novel regulators of secretory membrane trafficking, and serves as a basis for further functional characterization.

Zusammenfassung

Sekretorischer Membrantransport ist essenziell für die Homöostase der zellulären Organellen und für die Sekretion verschiedener Cargoproteine, wie z. B. Verdauungsenzyme, Hormone, Wachstumsfaktoren, Antikörper, Proteine der extrazellulären Matrix. Rab und Arf GTPasen (zwei Untergruppen aus der Superfamilie der kleinen GTPasen) spielen eine zentrale Rolle bei der Regulation dieses Transports. Trotz der wichtigen Rolle dieser kleinen GTPasen ist ihre genaue Funktionsweise nicht völlig klar.

Es wurden Mikroskopie-basierte RNAi-Screens durchgeführt, um regulatorische GTPasen mit einer Funktion beim Transport des prototypischen Cargoproteins ts-O45-G in HeLa Zellen zu identifizieren. In diesen RNAi-Screens konnten 18 kleine GTPasen als potenzielle Regulatoren des sekretorischen Transports identifiziert werden. Für 14 von ihnen konnte eine mögliche Rolle beim Transport von ts-O45-G zum ersten Mal belegt werden.

Eine der identifizierten GTPasen wurde für eine weitergehende Charakterisierung gewählt: Rab42 erschien besonders interessant, da sie nicht charakterisiert ist und die mRNA von Rab42 Pseudogen in HeLa Zellen nachweisbar ist. Spezifischer Knockdown von RAB42 in HeLa Zellen verhindert den Transport von ts-O45-G vom ER zur Plasmamembran. Außerdem konnte gezeigt werden, dass der siRNA-induzierte Block der Sekretion von ts-O45-G durch Transfektion siRNA-resistenter RAB42-cDNA aufgehoben werden kann. Detaillierte Untersuchungen zeigten, dass der Transport der ts-O45-G vom TGN zur Plasmamembran inhibiert wird. Analysen mittels Immunfluoreszenzmikroskopie demonstrieren darüber hinaus, dass RAB42 hauptsächlich im Cytoplasma und an der Plasmamembran sowie in geringerem Maße in intrazellulären punktartigen Strukturen, die sich in unmitterlbarer Nähe des Nukleus befinden, lokalisert.

Eine weitere wenig charakterisierte Rab GTPase, Rab40c, wurde während meiner Doktorarbeit als potenziell regulatorisches Protein für den Transport von Typ I Prokollagen (PC I) in RNAi-Screens in NIH3T3 Fibroblasten identifiziert. Knockdown von Rab40c verhindert Transport von PC I und ts-O45-G in NIH3T3 Fibroblasten, dagegen konnte ein entsprechender Block des Transports von ts-O45-G in HeLa Zellen in meinen Untersuchungen nicht belegt werden. Meine Experimente belegen, dass Knockdown von Rab40c in NIH3T3 Fibroblasten zu einem Block der frühen Sekretion von PC I führt. Außerdem zeigen die Analysen, dass Lokalisation von FLAG-markiertem Rab40c abhängig vom untersuchten Zelltyp ist. In NIH3T3 Fibroblasten lokalisert FLAG-markiertes Rab40c im Golgi-Komplex, in HeLa Zellen wird es demgegenüber in perinukleären, tubulovesikulären Strukturen und im Zytoplasma gefunden. Rab40c enthält – anders als die meisten anderen GTPasen – zusätzlich zur GTPase Domäne eine sog. SOCS-Box. Durch immunfluoreszenmikroskopische Analysen konnte gezeigt werden, dass die SOCS-Box Domäne für die Lokalisation von Rab40c im Golgi-Komplex essenziell ist.

Zusammenfassung: In der vorliegenden Doktorarbeit werden GTPasen mit einer möglichen Funktion bei der Regulation des sekretorische Membrantransports vorgestellt, wobei für die meisten von ihnen eine solche Rolle zum ersten Mal belegt wird. Detailliertere Untersuchungen zu zwei der identifizerten GTPasen – RAB42 und Rab40c – zeigen, dass die vorgestellten Arbeiten als valide Grundlage für eine funktionale Charakterisierung auch weiterer GTPasen dienen kann.

1 Introduction

1.1 Membrane trafficking

Eukaryotic cells are characteristic of their compartmentalization into membrane-bounded organelles. Each organelle has a specific function, which is carried out by its constituent proteins and lipids. Therefore transport of proteins and lipids between these membrane-bounded organelles is important for cellular function. Various biochemical, genetic and morphological approaches have been taken to investigate the molecular mechanisms underlying protein transport and membrane assembly (Palade, 1975; Rothman, 1994; Schekman and Orci, 1996). These studies have established the concepts and pictures of secretory pathway and membrane traffic.

1.1.1 Secretory pathway

Most secretory proteins and membrane proteins contain N-terminal or internal signal peptides that mediate their sorting to the ER. Signal recognition particle (SRP) binds to the signal peptide in a nascent polypeptide chain and the ribosome. The complex is then targeted to the ER membrane via the interaction of SRP and SRP receptor. By a co-translational translocation mechanism, nascent proteins enter the ER through the protein-conducting channel, which is formed by the Sec61 complex (Osborne et al., 2005). The signal peptide is cleaved at some point during translocation. The newly synthesized proteins leave the ER at specialized membrane domain termed ER exit sites, from which the formation of coat protein complex II (COPII) vesicles occurs. The newly synthesized proteins are transported to the Golgi complex, where they are modified, processed, sorted and dispatched toward

their final destination (Griffiths and Simons, 1986). Distinct transport pathways are taken to deliver these "cargoes" to the their final destinations, which include the plasma membrane, early endosome, late endosome, lysosome, recycling endosome, and secretory granule/vesicle (Fig. 1). The diversity of these transport pathways implicates the underlying regulatory machinery of membrane trafficking.

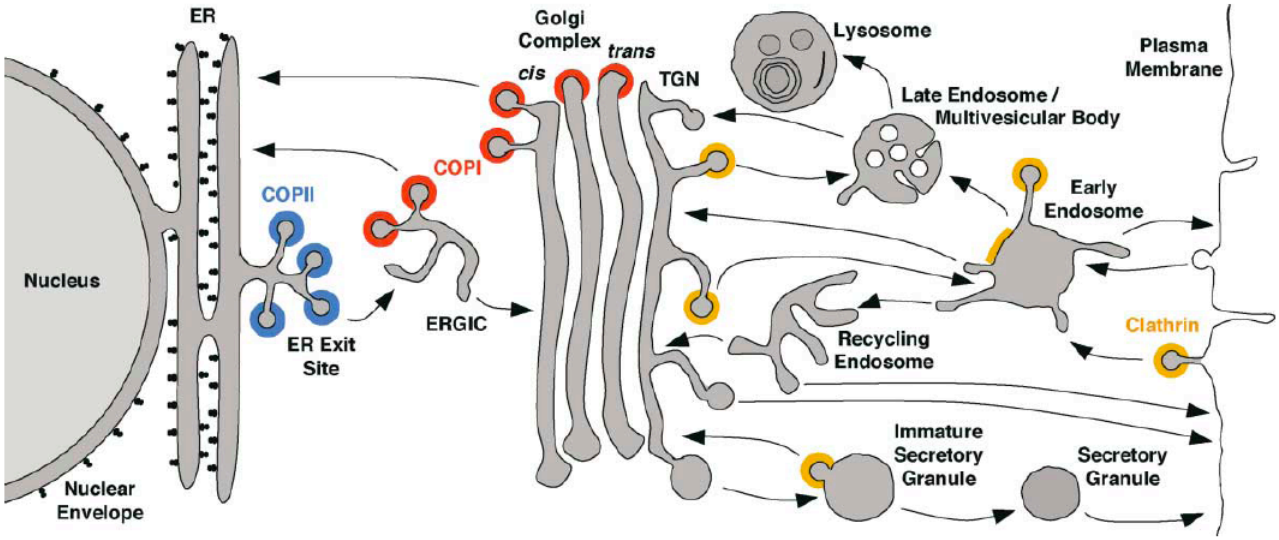

Figure 1 Overview of membrane trafficking

This figure depicts the compartments of the secretory, lysosomal/vacuolar, and endocytic pathways. Transport steps are indicated by arrows. Colors indicate the locations of COPII (blue), COPI (red), and clathrin (organge). This figure is adapted from a review article (Bonifacino and Glick, 2004).

1.1.2 Intra-Golgi cargo transport

The Golgi is the intracellular organelle, where the processing of oligosaccharide side chain on nascent glycoproteins and glycolipids occurs (Mellman and Simons, 1992). It consists of a stack of 3-8 flattened cisternae. These cisternae can be distinguished based on their biochemical reactivities (Dunphy and Rothman, 1985; Farquhar, 1985). The resident enzymes are distributed differentially across the stack. Cisternae at the *cis* side of the Golgi,

which faces the ER, contain the resident enzymes that act at the early steps of oligosaccharide processing. Neighboring cisternae in the medial portion of the stack contain the enzymes that act at the intermediate steps, whereas cisternae near the *trans* side of the Golgi contain the enzymes that act at late steps. How resident Golgi enzymes localize to distinct cisternae, and how secretory cargoes traverse the Golgi are major topics in membrane traffic.

Two models have been proposed for the membrane traffic through the Golgi: stationary cisternae model and cisternal maturation model (Fig. 2). In stationary cisternae model, resident Golgi proteins are retained in the cisternae while secretory cargoes are transported from one cisterna to the next in anterograde COPI vesicles (Rothman and Wieland, 1996). This model explains the polarity of Golgi complex by viewing Golgi as a series of distinct subcompartments. It also accounts for the observation that COPI vesicles are abundant around the Golgi, forming and fusing at the cisternal rims (Farquhar, 1985; Orci et al., 1986). However, the model fails to explain the transport of the secretory cargoes that are too large to fit in COPI vesicles. One of the examples is the transport of procollagen. It was shown that procollagen moves across the Golgi without ever leaving the lumen of the Golgi cisternae (Bonfanti et al., 1998). In addition, strong evidence supports retrograde COPI-dependent transport, but the evidence for anterograde COPI-dependent transport is less solid (Rabouille and Klumperman, 2005).

Cisternal maturation model was proposed to address these problems (Glick and Malhotra, 1998; Pelham, 1998). In this model, cisternae assemble at the *cis* side of the stack, progress through the stack while carrying the secretory cargoes forward. At the TGN, the cisternae produce COPI and clathrin vesicles and receive vesicles from the compartments of the endocytic pathways. The model fits with abundant morphological evidence that cisternae form at the *cis* side of the stack and peel off at the *trans* side (Mollenhauer and Morre, 1991). Furthermore, it provides the explanation for

the observation that bulky soluble protein procollagen and small transmembrane glycoprotein VSVG move through the Golgi at the same rate (Mironov et al., 2001). One characteristic of cisternal maturation model is that an individual cisterna matures from *cis* to *trans*. Therefore, the composition of the Golgi-resident proteins in a cisterna should change over time. Studies on the composition of the Golgi-resident proteins by live-cell fluorescence microscopy of Golgi cisterna in *Saccharomyces cerevisiae* supported cisternal maturation model (Losev et al., 2006; Matsuura-Tokita et al., 2006).

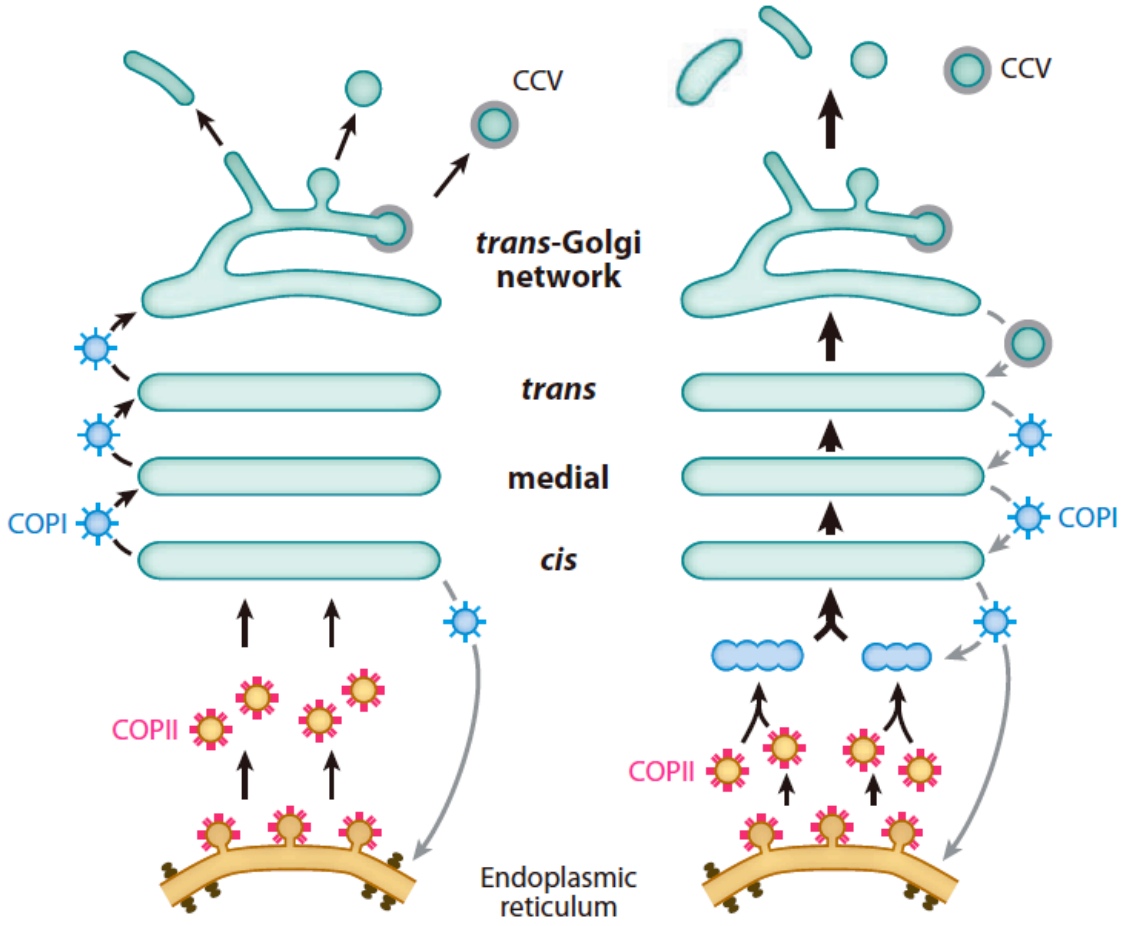

Figure 2 Two models for membrane traffic through the Golgi

Stationary cisternae model (left) suggests that Golgi cisternae are distinct stable compartments connected by the anterograde transport mediated by COPI vesicles, whereas the cisternal maturation model (right) predicts that a cisterna is a transient structure that forms *de novo* by the coalescence of COPII vesicles, matures from *cis* to *trans*, and breaks down into transport carriers at

the TGN. Maturation is driven by the retrograde transport of the Golgi-resident proteins. The retrograde transport involves COPI vesicles within the Golgi and may involve clathrin-mediated recycling from maturing TGN compartment. This figure is adapted from a review article (Glick and Nakano, 2009).

1.1.3 Post-Golgi cargo transport

After passing through the Golgi complex and reaching the TGN, different secretory cargoes are packaged into different vesicles, which carry them to their respective destinations, which may include the plasma membrane, early endosome, late endosome, lysosome, and secretory granule/vesicle (Fig. 1). A variety of experimental results suggest that TGN acts as the major sorting station for all newly synthesized secretory cargoes (Griffiths and Simons, 1986; Keller et al., 2001). The sorting signals in secretory cargoes mediate the physical segregation of cargoes into different TGN domains (Keller and Simons, 1997). The sorting processes involve the machineries that can decode the sorting signal motifs or create a lipid and protein microenvironment for which specific cargoes have a selective affinity. Important components of these machineries include Rab and Arf GTPases, adaptors, golgins, and lipids.

Clathrin-coated vesicles transport the secretory cargoes that exit the TGN. The formation of clathrin-coated vesicles is regulated by ARF1 (Bonifacino, 2004; Kirchhausen, 2000). Sec7-family GEFs at the TGN, such as BIG1 and BIG2 (brefeldin A inhibited GEF), activate ARF1 (D'Souza-Schorey and Chavrier, 2006). Activated ARF1 promotes the recruitment of cytosolic protein complexes that can recognize the sorting signal motifs and bind clathrin (Nie et al., 2003). These recruited protein complexes function as an adaptor between cargo proteins and the clathrin coat. These adaptor proteins

include AP-1, AP-3, AP-4 and GGAs (*G*olgi-localized, *g*amma-ear-containing, *A*RF-binding proteins) (D'Souza-Schorey and Chavrier, 2006). Interestingly, AP-3 and AP-4 are not enriched in clathrin-coated vesicles and might function independently of clathrin (Robinson, 2004).

Activation of ARF can also establish the TGN microdomains by tuning the local lipid composition. Activated ARF can promote the production of phosphatidylinositol 4-phosphate (PtdIns4P) by recruiting and activating PtdIns4-kinase (PI4K)IIIβ (De Matteis and Godi, 2004). PtdIns4P functions by recruiting a specific set of cytosolic proteins that contribute to forming the TGN microdomains (Shin and Nakayama, 2004). Furthermore, PtdIns4P participates in recruiting AP-1 and the GGAs to the TGN microdomains (Wang et al., 2007; Wang et al., 2003).

Golgins also participate in regulating the post-Golgi transport. The golgins that contain a GRIP domain (golgin-97, RanBP2α, Imh1p, and p230/golgin-245) are known to localize to the *trans* side of the Golgi (Munro, 2011). Knockdown of individual GRIP domain golgin can result in fragmentation of the Golgi, and defects in the retrograde transport of some cargoes from the endosomes to the TGN (Derby et al., 2007; Hayes et al., 2009; Lieu et al., 2007; Lu et al., 2004; Reddy et al., 2006; Yoshino et al., 2005). It has been suggested that some GRIP domain golgins are associated with the carriers leaving the Golgi for the plasma membrane and thus they participate in the post-Golgi transport (Kakinuma et al., 2004; Lieu et al., 2008; Lock et al., 2005).

When a TGN export domain is mature, it extrudes from the Golgi by interacting with suitable microtubule-based motor. Fission occurs at the thinnest section of the tubule extrusion by machineries based on dynamin, protein kinase D and brefeldin A-ribosylated substrates (BARS) (De Matteis and Luini, 2008).

1.1.4 Endocytic pathways

Endocytosis is a complex cellular process, through which cells regulate their homeostasis and interact with the extracellular environments by controlling the composition of proteins and lipids of the plasma membrane. The term "endocytosis" describes the internalization of molecules and particles into transport vesicles from the plasma membrane lipid bilayer. Cells have developed a number of endocytic pathways to internalize nutrients, bacterial toxins, viruses, immunoglobulins, surface receptors and their bound ligands, and various extracellular soluble molecules (Lanzetti and Di Fiore, 2008). Internalized molecules can be delivered to the lysosomes for degradation, or recycled to the cell surface. Endocytic pathway also allows receptors and their ligands to be sorted in the early or sorting endosomes.

Many endocytic pathways are discovered and can be divided into two types: clathrin-mediated and clathrin-independent (Conner and Schmid, 2003; Doherty and McMahon, 2009; Grant and Donaldson, 2009). Clathrin-mediated endocytosis has been extensively studied (Mills, 2007). In clathrin-mediated endocytosis, the cytoplasmic domains of the membrane proteins are specifically recognized by cognate adaptor proteins and packaged into clathrin-coated vesicles. The process is facilitated by numerous accessory proteins, and requires the GTPase dynamin for vesicle scission (Conner and Schmid, 2003). Internalization of transferrin receptors and low-density lipoprotein receptor (LDLR) serves as two classic examples to illustrate clathrin-mediated endocytosis (Brown and Goldstein, 1986).

Clathrin-independent endocytic pathways have been less well-studied and are drawing attention from cell biologists (Mayor and Pagano, 2007). Many transmembrane proteins on the plasma membrane lack cytoplasmic sequences for the recruitment and internalization into clathrin-coated vesicles. These proteins have been shown to be internalized by clathrin-independent

endocytic pathways (Naslavsky et al., 2004). Another evidence of clathrin-independent endocytic pathways comes from the studies on cellular uptake of bacterial toxins. Pharmacological perturbations that were thought to inhibit the formation of clathrin-coated pits did not block all endocytosis (Sandvig et al., 2008). Subsequent genetic manupulation on the clathrin-associated proteins, dynamin (Damke et al., 1995), Eps15 (Lamaze et al., 2001), and AP180 (Naslavsky et al., 2004) confirmed the endocytic pathways that do not depend on clathrin-associated machinery. A clathrin-independent endocytic pathway that requires dynamin and caveolae is characterized (Fig. 3). Caveolae are 50-80 nm flask-shaped plasma membrane invaginations that are characteristic of the presence of caveolin proteins. Biochemical and proteomic analysis of caveolar membrane fraction revealed they are enriched in sphingolipids, cholesterol, signalling proteins, and GPI-anchored proteins (Aboulaich et al., 2004; Lemaitre et al., 2005; Simons and Ikonen, 1997; Sprenger et al., 2004). There are also specialized actin-driven clathrin-independent pathways, phagocytosis and marcopinocytosis (Fig. 3). The former is used to internalize large particles, such as bacteria. The latter is used for the uptake of fluid or growth factors.

Some Rab and Arf GTPases are known to be involved in endocytic pathways (Maxfield and McGraw, 2004). ARF6 plays a regulatory role in the recruitment of clathrin adaptor protein 2 (AP2) and clathrin to the plasma membrane, which is the first step for the formation of endocytic vesicles (Krauss et al., 2003). RAB5 and early endosome antigen 1 (EEA1) regulate the fusion between primary endocytic vesicles with sorting endosomes (McBride et al., 1999). RAB4 and RAB11 are associated with recycling. RAB4 localizes to sorting endosomes and endocytic recycling compartment, and regulates the recycling of membrane from sorting endosomes back to the plasma membrane (van der Sluijs et al., 1992). RAB11 localizes to endocytic recycling

compartment and TGN and regulates the recycling back to the plasma membrane (Chen et al., 1998; Ren et al., 1998).

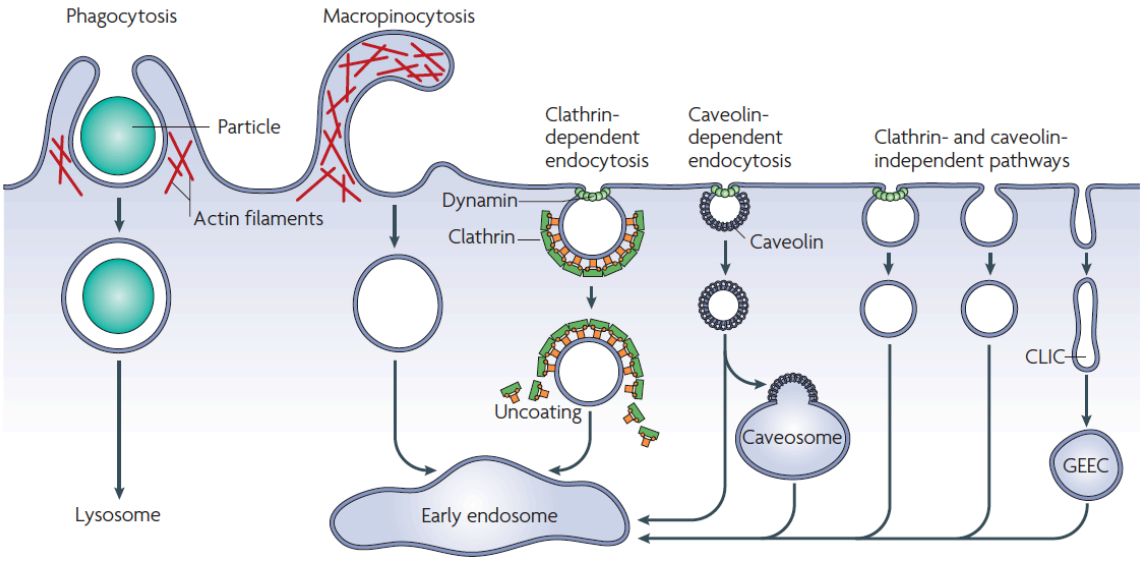

Figure 3 Overview of endocytic pathways

Large particles can be internalized by phagocytosis, and upake of fluid can occur by marcopinocytosis. Both processes require actin-mediated remodelling of the plasma membrane. The vesicles formed from phagocytosis and macropinocytosis is much larger than the vesicles from other endocytic pathways. Various endocytic pathways are classified based on their dependency on clathrin, caveolin and dynamin. Most internalized cargoes are transported to the early endosome via vesicular (clathrin- or caveolin-coated vesicles) or tubular intermediates (known as clathrin and dynamin-independent carriers (CLICs)) that are derived from the plasma membrane. Some cargoes may first travel to intermediate compartments, such as caveosome or GPI-anchored protein enriched early endosomal compartments (GEECs), *en route* to the early endosome. This figure is adapted from a review article (Mayor and Pagano, 2007).

1.2 The Ras superfamily proteins

The Ras superfamily consists of over 150 human proteins (Wennerberg et al., 2005). Similar to the α subunit of heterotrimeric G protein in biochemistry and function, they function as monomeric G proteins, alternating between GTP-bound active state and GDP-bound inactive state. They are proteins of low molecular weight (20-25 kDa) and share a common enzymatic activity, catalyzing the hydrolysis of GTP. Therefore, they are also commonly referred to as small GTPases, G proteins, or GTP-binding proteins. Based on the similarity of sequence and function, Ras superfamily proteins can be categorized into 5 families: Ras, Rho, Ran, Rab, and Arf (Wennerberg et al., 2005) (Fig. 4).

The founding member of Ras family is the Ras protein. The acronym Ras is derived from the word *ra*t *s*arcoma, as it was first identified as the transforming factor of rat sarcoma viruses (Barbacid, 1987).

Rho (*R*as *ho*mologous) family proteins have been the focus of many research studies since the discovery of their primary roles in the reorganization of the actin cytoskeleton. Ran (*Ra*s-like *n*uclear) family proteins are the most abundant small GTPases in the cell and are known for its function in nucleo-cytoplasmic trafficking (Cook et al., 2007). Rab (*Ra*s-like proteins in *b*rain) and Arf (*A*DP-*r*ibosylation *f*actor) are known for their roles in regulating intracellular vesicular transport of the endocytic and secretory pathways (Nie et al., 2003; Zerial and McBride, 2001).

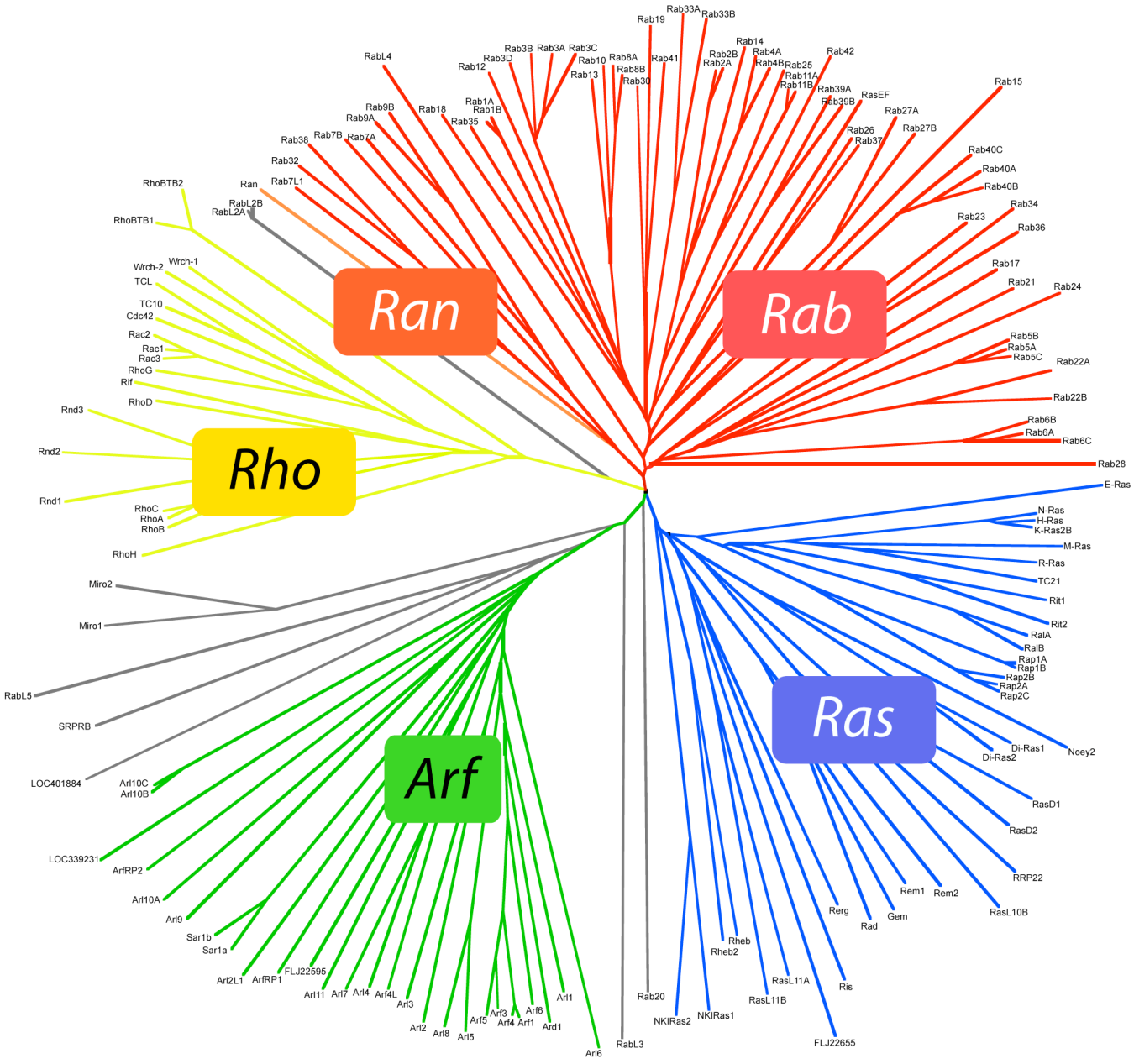

Figure 4 Phylogenetic tree of the Ras superfamily proteins

This figure is adapted from a review article (Wennerberg et al., 2005)

1.2.1 Arf GTPases

Arf family GTPases consist of Arf, Arl (*Arf-l*ike), and Sar (*S*ecretion-*a*ssociated and *R*as-related) proteins. Arf family GTPases bear a lipid moiety. A myristoyl lipid moiety is usually attached to N-terminus of the Arf protein, following removal of initiator methionine and exposure of a glycine at

position 2. One structural feature shared by the Arf family GTPases is the N-terminal amphipathic helix. In the GDP-bound conformation, the hydrophobic residues of this amphipathic helix are masked inside a hydrophobic pocket on the core of the GTPase (Pasqualato et al., 2002). The GTPase undergoes conformational change, when the exchange of GDP for GTP is catalysed by a specific GEF. In the GTP-bound form, N-terminal amphipathic helix is pushed out of its pocket and interacts with an adjacent lipid bilayer (Goldberg, 1998; Robert et al., 2004).

ARF was first discovered, purified and functionally defined as the protein cofactor required for enhancing the cholera toxin-catalyzed ADP-ribosylation of the α subunit of heterotrimeric G protein ($G\alpha_s$) (Enomoto and Gill, 1980; Kahn and Gilman, 1984). Shortly afterward Arf was shown to be a GTP-binding protein (Kahn and Gilman, 1986). The initial criteria for designating proteins as "Arfs" were functional. Only proteins that were able to (1) act as cofactor for cholera toxin, (2) rescue the lethal *arf1arf2*$^-$ deletion in *Saccharomyces cerevisae*, and (3) directly activate phospholipase D were given the name Arf (Kahn et al., 2006). There are 6 Arfs in mammals. Based on amino acid sequence similarity, Arf proteins have been categorized into 3 classes: Class I (ARF1, ARF2, and ARF3 share >96% sequence identity to each other), Class II (ARF4 and ARF5 share 90% sequence identity to each other and 80% sequence identity to the other Arfs) and Class III (ARF6 shares 64-69% sequence identity to the other Arfs). ARF1 and ARF3 regulate the assembly of different types of "coat" complexes onto budding vesicles along the secretory pathway, and activate lipid-modifying enzymes (Bonifacino and Glick, 2004). The functions of ARF4 and ARF5 are still unclear. However, some studies have indicated that ARF5 might play a role in early Golgi transport and in recruiting coat components to *trans*-Golgi membranes. ARF6 is thought to regulate endosomal membrane traffic and structural organization at the cell surface (D'Souza-Schorey and Chavrier, 2006).

Arl proteins are ca. 50-60% identical to each other and to Arf proteins. The term "Arl" doesn't denote a protein with one or more specific functions, as does the term Arf. It indicates only that the protein is structurally related to Arfs (Kahn et al., 2006). There are about 20 ARLs in mammals (Kahn et al., 2006; Pasqualato et al., 2002), but the biological and physiological functions of most ARL proteins are poorly characterized. The best-characterized ARL protein, ARL1, is localized to the trans-Golgi network (TGN) and regulates trafficking in the TGN-endosomal pathways (Lu et al., 2004). ARL2 and ARL3 regulate microtubule dynamics (Zhou et al., 2006). Human ARL4A, ARL4C, and ARL4D are three closely related ARLs that appear to have diverged in recent evolution because they all have orthologs in other vertebrates but a single ortholog in *Drosophila* (Jacobs et al., 1999; Li et al., 2004). They are distinguished from other members of the Arf family of GTPases by a C-terminal extension of 10-15 mostly basic residues and a short insertion in the loop between the two switch regions (Hofmann et al., 2007; Lin et al., 2000; Pasqualato et al., 2002).

Sar proteins are only slightly closer in sequence to Arf proteins (<30% identity) than to other families of GTPases. However, they are functionally related in that they coordinate the recruitment of coat proteins or complexes to initiate vesicle budding (Kahn et al., 2006). One of the representative Sar proteins is SAR1. It was first identified as a suppressor of temperature-sensitive mutation of *sec12* in genetic screens in the yeast *Saccharomyces cerevisiae* (Nakano and Muramatsu, 1989). SAR1 has been known to regulate the formation of coat protein complex II (COPII) vesicles on the ER membrane (Jensen and Schekman, 2011). The formation of COPII vesicles begins with the recruitment of SAR1 to the ER. This event is promoted by the membrane-bound factor Sec12, which acts as a GEF of SAR1, catalyzing the exchange of GDP for GTP on SAR1. GTP-bound SAR1 can be inserted into the outer leaflet of the ER membrane via its exposed N-terminal amphipathic helix, and

recruit cytosolic Sec23-Sec24 heterodimer. Sec24 is the subunit responsible for binding the membrane cargo proteins and concentrating them into the forming vesicles (Miller et al., 2002). SAR1 and cargo-bound Sec23-Sec24 heterodimer form pre-budding complex on the ER membrane. Sec13-Sec31 heterodimer binds and captures the pre-budding complexes, forming an outer coat layer that sustains membrane curvature and promotes the vesicle fission from the ER membrane (Fath et al., 2007). The vesicle fission is mediated by the hydrolysis of GTP on SAR1 (Lee et al., 2005), which is stimulated by Sec23 (as the GAP of SAR1) and further accelerated by Sec13-Sec31 heterodimer (Antonny et al., 2001).

1.2.2 Rab GTPases

Rab family GTPases is the largest branch of Ras superfamily proteins. These proteins are conserved across evolution. Members of Rab GTPases have been identified in various evolutionary distant organisms: Caenorhabditis elegans (29 members), Drosophila melanogaster (29), Homo Sapiens (ca. 70), Arabidopsis thaliana (57), Saccharomyces cerevisiae (11) (Hutagalung and Novick, 2011; Pereira-Leal and Seabra, 2001). Rabs in general possess the GTPase fold, which is composed of 6 β-sheets flanked by 5 α-helices (Hutagalung and Novick, 2011; Wittinghofer and Vetter, 2011). At the C-terminus of the Rab there are the hypervariable region and the CAAX boxes. Newly synthesized Rab protein is associated with Rab escort protein (REP), which delivers the Rab protein to Rab geranylgeranyl transferase (RabGGT) that catalyzes the addition of geranylgeranyl lipid moieties to the CAAX box of the Rab at the C-terminus (Pereira-Leal et al., 2001). The geranylgeranyl tails are essential for the interaction between Rabs and membranes.

Rab GTPases cycle between a GTP-bound state and a GDP-bound state. Guanine nucleotide exchange factor (GEF) and GTPase-activating protein

(GAP) are two classes of proteins that regulate the GDP-GTP cycle. A GEF acts by inducing the release of the bound GDP, which can be replaced by the more abundant GTP. A GAP protein provides a critical catalytic group to stimulate the activity of GTP hydrolysis (Bos et al., 2007). The nucleotide-bound state of Rab GTPase controls its localization, conformation and activity. GTP-bound Rab GTPase is considered to be active, as this conformation can interact with the effector proteins that regulate the specific membrane traffic pathway.

As other small GTPases, Rab GTPases contain 5 conserved sequence motifs, which have been called the G1, G2, G3, G4, and G4 domains (Bourne et al., 1991). These G domains are associated with guanine nucleotide binding. G1 is often referred to as the P-loop (Saraste et al., 1990), and has the consensus sequence GXXXXGKS/T, which is involved in the interaction with the nucleotide phosphates. G2 is also known as switch I loop, while G3 is called switch II region. G2 and G3 are called switch regions, as these regions undergo significant conformational change upon GTP hydrolysis. G3 with the DXXGQ motif is involved in the interaction with the γ-phosphate of GTP and Mg^{2+}. G4 and G5 are involved in the interaction with guanine base (Itzen and Goody, 2011). Mechanistic understanding of how G domains interact with guanine nucleotide and the components involved in GTP hydrolysis is important. It provides the basis to understand the diseases caused by the mutation of small GTPases and contributes to the generation of Rab GTPase mutants that are either GDP-locked or GTP-locked (Adari et al., 1988; Nuoffer et al., 1994; Saraste et al., 1990; Vetter and Wittinghofer, 2001).

Rab GTPases have been established as key regulators of membrane organization and intracellular membrane trafficking (Stenmark, 2009). They are known to be associated with specific organelles, where they regulate the recruitment of a variety of proteins, including molecular motors and tether factors (Pfeffer, 2001; Zerial and McBride, 2001). For example, Rab6 localizes

to the trans-Golgi where it recruits Bicaudal D, an accessory protein for the microtubule motor dynein (Matanis et al., 2002; Short et al., 2002), and TMF1, a coiled-coil protein involved in membrane traffic (Fridmann-Sirkis et al., 2004). Rab5 localizes to the early endosomes. One of the various proteins Rab5 recruits is EEA1, a tethering factor for endosome fusion (Simonsen et al., 1998).

There are about 70 human Rab GTPases identified. However, functions of many Rabs are not characterized. Identification of the effector proteins of a specific Rab GTPase is an important approach to investigate the Rab-mediated membrane traffic pathways. Large-scale screening for the effectors of Rab GTPases by yeast two-hybrid assay and GST pull-down assay have been performed (Fukuda et al., 2008; Kanno et al., 2010). The results of these screens have revealed a number of previously unknown Rab-mediated pathways.

The biological relevance of some Rab GTPases remains elusive. Rab40c is one of these Rabs. Mammalian Rab40c was shown to be involved in vesicle transport in oligodendrocytes (Rodriguez-Gabin et al., 2004). A homolog of Rab40c in *Xenopus*, XRab40, was shown to participate in the gastrulation of *Xenopus* embryo, localize at the Golgi complex and interact with Cullin5 and Elongin B to form a E3 ubiquitin ligase complex that regulates noncanonical Wnt pathway (Lee et al., 2007). A recent study demonstrated Rab40c associates with lipid droplets and regulates the biogenesis of lipid droplets (Tan et al., 2013). However, there are some inconsistencies concerning the localization and function in these studies.

There are Rab GTPases that have not been studied. To our knowledge, localization and functions of RAB42 and RAB44 are unknown.

1.3 Cargo proteins in the secretory pathway

Transmembrane proteins and glycosylphosphatidylinositol-anchored proteins (GPI-anchored proteins) are two types of membrane proteins. They are typical secretory cargo proteins and both have the N-terminal signal peptide sequence that directs their entry into the ER. However, transmembrane proteins and GPI-anchored proteins are associated with membrane by distinct molecular interactions. Transmembrane proteins have membrane-spanning domains that traverse the lipid bilayer (*e.g.* ts-O45-G-YFP) (Fig. 5). By contrast, GPI-anchored proteins (*e.g.* CFP-GL-GPI) are attached to the extracellular or lumenal leaflet of the membrane through the glycolipid structure, GPI (Fig. 5).

Secretory cargo proteins also include soluble proteins, such as zymogen and collagen. They are secreted extracellularly.

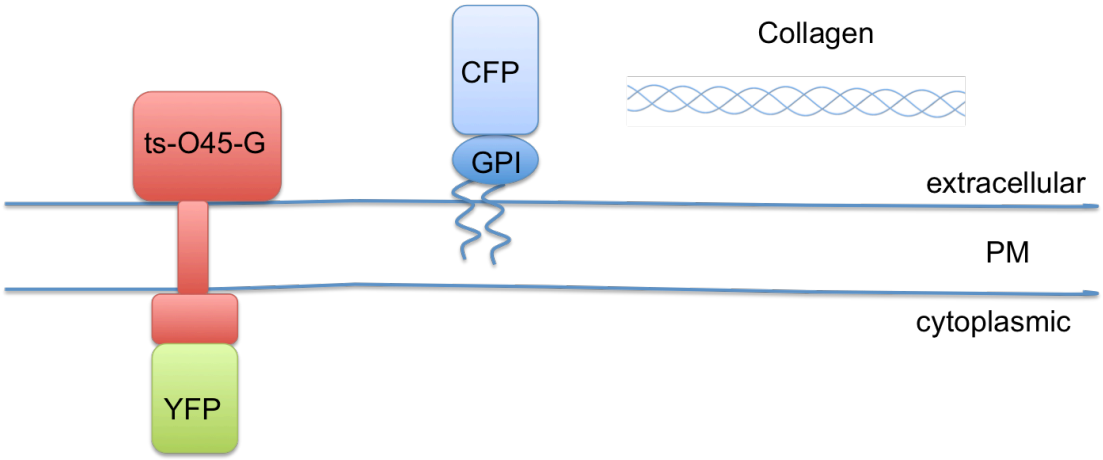

Figure 5 Schematic presentation of cargo proteins

The drawing depicts the association of the cargo proteins (ts-O45-G-YFP, CFP-GL-GPI, and collagen) with the PM. ts-O45-G-YFP are inserted in the PM via a transmembrane domain. CFP-GL-GPI are attached to the outer leaflet of the PM by the lipid moiety of the GPI anchor. Collagens, such as type I procollagen (PC I), are secreted into the extracellular matrix.

1.3.1 Vesicular stomatitis virus glycoprotein (VSVG)

Enveloped viruses, such as vesicular stomatitis viruses (VSV), provide simple and useful model systems for the study of the structure, biosynthesis, and function of membrane proteins. VSV virion membrane contains cell-derived lipid and glycolipids, in addition to two viral proteins: the matrix protein (M) and the glycoprotein (G). The glycoprotein G of VSV (VSVG) is an integral transmembrane protein and forms spikes on the surface of the virion. This 70 kDa glycoprotein have two N-linked complex oligosaccharides (Etchison et al., 1977; Reading et al., 1978) and is positioned in the virion such that almost 90% of the polypeptide chain is external to the lipid bilayer (Rose et al., 1980; Schloemer and Wagner, 1975). VSVG is responsible for binding of the viruses to susceptible host cells and inducing the uptake of the virus by the cells (Bishop et al., 1975; Cartwright et al., 1969).

Many studies focused on the biosynthesis of VSVG and the transport of VSVG to the PM (Lingappa et al., 1978; Rothman and Lodish, 1977). VSVG consists of a single polypeptide chain of 511 amino acids and contains a N-terminal signal peptide (Lingappa et al., 1978). It is co-translationally glycosylated and inserted into the rough ER membrane (Rothman and Lodish, 1977). From the rough ER it is transported first to the Golgi complex and then to the PM, where assembly and budding of viruses occurs (Lodish et al., 1980). The transport of VSVG to the PM is critical for the life cycle and infectivity of VSV. Some temperature-sensitive mutants of VSV have been isolated and are known to have defects in the transport of the glycoprotein (Lodish and Weiss, 1979; Zilberstein et al., 1980). A temperature-sensitive mutant of VSV, Orsay-45, isolated by Flammand, have been studied extensively (Flamand, 1970; Lafay, 1974). This mutant has a reversible block in transport of the glycoprotein G from the rough ER to the Golgi apparatus (Bergmann et al., 1981). Its glycoprotein G is commonly referred to as ts-O45-G. At restrictive

temperature 39.5°C, ts-O45-G cannot exit the rough ER. Upon shifting to permissive temperature 32°C, ts-O45-G rapidly leaves the rough ER and moves towards the Golgi apparatus. The defect is caused by a single amino acid substitution in ts-O45-G (Gallione and Rose, 1985). Later on it was demonstrated that oligomerization is required for the transport of ts-O45-G from the rough ER (Kreis and Lodish, 1986). Temperature-sensitivity of ts-O45-G makes ts-O45-G an important tool to analyze the dynamics and molecular machinery of the early secretory pathway (Keller et al., 2001; Presley et al., 1997; Toomre et al., 1999).

1.3.2 Collagens

Collagen is the most abundant component of the extracellular matrix. It consists of 3 polypeptide α chains, which form a triple helix. Each polypeptide chain has a X-Y-Gly repeating pattern in which Glycyl residues occupy every third position and the X and Y positions are frequently occupied by proline and 4-hydroxyproline, respectively (Kadler et al., 2007). Proline and 4-hydroxyproline residues stablize the triple helix by limiting the rotation of the polypeptide chains. The triple helix is further stabilized by the interchain hydrogen bonds and water bridges (Bella et al., 1995; Prockop and Kivirikko, 1995). Furthermore, the side chains of proline and 4-hydroxyproline in the triple helix are exposed to solvent. This conformation accounts for the ability of collagens to polymerize (Prockop and Kivirikko, 1995).

Biosynthesis of collagens is a complex process. Collagen is first synthesized as a procollagen molecule comprised of 3 procollagen polypeptide chains (Tromp et al., 1988). Procollagen is known to traverse the rough ER and the Golgi complex of the cell before its secretion into the extracellular matrix (Fessler and Fessler, 1978). Collagens are generated when

the propeptides of procollagen molecules are cleaved in the extracellular matrix (Myllyharju and Kivirikko, 2004). Collagen fibrils are formed by the self-assembly of collagen molecules.

As many secreted proteins in eukaryotic cells, the precursor of procollagen polypeptide contains a N-terminal signal peptide (Palmiter et al., 1979). In the ER, procollagen polypeptides undergo extensive post-translational modification before the triple helix formation. Numerous enzymes and molecular chaperones assist in their correct folding and trimerization. Collagen prolyl 4-hydroxylase is essential for collagen biosynthesis, because 4-hydroxyproline residues are required for the formation of collagen triple helix (Myllyharju and Kivirikko, 2004). Enzymatic activity of prolyl 4-hydroxylase requires the cofactor ascorbate (Peterkofsky, 1991).

The export of procollagen molecules from the ER depends on COPII vesicles (Stephens and Pepperkok, 2002; Townley et al., 2008). The rigid rod-like procollagen molecule of 300 nm was thought to be too large to fit into the conventional 60-80 nm COPII vesicles (Schekman and Orci, 1996). Various studies have been undertaken to investigate this question. A genome-wide RNAi screen in *Drosophila* tissue culture cells has identified new components that are required for protein secretion and Golgi organization. These proteins are termed TANGO, for *t*ransport *an*d *G*olgi *o*rganization (Bard et al., 2006). One of these proteins, TANGO1, is required for the export of Collagen VII from the ER (Saito et al., 2009). Another line of evidence comes from the study on the X-linked skeletal disorder Spondyloepiphyseal dysplasia tarda (SEDT), which is characterized by short stature, a short trunk, and precocious osteoarthritis. SEDT is caused by mutations in the gene *SEDL* (Gedeon et al., 1999). As a consequence, the chondrocytes are unable to properly secrete extracellular matrix components, leading to a derangement in chondrogenesis (Tiller et al., 2001). The *SEDL* product, Sedlin, is a component of TRAPP, a

highly conserved multisubunit complex which functions at various steps in intracellular transport (Barrowman et al., 2010). Later on, it was reported that TANGO1 recruits Sedlin and their joint action regulates the ER export of procollagens (Venditti et al., 2012). Furthermore, a recent study demonstrated that an ubiquitin-dependent mechanism regulates the size of COPII vesicles (Jin et al., 2012). Ubiquitination of the components of COPII vesicles, SEC31, facilitates the formation of large COPII vesicles.

1.3.3 GPI-anchored proteins

1.3.3.1 Discovery of GPI-anchored proteins

The discovery of GPI-anchored proteins came from the observation that highly purified phosphatidylinositol-specific phospholipase C (PI-PLC) from bacteria can specifically release alkaline phosphatase (AP), acetylcholinesterase (AChE) and 5'-nucleotidase from the PM of various mammalian tissues in late 1970s (Ikezawa et al., 1976; Low and Finean, 1977; Low and Finean, 1978; Shukla et al., 1980). Later on the GPI moiety of GPI-anchored proteins of *Torpedo* electric organ AChE, human erythrocyte AChE, rat brain and thymocyte Thy-1, variant surface glycoprotein (VSG) protein of *Trypanosoma brucei* were structurally characterized (Ferguson et al., 1985; Ferguson et al., 1988; Futerman et al., 1985; Roberts and Rosenberry, 1985; Tse et al., 1985).

1.3.3.2 Biosynthesis of GPI-anchored proteins

Biosynthesis of GPI moiety occurs in the ER and requires at least 10 reactions (Fujita and Kinoshita, 2012). So far more than 20 genes that are associated with these reactions have been identified (Fujita and Kinoshita,

2010; Kinoshita et al., 2008). N-terminal signal peptide and C-terminal GPI attachment signal peptide are two important features of GPI-anchored proteins. These two features are critical for the biosynthesis of GPI-anchored proteins. N-terminal signal peptides direct their sorting to the ER. In the ER, GPI moieties are transferred *en bloc* by GPI transamidase to the C-termini of proteins that have a GPI attachment signal peptide. GPI transamidase recognizes the GPI attachment signal peptide and cleave off the signal peptide, resulting in the formation an enzyme-substrate intermediate linked via thioester. Nucleophilic attack by the terminal amino group of GPI moiety breaks the thioester, generating GPI-anchored proteins (Orlean and Menon, 2007; Udenfriend and Kodukula, 1995).

Functions of GPI-anchored proteins are diverse. There are GPI-anchored proteins that function as enzymes, adhesion molecules, surface antigens, and receptors (Chatterjee and Mayor, 2001). The functions of GPI moiety have been intensely studied. Various putative functions in the context of membrane trafficking have been proposed. GPI moiety might be related to the export of GPI-anchored proteins from the ER. Recent studies indicated that only the properly processed GPI-anchored proteins are transported efficiently (Castillon et al., 2011; Fujita et al., 2011). GPI moieties might act as ER export signals for GPI-anchored proteins. Polarized cells, such as epithelial cells, have at least two different plasma membrane domain, basolateral and apical membrane domains. Apical-basolateral sorting was occurred in the TGN or recycling endosomes (Rodriguez-Boulan et al., 2005). In most polarized cells, GPI-anchored proteins localize to the apical membrane domain (Brown and Rose, 1992; Lisanti et al., 1989; Paladino et al., 2006). These observations postulated GPI moiety could act as apical sorting signal, but the underlying mechanisms are not clear.

1.3.4 Rab and Arf GTPases associated with the trafficking of ts-O45-G, PC I, and GPI-anchored proteins

A number of Rab and Arf GTPases are associated with the trafficking of ts-O45-G. Down-regulation of RAB1A/1B, RAB6A, RAB18, RAB34, RAB7B, ARF1, ARF3, ARF5 and ARFRP1 have been reported to inhibit ts-O45-G secretion in HeLa cells (Dejgaard et al., 2008; Goldenberg et al., 2007; Haas et al., 2007; Miserey-Lenkei et al., 2010; Nishimoto-Morita et al., 2009; Progida et al., 2010; Tisdale et al., 1992; Volpicelli-Daley et al., 2005). Over-expression of RAB2, RAB31, RAB34 mutants inhibited ts-O45-G secretion (Goldenberg et al., 2007; Ng et al., 2009; Tisdale et al., 1992).

Much less Rab and Arf GTPases are known to be associated with PC I secretion. Over-expression of ARF1 mutant inhibited PC I secretion (Stephens and Pepperkok, 2002). Interestingly, some Rabs are suggested to be potential regulators of PC I secretion based on the study investigating osteoblast differentiation (Nabavi et al., 2012). Ascorbate induces osteoblast differentiation, and the concomitant increased expression of bone related genes, including type I collagen (Kitching et al., 2002). Impaired PC I secretion was observed in the osteoblasts expressing RAB1, RAB3D and RAB27B mutants (Nabavi et al., 2012).

There are a few studies examining the role of Arf GTPases in the secretion of GPI-anchored proteins. The homolog of ARL1 in *Trypanosoma brucei*, TbARL1, is involved in the secretion of the GPI-anchored protein, variant surface glycoprotein (VSG) from the TGN to the cell surface (Price et al., 2005). In yeast, Arl1p was shown to be involved in the transport of the GPI-anchored protein, Gas1p, from the late Golgi to the plasma membrane (Liu et al., 2006). ARL1 has been shown to target GRIP domain-containing golgins to the Golgi complex (Panic et al., 2003). A GRIP domain-containing golgin, p230, is shown to be involved in the transport of GPI-anchored

proteins from the Golgi complex to the cell surface (Kakinuma et al., 2004). These studies suggested the post-Golgi transport of GPI-anchored proteins involves ARL1 and golgins.

1.4 Microscopy-based RNAi screening

Microscopy-based RNAi screening is emerging as a powerful method for functional genomic studies. This method requires a number of diverse technologies, including RNAi technology, microscopy, image processing and automation.

1.4.1 RNAi technology

RNAi is a conserved gene silencing mechanism (Fire et al., 1998; Meister and Tuschl, 2004). RNAi technology has been commonly utilized to investigate the gene function. Chemically synthesized short double-stranded RNA (dsRNA) oligomers (siRNAs) are the most widely used reagent to induce RNAi in mammalian cells (Elbashir et al., 2001). siRNAs can be efficiently transfected by chemical transfection reagents, which are available from major biotechnology companies. However, the preparation of transfection complex involves intensive liquid-handling procedures, which might conceivably restrict the scale of transfection. One of the solutions to circumvent the tedious liquid-handling procedures is the development of solid-phase reverse transfection. In solid-phase reverse transfections, dried transfection mixtures of siRNA oligonucleotides, transfection reagents and matrix reagents are coated on the culture plates before the transfection. The cells are then seeded on the well coated with dried transfection mixture and are transfected. This technology has been exploited in RNAi screening, in which large-scale transfection is indispensable (Erfle et al., 2007; Erfle et al.,

2008; Ziauddin and Sabatini, 2001). The information of genome sequences contributes to the improvement of siRNA design. Various sets of siRNAs targeting specific gene families can be obtained as a library commerically.

1.4.2 Fluorescence microscopy and GFP

Fluorescence microscopy is an important imaging method in cell biology. Intracellular localization of the proteins can be examined by fluorescence microscopy in conjunction with immunofluorescence techniques. The discovery, cloning, and heterologous expression of GFP revolutionize the field of cellular imaging (Chalfie et al., 1994; Prasher et al., 1992; Shimomura et al., 1962; Tsien, 1998). GFP can be used to label nearly all cellular proteins under physiological condition in living cells (Giepmans et al., 2006). The development of GFP and its spectral variants broadens the application of fluorescence microscopy (Lippincott-Schwartz et al., 2003; Miyawaki et al., 2005). Complex biological processes, such as protein dynamics and protein-protein interactions can be analyzed with high spatiotemporal resolution. Furthermore, GFP-based reporters have been developed to monitor the pH, enzyme activity, redox state of the ER, cyclic AMP and Ca^{2+} concentrations in living cells (Birk et al., 2013; Meyer and Dick, 2010; Miyawaki, 2005; Phizicky et al., 2003; Wouters et al., 2001).

1.4.3 Automated microscopy

Automation of microscopy is essential for RNAi screening application because of the scale of screening experiments. The advance of robotics provides the possibility to automate microscopy. Epifluorescence microscopes equipped with motorized control of stage positioning, fluorescence filters, and camera acquisiton are available from major microscope providers

(Conrad and Gerlich, 2010; Pepperkok and Ellenberg, 2006). Automated image processing is required to perform quantitative measurements on each individual cell. One of the challenge is the identification of cells. Segmentation algorithms based on the property of the cell have been developed to overcome this challenge.

1.4.4 RNAi screening

The core of microscopy-based RNAi screening is the cell-based assay. The assay is desgined to analyze the biological process of interest. A variety of assays have been developed to score the expression of marker genes (Loo et al., 2007), lipoprotein uptake (Bartz et al., 2009), virus entry into cells (Pelkmans et al., 2005), ts-O45-G and PC I secretion (Starkuviene et al., 2008).

Phenotypes from RNAi screening need to be interpreted with caution. The lack of a phenotype by RNAi can be caused by genetic or functional redundancy. Phenotypes can confirmed by combinatorial RNAi, or combining RNAi with dominant-negative mutants or small molecule inhibitiors (Macia et al., 2006; Sahin et al., 2007). Furthermore, phenotypes can be complicated by a potential indirect effect of gene silencing.

2 Materials and Mathods

2.1 Materials

2.1.1 Cell-lines

NIH3T3 mouse fibroblasts (ATCC, CRL-1658) were cultured in low glucose DMEM (Life Technologies, Grand Island, NY, USA) supplemented with 10% newborn calf serum, 100 units/ml penicillin, 100µg/ml streptomycin and 2 mM L-glutamine.

HeLa cells (ATCC CCL-2.1) were cultured in low glucose DMEM supplemented with 10% fetal bovine serum, 100 units/ml penicillin, 100µg/ml streptomycin and 2 mM L-glutamine.

HEK293T cells (ATCC CRL-11268) were cultured in low glucose DMEM supplemented with 10% fetal bovine serum, 100 units/ml penicillin, 100µg/ml streptomycin and 2 mM L-glutamine.

2.1.2 Plasmids

CFP- and GFP-tagged versions of human RAB GTPases were a gift from Prof. Bruno Goud (Institut Curie, Paris, France). ts-O45-G-YFP was a gift from Dr. Rainer Pepperkok (EMBL Heidelberg, Germany). mRFP1-KDEL was a gift from Dr. Nathan Brady (DKFZ, Heidelberg, Germany).

2.1.3 siRNAs

siRNAs were from Qiagen (Hilden, Germany).

2.1.4 Primary Antibodies

Following mouse monoclonal primary antibodies were used: anti-GM130, anti-EEA1 (BD Bioscience, San Diego, CA, USA), anti-α-tubulin (Cell Signaling Technology, Danvers, MA, USA), anti-GFP (Roche), anti-RAB42 (Abnova, Taiwan).

Mouse monoclonal anti-LAMP1 (H4A3 clone) was a gift from Dr. Jacomine Krijnse-Locker. Mouse monoclonal anti-VSVG was a gift from K. Simons (MPI-CBG, Dresden, Germany).

Rabbit polyclonal anti-FLAG (Sigma-Aldrich), anti-PC I and anti-Rab40c (Millipore, Temecula, CA, USA), sheep polyclonal anti-TGN46 antibody (AbD serotec) were used.

2.1.5 Secondary antibodies

Commercial secondary antibodies were as follows: AlexaFluor488- and AlexaFluor647-coupled anti-mouse IgG, anti-rabbit IgG and anti-sheep antibodies (Life Technologies, Grand Island, NY, USA), Cy3- and Cy5-coupled anti-rabbit antibodies, HRP-coupled anti-mouse and anti-rabbit antibodies (GE Healthcare, Pittsburgh, PA, USA).

2.1.6 Chemicals

All chemical reagents were purchased from Sigma-Aldrich (St. Louis, MO, USA), if not stated otherwise.

2.2 Molecular biology methods

2.2.1 RT-PCR

Total RNA in HeLa cells was isolated using TRIZOL (Life Technologies, USA) in accordance with the manufacturer's protocol. For reverse transcription, 24 μl of RNA solution containing 1 μg RNA and 100 pmole oliogo(dT) incubated in a tube at 70°C for 3 min. The tube was then spinned down and placed on ice. First Strand Synthesis Buffer, 5 nmole dNTP mix, 50 U M-MLV reverse transcriptase (Life Technologies, USA) and 60 U RNase inhibitor (Life Technologies, USA) were added in the tube (final volume: 30 μl). Synthesis of cDNA was initiated by incubation at 42°C for 1 hour. After that the tube was incubated at 92°C for 10 minutes to inactivate the reverse transcriptase. The cDNA sample was stored at -20°C before PCR.

For PCR, the cDNA sample and corresponding forward and reverse primers (Sup. Table 2) were mixed with Taq 2X master mix (New England Biolabs, USA).

2.2.2 Cloning of RAB42

DNA fragment encoding RAB42 was amplified from cDNA of HeLa cells by PCR. The primers used were RAB42-F and RAB42-R. The PCR fragment was used as the template for subsequent cloning. For subcloning the FLAG-tagged RAB42 expression vectors, the fragment was modified by PCR, with a EcoRI site at the 5′ end and a BamHI site at the 3′ end. The primers used were Flag-RAB42-5-EcoRI and RAB42-3-BamHI-R. The EcoRI/BamHI digested fragment was inserted into the EcoRI/BamHI digested pcDNA3.1(-) to generate FLAG-RAB42.

Primer	Sequence (5′->3′)
RAB42-F	**CATGGAGGCCGAGGGCTGCCGCTACCAATTTCG**
RAB42-R	**ACCAGGTGGGCTAAGGCTGGGACTGCTTTAACC**

Flag-RAB42-5-EcoRI	**CCGGAATTCACCATGGACTACAAAGACGATGACGAT AAAATGGAGGCCGAGGGC**
RAB42-3-BamHI-R	**GAACGCGGATCCTCAACACTGGCATGGGC**

2.2.3 Subcloning CFP-GL-GPI into pRevTRE2 vector

pRevTRE2 is a expression vector with a doxycycline transactivator responsive element, which allows doxycycline-dependent mRNA transcription. Following steps were taken to subclone CFP-GL-GPI into pRevTRE2. First, cDNA encoding CFP-GL-GPI were amplified by PCR with the forward primer (5′-AGCTTTGTTTAAACCACCATGGAGCT-3′) and the reverse primer (5′-GTTTGGACAAACCACAAC-3′) using CFP-GL-GPI plasmid as the template. The amplified fragments were digested by MssI and NotI restriction enzymes. Then, MssI/NotI digested fragments were ligated with MssI/NotI digested pRevTRE2 vector. After ligation and transformation, the plasmids of pRevTRE2-CFP-GL-GPI transformants were sequenced.

2.2.4 Site-directed mutagenesis

PCR was applied for site-directed mutagenesis. PCR was performed using the Phusion High-Fidelity DNA polymerase (New England Biolabs, USA) and the 5′ phosphorylated mutagenic primers (Sup. Table 6) that introduce the desired mutation. The PCR product was analysed by agarose electrophoresis. The amplified DNA fragments of correct size were purified and circularized by ligation with T4 DNA ligase (New England Biolabs, USA), and afterwards used for transforming chemically competent E. coli cells. The plasmids of transformants were purified and sequenced.

2.3 Cell biology methods

2.3.1 Reverse transfection

Reverse transfection of siRNA were performed using 96-well plate (ibidi, Martinsried, Germany). siRNA-gelatin source solution was prepared as described (Erfle et al., 2008) with the following modifications. Briefly, 5 µl of 30 µM siRNA solution, 3.5 µl Lipofectamine 2000 and 3 µl Opti-MEM (Life Technologies, USA) containing 0.4 M sucrose were mixed and incubated for 30 minutes at room temperature. After incubation, 7.25 µl 0.2% gelatin (Sigma-Aldrich, USA) and 3.5×10^{-4}% fibronectin (Sigma-Aldrich, USA) were added. Transfection solution was prepared by mixing 1 µl siRNA-gelatin source solution and 50 µl water. 50 µl transfection solution was spotted on each well of the 96-well plate. After the transfection solution dried, the plate was ready for reverse transfection.

2.3.2 Transfection of siRNAs and plasmids

Transfection of siRNA and plasmid was performed using Lipofectamine 2000 (Life Technologies, USA) in accordance with the manufacturer's protocol. For siRNA transfection, 1.25×10^4 Hela cells were plated on the 24-well plate (Greiner Bio-One, Frickenhausen, Germany) in 500 µl growth medium without antibiotics one day before transfection. Prior to transfection, transfection complex was prepared by mixing 50 µl siRNA solution (30 pmole siRNA in 50 µl Opti-MEM) with 50 µl Lipofectamine 2000 solution (0.6 µl Lipofectamine 2000 in 50 µl Opti-MEM). After incubation for 20 minutes at room temperature, 100 µl transfection complex was added to each well. Transfection complex was removed by changing the medium after 4 hours of incubation at 37°C, and the cells were incubated at 37°C until 48 hours post-transfection.

For plasmid DNA transfection, 2.5×10^4 HeLa cells were plated on the 24-well plate in 500 µl growth medium without antibiotics one day before transfection. Prior to transfection, transfection complex was prepared by mixing 50 µl DNA solution (320 ng DNA in 50 µl Opti-MEM) with 50 µl Lipofectamine 2000 solution (0.6 µl Lipofectamine 2000 in 50 µl Opti-MEM). After incubation for 20 minutes at room temperature, 100 µl transfection complex was added to each well. Medium was changed after 4 hours of incubation at 37˚C.

2.3.3 Primary screen and ts-O45-G transport assay

3.2×10^3 HeLa cells in 200 µl growth medium without antibiotics were seeded on ready-to-transfect 96-well plates. After 40 hours, HeLa cells were infected by an adenovirus vecotor for the expression of ts-O45-G-YFP and subjected to ts-O45-G transport assay as described (Starkuviene et al., 2008). Briefly, adenovirus encoding ts-O45-G-YFP was diluted 1:40 in the medium. HeLa cells were incubated in the adenovirus-containing medium (70 µl/well) for 45 minutes at 37˚C, then washed once with the medium, and incubated for 30 minutes at 37˚C. For the accumulation of ts-O45-G in the ER, HeLa cells were incubated at 39.5˚C for 6 hours. ER-exit block of ts-O45-G was released by shifting the incubation temperature to 32˚C. After incubation in the medium containing 100 µg/ml cycloheximide (Sigma-Aldrich) at 32˚C for 60 minutes, the cells were fixed in 3% paraformaldehyde solution (3% paraformaldehyde in PBS) at room temperature for 20 minutes. The cells were then washed once with PBS, incubated in the PBS containing 30mM glycine to quench the residual formaldehyde.

2.3.4 ts-O45-G post-TGN transport assay

To investigate ts-O45-G post-TGN transport, we adopted the ts-O45-G transport assay by including a 20˚C incubation step. In brief, HeLa cells were transfected with siRNAs as described above. Following 65 hours of incubation, cells were infected with adenoviruses encoding ts-O45-G. 1 hours after the infection, cells were transferred to 39.5˚C to accumulate ts-O45-G molecules in the ER and incubated for additional 3 hours. Then, the cells were incubated at 20˚C in the growth medium containing 20 mM HEPES (pH 7.4) for 2 hours. Finally, the cells were moved to the permissive temperature 32˚C in growth medium containing 100 μg/ml cycloheximide for 1 hour to induce and follow the secretion of ts-O45-G-YFP. Cells were then fixed with 3% paraformaldehyde solution, incubated in the PBS containing 30 mM glycine and stained with anti-VSVG antibody.

2.3.5 CFP-GL-GPI transport assay

HeLa cells were infected with adenoviruses encoding CFP-GL-GPI. 4 hours after the infection, the cells were incubated in the medium containing cycloheximide to start the chase. The cells were fixed 60 minutes after the chase with 3% paraformaldehyde solution, incubated in the PBS containing 30 mM glycine and stained with anti-GFP antibody.

Immunofluorescence microscopy was performed on an inverted IX81 wide-field screening microscope (Olympus Biosystems, Japan). 20 or 36 images per well were taken using a 10x air objective (Olympus, UPLSAP 10 X). Images were analyzed and quantified by Scan^R analysis software (Olympus Biosystems, Japan). Scan^R first identified cell nuclei by a fixed threshold segmentation based on the Hoechst 33342 nuclear staining. Each nuclear area was dilated by a distance of 20 pixels to generate the mask that encompasses a maximum area of cell without touching the neighboring cells. The mask served as the region of interest to quantify the CFP-specific and

PM-specific fluorescence. CFP-GL-GPI transport rate was calculated by taking the ratio of PM-specific fluorescence intensity (PM GPI) to CFP-specific fluorescence intensity (Total GPI)

2.3.6 Viral transduction

Retrovirus particles were used as the vector to stably integrate the reporter genes into the genome of target cells (HeLaMT cells). The procedure took 5 days and includes preparation of plasmids encoding the virus components and the reporter gene, production of retrovirus particles using HEK293T cells, harvesting the retrovirus particles and infection of target cells.

On day 1, 9 μg of the plasmids encoding the virus components and the reporter gene (pRevTRE2-CFP-GL-GPI, pVPack-GP and pVPack-Eco) were precipitated using 1 ml 100% (v/v) ethanol and 0.1 × volume 3M sodium acetate, pH 5.2. After incubation at -80°C for 30 minutes, the DNA pellet was collected by centrifugation (12000 ×g, 4°C, 10 minutes). The supernatant was discarded, and the DNA pellet was washed by adding 1 ml 70% (v/v) ethanol. After centrifugation (12000 ×g, 4°C, 10 minutes), the supernantant was carefully discarded and the wet DNA pellet was stored at 4°C overnight. HEK293T cells were seeded on 10-cm culture dish for the transfection on the next day. On day 2, HEK293T cells were transfected with plasmid using MBS Mammalian Transfection Kit (Stratagene, USA) in accordance with the manufacturer's manual. The transfected HEK293T cells were incubated at 37°C for 72 hours to produce retrovirus particles. On day 4, target cells (HeLaMT cells) were seeded on 10-cm culture dishes for the infection on the next day. On day 5, the medium containing retrovirus particles were harvested from the transfected HEK293T cells, and filtered. This medium was supplemented with 10 μg/ml DEAE-dextran and was then added to the culture dishes containing the target cells. After incubation at 37°C for 3 hours,

normal growth medium was added, and the cells were incubated for 3 days with retrovirus particles. The cells were incubated in the medium containing doxycycline and analyzed by FACS based on CFP fluorescence intensity.

2.4 Microscopy

2.4.1 Image acquisition and analysis of ts-O45-G transport assay

Immunofluorescence microscopy was performed on an inverted IX81 wide-field screening microscope (Olympus Biosystems, Japan). 20 or 36 images per well were taken using a 10x air objective (Olympus, UPLSAP 10 X). Images were analyzed and quantified by Scan^R analysis software (Olympus Biosystems, Japan). Scan^R first identified cell nuclei by a fixed threshold segmentation based on the Hoechst 33342 nuclear staining. Each nuclear area was dilated by a distance of 20 pixels to generate the mask that encompasses a maximum area of cell without touching the neighboring cells. The mask served as the region of interest to quantify the YFP-specific and ts-O45-G-specific fluorescence. ts-O45-G transport rate was calculated by taking the ratio of ts-O45-G-specific fluorescence intensity (PM VSVG) to YFP-specific fluorescence intensity (Total VSVG).

2.4.2 Speicmen preparation for confocal microscopy

Cells on coverslips were fixed in PBS containing 3% paraformaldehyde (Polysciences, Inc., USA) for 20 minutes at room temperature. After washed twice with PBS, the cells were permeablized by incubation in PBS containing 0.1% Triton X-100 at room temperature for 5 minutes. For immunostaining, the cells were incubated sequentially in primary antibody and secondary antibody solution (diluted in PBS). Nuclei were stained by Hoechst 33342. The

coverslips were then mounted in Mowiol 4-88 solution (Carl Roth, Karlsruhe, Germany) in accordance with the manufacturer's protocol.

2.4.3 Confocal microscopy

Confocal images were acquired on a Leica TCS SP5 DMI6000 inverted microscope using a 63x oil immersion objective (HCX PL APO lambda blue 63x, NA 1.4). Cells were optically sectioned into z-stacks, with the pinhole set to 1 Airy unit. 488 nm, 594 nm and 633 nm laser lines were used for the excitation of AlexaFluor488, mRFP1 and AlexaFluor647, respectively. Sequential acquisition was used to avoid bleed-through.

2.5 Biochemical methods

2.5.1 Western blot

SDS-polyacrylamide gel electrophoresis was performed according to the method of Laemmli (Laemmli, 1970). Cells were lysed in sample buffer (58 mM Tris-Cl, pH 6.8, 1.67% SDS, 5% glycerol, 0.02 mg/ml bromphenol blue, 92 mM DTT) containing protease inhibitor (Roche applied science, Germany). For immunoblotting analysis, proteins were separated on SDS-polyacrylamide gel and electroblotted onto PVDF membrane (Millipore) immersed in transfer buffer (48 mM Tris-Cl, 39 mM glycine, 0.02% SDS, methanol 15% (v/v), pH 8.3). 2.5% milk (Carl Roth, Karlsruhe, Germany) in PBST (PBS containing 0.1% Tween 20) were used for blocking and antibody dilution. Primary antibody and horseradish peroxidase (HRP) coupled secondary antibody were incubated with the membranes for 1 hour at room temperature or overnight at 4˚C. After incubation with antibody, membranes were washed 3 times with PBST. After immersing the membrane in

luminescent solution (GE Healthcare, Pittsburgh, PA, USA) the chemiluminescence of the immunoreactive bands can be detected by X-ray film exposure or ChemoCam imager (INTAS Science Imaging Instruments GmbH, Germany).

2.6 Data analysis

2.6.1 Statistical analysis

Dr. Bettina Knapp performed the statistical analysis. For the statistical data processing of the primary screen we used the software R (http://cran.r-project.org/) and the RNAither package from Bioconductor (http://www.bioconductor.org). First, the cells which have a measured total VSVG intensity in a predefined range as well as a PM intensity less than a predefined threshold were selected. The thresholds have been assessed based on manual inspection for each set (3 96-well plates) of the 3 replicates. For each well, we then summarized all the selected cells (measured in 20 positions per well) by taking the median of the ratio of the intensity PM VSVG and total VSVG. After a z-score transformation of the computed ratios of each plate we used additionally the B-score method to remove spatial effects within plates. The four replicate measurements have been summarized by the mean and hits have been identified using a threshold of +1.5/-1.5. Furthermore, a one-sided, one-sample Welch's t-test was used to compute significance values for each siRNA on the null-hypothesis of nonzero normalized ratios.

For the analysis of the validation experiments we did the same same preprocessing of the data as for the primary screen. Since the siRNAs have been selected for validation based on the hits of the primary screen, we cannot assume that most of siRNAs do not have an effect on VSVG trafficking and a normalization like z-score or B-score cannot be used. Therefore, we

normalized the median ratios computed for each well by subtracting the median of the negative controls and dividing by the standard deviation of the negative controls of the respective plate. Again a threshold of +1.5/-1.5 has been used for hit selection.

Two-tailed Student's t-Test was used to calculate the p-value of independent replicate experiments.

3 Results

3.1 Secretion of ts-O45-G

3.1.1 Targeted siRNA screens identify small GTPases that regulate the secretion of ts-O45-G

A high-content screening microscopy platform was developed to quantify ts-O45-G secretion (Starkuviene et al., 2008). We applied this platform to screen a library of ca. 200 siRNAs targeting 68 Rab GTPases and 25 Arf GTPases. 2 siRNAs were used to down-regulate each gene for 48 hours in primary screen. Solid-phase reverse transfection allows us to transfect HeLa cells with siRNAs simultaneously (Erfle et al., 2007). HeLa cells were infected with adenovirus for the expression of cargo protein ts-O45-G-YFP, and incubated at 39.5˚C to accumulate the cargo in the ER. Then the cells were incubated at 32˚C for 60 minutes. After that the cells were fixed and immunostained for ts-O45-G-YFP on the PM. Immunofluorescence analysis revealed the intense ts-O45-G-specific flourescence in control cells, indicating most of the cargo proteins were transported to the PM (Fig. 9). As a postitive control, we used siRNA targeting the component of COPI coat (α-COP), which regulates the protein transport through the Golgi complex (Beck et al., 2009; Pepperkok et al., 1993). In the cells transfected with α-COP siRNA, hardly any ts-O45-G-specific fluorescence can be observed, indicating defective transport of ts-O45-G (Fig. 9). Importantly, in the cells transfected with siRNAs targeting RAB3B, RAB6A and RAB11A, the PM-specific fluorescence is relatively dim, suggesting the transport of ts-O45-G to the PM was inhibited (Fig. 9). ts-O45-G transport rate was calculated by taking the ratio of PM-specific fluorescence intensity to YFP-specific fluorescence intensity, both fluorescence intensities were quantified by image analysis

software, Scan^R. The measurements of approximately 2400 cells for each siRNA from 3 replicate experiments were taken for statistical analysis. We normalized ts-O45-G transport rate based on the median of ratios of all wells on the 96-well plate and summarized the effect of siRNA as z-score. The z-scores of positive control and negative control calculated from three independent experiments are -6.67 and -0.16, respectively. siRNA was considered as a hit when the z-score was either smaller than -1.5 (inhibitory hit) or larger than 1.5 (facilitating hit). 7 siRNAs with the z-score smaller than -3.0 were regarded as strong inhibitors (targeting RAB2B, RAB6A, RAB15, ARF1, ARF3 and ARL5B). There are no siRNAs with the z-score larger than 3.0 to be considered as strong facilitators. Primary screen identified 14 Rabs and 7 Arfs as inhibitory hits and 12 Rabs as facilitating hits (Fig. 6, Sup. Table 1). Nearly all hit genes were obtained based on the effect of one of two siRNAs used in primary screen, except RAB6A and RAB11A, of which both two siRNAs showed effects. Both RAB6A siRNAs showed inhibitory effect on ts-O45-G transport. However, one of the RAB11A siRNAs showed inhibitory effect, and the other one showed facilitating effect on ts-O45-G transport. Five of the 32 hit genes (RAB6A, RAB11A, RAB18, RAB34, and RAB37) were also identified as effectors in a recent published screen (Simpson et al., 2012) (Fig. 7).

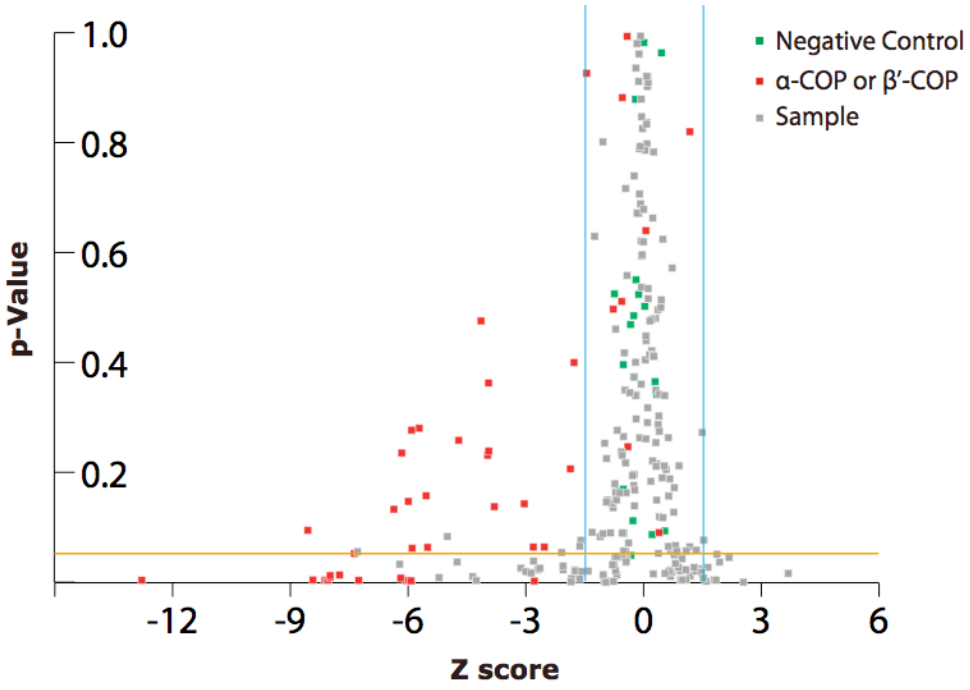

Figure 6 Result of VSVG primary screens

Result of ts-O45-G primary screens was shown. Z scores (normalized ratio) and p-values were calculated based on the data from 3 replicate experiments and the result of each siRNA is represented by a dot. Thresholds for hit classification are indicated in blue (z score > 1.5 or < 1.5) and orange (p-value < 0.05) lines.

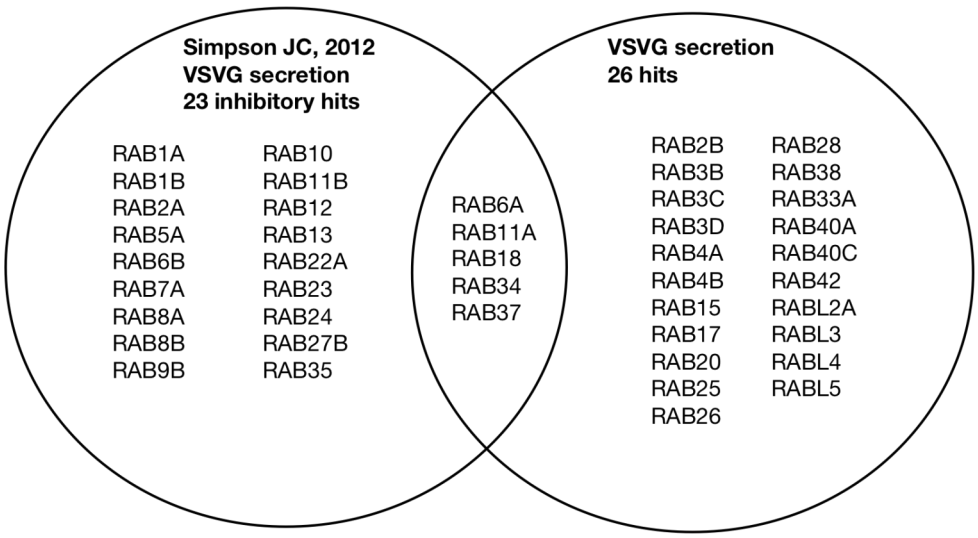

Figure 7 Comparison of the hits from our primary screen with the hits from a published screen (Simpson et al., 2012)

3.1.2 Confirmation of the expression of small GTPases in HeLa by RT-PCR

To eliminate potential false positive hits, we looked into the expression of the genes in HeLa cells. Various hit genes are clearly expressed in the HeLa cells according to published studies and expression profile database, BioGPS (http://biogps.org/) (Wu et al., 2009a). However, expression profiles of some small GTPases in the HeLa cells were not available. Therefore we sought to probe their expression by RT-PCR using gene-specific primer pairs (Sup. Table 2). We didn't detect the expression of RAB25, RAB37, and ARL13A in the HeLa cells by RT-PCR. The RT-PCR results are consistent with published studies of RAB25 and RAB37 (Amornphimoltham et al.; Wu et al., 2009b). The expression of these 3 genes in the HeLa cells might be either absent or too low to be detected. The phenotypes we observed might be caused by the off-target effects of the siRNAs. Therefore, these genes were excluded in subsequent experiments.

3.1.3 Validation experiments of VSVG screen

We went on to further confirm the RNAi-mediated effect in validation experiments using the hit siRNA from the primary screen and a third siRNA. In addition to the hit genes from the primary screen, we included some conventional regulators (RAB1A, RAB1B, and RAB7B) and a subset of randomly chosen genes (RAB4B, RAB7A, RAB8B and RAB22A) in validation experiments. In contrast to primary screens, direct transfection of siRNAs was performed in validation experiments. The effect of siRNA-mediated inhibition on ts-O45-G transport was summarized as z-score by normalization against negative control. The z-score for positive control and negative control are -12.7 and 0, respectively. siRNA was considered as a hit when the z-score was

either smaller than -1.5 (inhibitory hit) or larger than 1.5 (facilitating hit). 13 siRNAs with z-score smaller than -6.0 were regarded as strong inhibitors. All of the strong inhibitors in primary screen came up as strong inhibitors in validation experiments. Genes were considered as validated hits when both the hit siRNA and the third siRNA caused the change in ts-O45-G transport. 14 Rabs (including 6 inhibitory hits and 1 facilitating hit) and 4 Arfs (all as inhibitory hits) GTPases were identified as validated hits involved in the transport of ts-O45-G (Sup. Table 3). The effect of siRNA-mediated gene silencing RAB2B, RAB3D, RAB4A, RAB8B, RAB26, RAB40C, and RAB42 on ts-O45-G secretion remained to be confirmed, because the two siRNAs used in validation experiments showed opposite effects—one showed inhibitory effect, the other showed facilitating effect. RAB6A, ARF3, ARF4 and ARFRP1, the small GTPases that are known to be associated with the secretion of ts-O45-G (Miserey-Lenkei et al., 2010; Nishimoto-Morita et al., 2009), are identified in our screen. Furthermore, we identified 14 small GTPases as novel regulators of ts-O45-G secretion (Table 1).

14 of the 18 identified small GTPases are associated with exocytosis and anterograde transport (Hutagalung and Novick, 2011). With regard to the remaining 4 small GTPases, RAB38 is involved in TGN-to-melanosome transport and RAB40C, RAB42 and ARL5B have no characterized functions. The result is consistent with the fact that ts-O45-G is an anterograde marker and the assay is focused to examine the anterograde transport.

We looked into the phenotypes of the cells in the validation experiments. In RAB3B, RAB3C, RAB4B, RAB6A, ARF3, ARF4, and ARL5B siRNA transfected cells, we observed ts-O45-G accumulated in the perinuclear region and the PM-specific fluorescences were dim. In RAB11A siRNA transfected cells, ts-O45-G were distributed in the vesicular punctate structures in cytoplasm (Fig. 9). The phenotypes of these cells suggested that ts-O45-G left

the ER and moved forward to the Golgi. The inhibition of ts-O45-G transport may not be occurred at the level of ER exit.

Down-regulation of RAB1A, RAB1B, RAB18, RAB34, RAB7B or ARF1 is reported to inhibit ts-O45-G secretion (Dejgaard et al., 2008; Goldenberg et al., 2007; Haas et al., 2007; Progida et al., 2010; Tisdale et al., 1992; Volpicelli-Daley et al., 2005). They were not identified as hits in our screens. This could be explained partly by the functional redundancy of the Rab and Arf isoforms. For example, RAB1A and RAB1B were not identified as hits, as only one siRNA showed effect in the validation experiments. Since RAB1A and RAB1B are protein isoforms, RAB1B can presumably compensate the function of RAB1A in the RAB1A-depleted cells. If this is the case, combinatory double knockdown of RAB1A and RAB1B may show stronger effect on the inhibition of ts-O45-G secretion. We tested this hypothesis by examining the transport inhibition in the HeLa cells upon combinatory double knockdown of RAB1A and RAB1B. Indeed, the transport inhibition of combinatory double knockdown was stronger (score -12.19) than that of RAB1A or RAB1B single knockdown (score -1.93 and -2.35, respectively) (Sup. Fig. 1). It was reported that paired knockdown of ARF1 with ARF3 or ARF4 lead to defective ts-O45-G transport, whereas individual Arf knockdown didn't markedly affect the secretory membrane trafficking (Volpicelli-Daley et al., 2005). Another explanation might be the efficiency of RNAi. 48 hours of RNAi might not be sufficient to deplete the protein. Therefore, the phenotypes could be manifest when the cells were transfected with siRNAs for longer period.

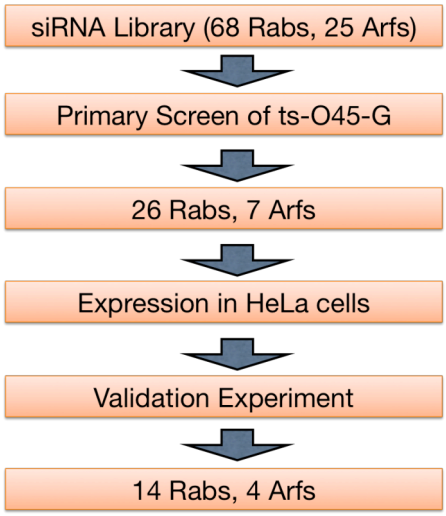

Figure 8 Overview of the VSVG RNAi screen

Gene	Localization	Function
RAB2B*	ER, ER-Golgi intermediate compartments, Golgi	ER to Golgi
RAB3B/3C/3D*	Secretory vesicles, PM	Exocytosis, neurotransmitter release
RAB4A/4B*	Early endosomes	Protein recycling/transport to PM
RAB6A	Golgi	Endosome to Golgi, intra-Golgi transport, Golgi to ER
RAB8B*	Cell membrane, vesicles	Exocytosis, TGN/RE to PM
RAB11A*	Golgi, RE, EE	TGN/RE to PM
RAB26*	Secretory granules	Exocytosis
RAB33A*	Golgi	Autophagosome formation
RAB38*	Melanosomes	TGN to melanosomes
RAB40C*	Golgi, RE	Endosome/intracellular transport
RAB42*	unknown	unknown
ARF3	Golgi, TGN	ER-Golgi traffic
ARF4	Golgi	ER-Golgi traffic
ARL5B*	Golgi	unknown
ARFRP1	TGN	Recruitment of ARL1 to the TGN

Table 1 Validated hits of VSVG screen

* Novel regulators of ts-O45-G secretion

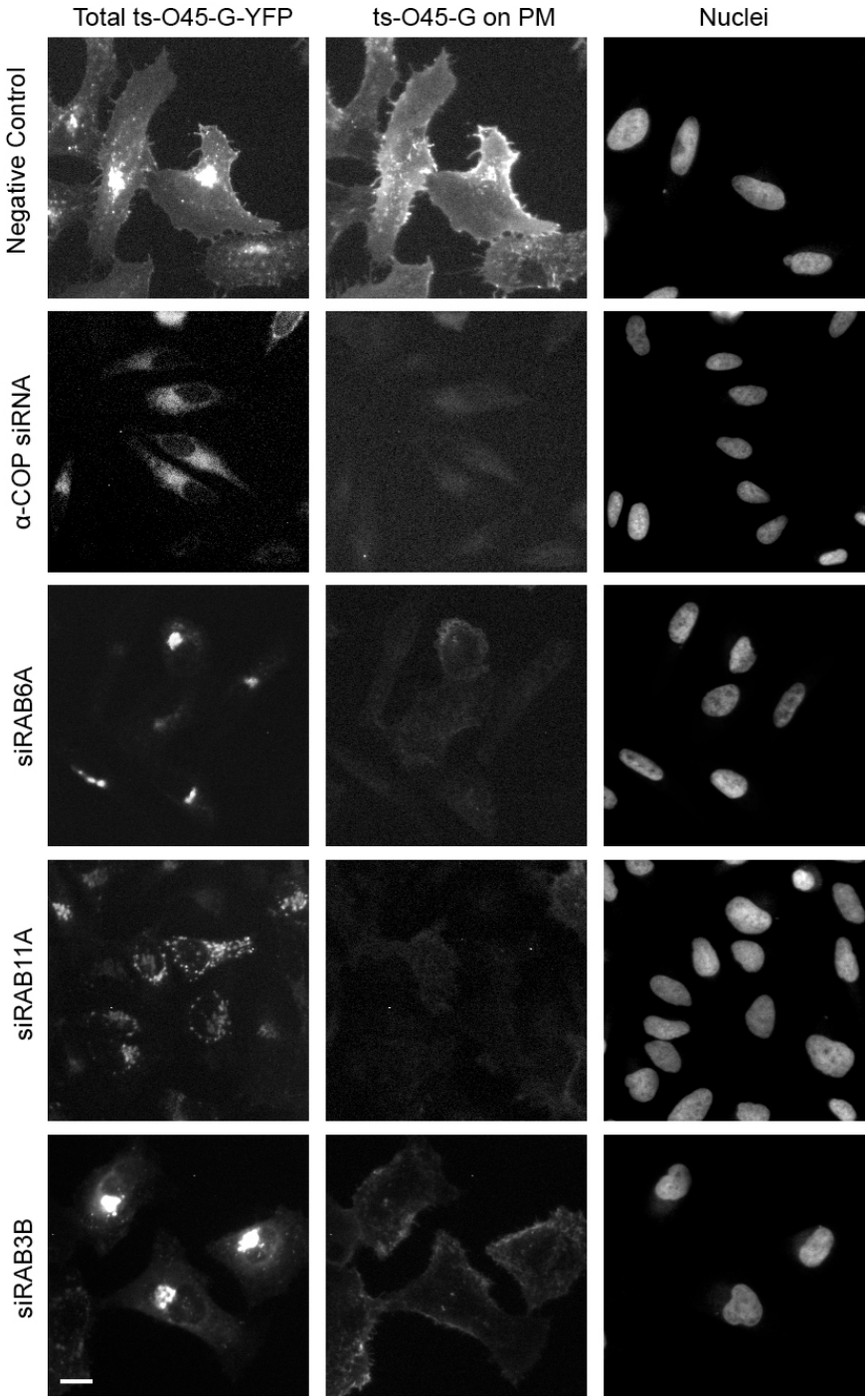

Figure 9 RNAi-mediated down-regulation of small GTPases inhibited ts-O45-G secretion

ts-O45-G transport assay was performed on the HeLa cells transfected with positive and negative control and siRNAs targeting various Rabs. After fixation, the cells were immunostained with anti-VSVG. Images were acquired by wide-field microscopy. ts-O45-G secretion is inhibited when RAB3B, RAB6A and RAB11A were depleted. Scale bar, 20 μm.

3.2 Characterization of a putative regulator of ts-O45-G secretion, RAB42

3.2.1 Specific down-regulation of RAB42 in the HeLa cells

RAB42 is one of the novel regulators of ts-O45-G secretion identified in our screen. It is an uncharaterized and interesting Rab GTPase. Bioinformatics study suggested that the existence of RAB42 retrogene, RAB42P1. The open reading frames of RAB42P1 and RAB42 share 97% sequence similarity. Transcript of RAB42P1 is expressed in HeLa cells (data from S. Roy). RAB42P1 might potentially function as a retrogene. We wonder the roles of RAB42 and RAB42P1 in ts-O45-G secretion. To investigate this question, we designed RAB42-specific and RAB42P1-specific siRNAs. Then we evaluated the efficiency of the RAB42 and RAB42P1 siRNAs in down-regulation of RAB42 and RAB42P1. We performed Western blot to quantify RAB42 protein level. Compared to the control cells, we observed an at least 75% reduction in RAB42 protein level in the cells transfected with either siRNA specifically targeting RAB42 (Fig. 10). On the contrary, there is no siginificant reduction in RAB42 protein level in the cells transfected with either siRNA specifically targeting RAB42P1. The Western blot result confirmed siRNA-specific down-regulation of RAB42 in HeLa cells.

A

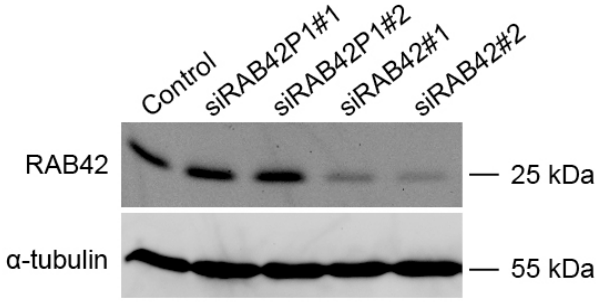

B

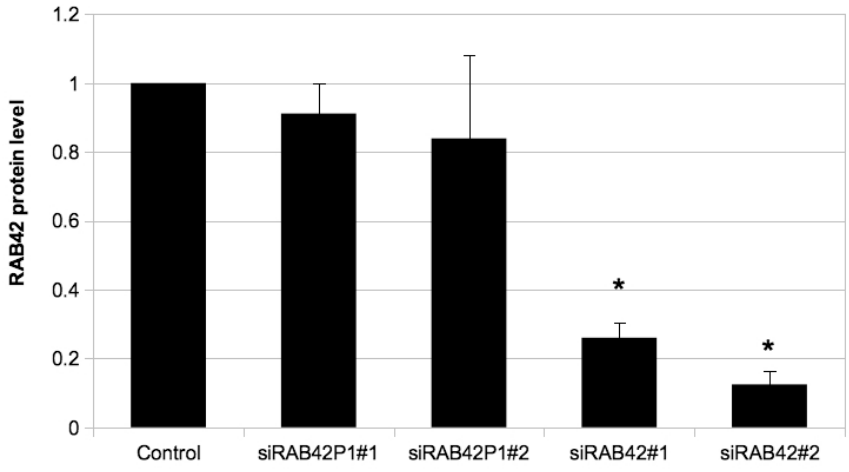

Figure 10 Specific down-regulation of RAB42 in the HeLa cells

HeLa cells were transfected with RAB42 siRNA for 72 hours. (A) Western blotting with RAB42 antibody confirmed the depletion of RAB42. Tubulin served as loading control and was used to quantify RAB42. (B) Quantification of RAB42 protein level. The error bars indicated the s.e.m. derived from 2 independent experiments. *, $p < 0.05$

3.2.2 ts-O45-G transport was inhibited in the RAB42-depleted HeLa cells

We went on to ask whether both RAB42 and RAB42P1 regulate ts-O45-G transport. To examine the function of RAB42 and RAB42P1 in regulating ts-O45-G transport, we performed ts-O45-G transport assay on the HeLa cells that were transfected with individual RAB42 and RAB42P1 siRNA, or a combination of both siRNAs for 72 hours. Inhibited ts-O45-G transport was observed in the RAB42 and RAB42P1 siRNA-transfected HeLa cells (Fig. 11A). We didn't observed significant enhancement of ts-O45-G transport inhibition in the cells transfected with both RAB42 and RAB42P1 siRNAs (Fig. 11A). The result suggested RAB42 and RAB42P1 could function in the same pathway that regulates ts-O45-G transport. Next, we want to determine whether inhibited ts-O45-G transport was due to down-regulation of RAB42 and not

due to off-target effect of RAB42 siRNA by performing rescue experiments. HeLa cells were transfected with RAB42 siRNA for 24 hours, followed by the transfection of plasmid encoding siRNA-resistent form of RAB42 (FLAG-tagged RAB42). Over-expression of FLAG-tagged RAB42 was confirmed by Western blot and immunofluorescence analysis. Two types of localizations of FLAG-tagged RAB42 can be observed in the HeLa cells: cytoplasm and the PM (90%) and the intracellular punctate structures (10%). The punctate structures did not co-localize with EEA1, mannose-6-phosphate receptor, and LAMP1 (data not shown). RNAi-mediated down-regulation of RAB42 caused 14% inhibition of ts-O45-G transport. Over-expression of FLAG-tagged RAB42 restores ts-O45-G transport (Fig. 11B). Our result indicated down-regulation of RAB42 inhibited ts-O45-G secretion.

Interestingly, we observed that the level of intracellular ts-O45-G-YFP was reduced in the siRAB42#1 transfected HeLa cells. The level of intracellular ts-O45-G-YFP was increased in siRNA42P1#2 transfected HeLa cells (Fig. 12).

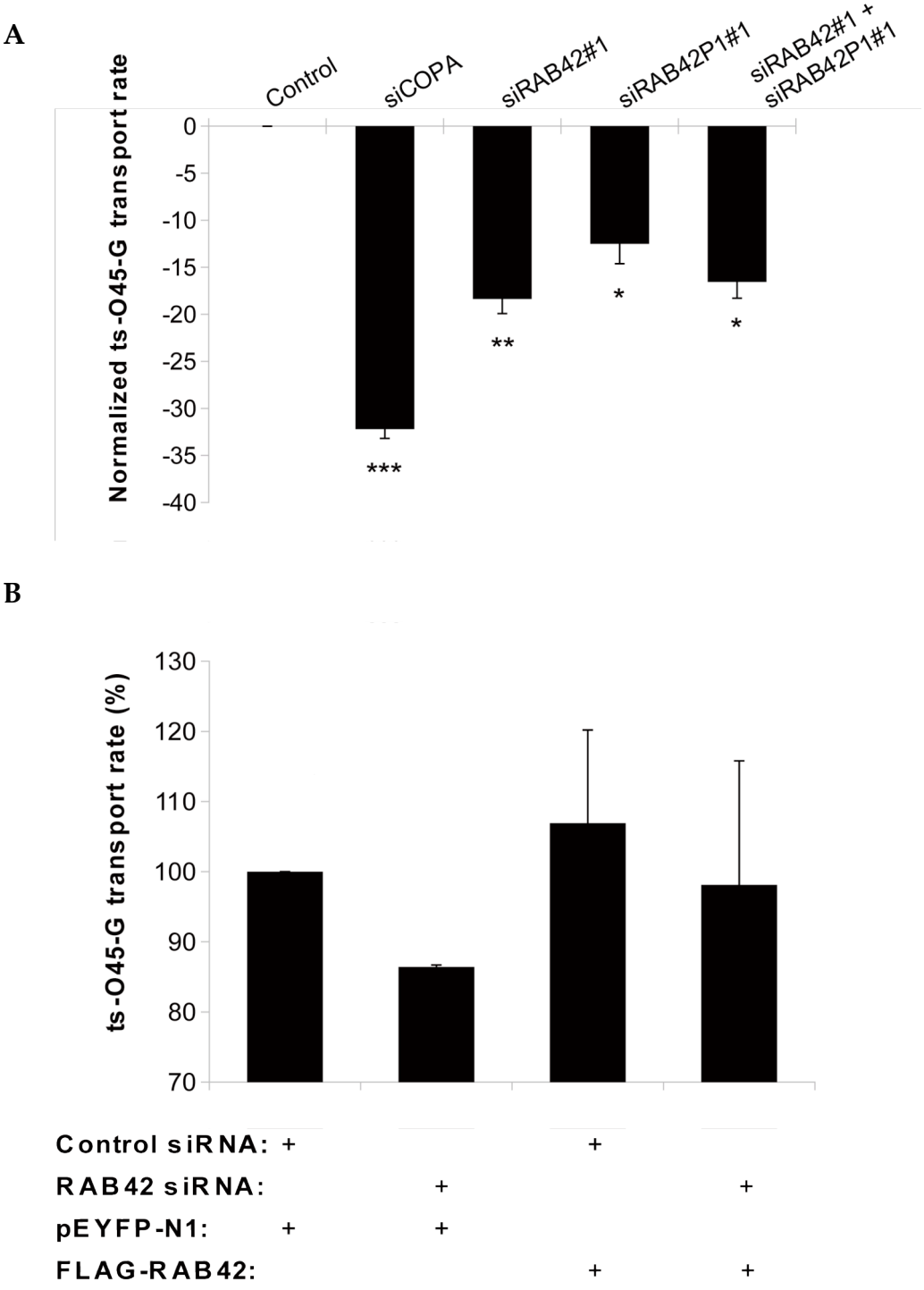

Figure 11 Down-regulation of RAB42 inhibited ts-O45-G secretion

(A) ts-O45-G transport assay was performed on the HeLa cells transfected with control and RAB42 siRNAs. Effect of siRNAs on ts-O45-G secretion are summarized. Bars represent the ts-O45-G transport rate, and the error bars indicate the s.e.m. derived from 2 independent experiments. *, $p < 0.05$; **, $p < 0.005$; ***, $p < 0.001$ (B) ts-O45-G transport assay was performed on the HeLa

cells sequentially transfected with siRNA and plasmid. Over-expression of a siRNA-resistent RAB42 rescued the RNAi-mediated inhibition of ts-O45-G secretion. The error bars indicate the s.e.m. derived from 2 independent experiments. *, significant at $p < 0.05$.

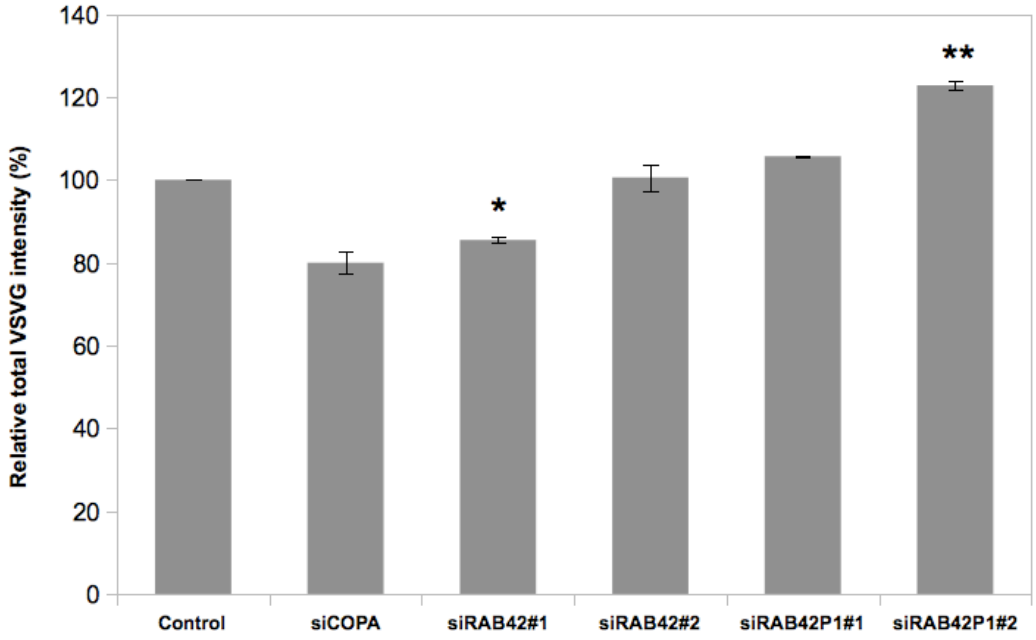

Figure 12 Down-regulation of RAB42 affected the level of intracellular ts-O45-G-YFP

ts-O45-G transport assay was performed on the HeLa cells transfected with control and RAB42 siRNAs for 72 hours. Effect of siRNAs on the intracellular ts-O45-G-YFP level are summarized. Bars represent the relative ts-O45-G-YFP intensity, and the error bars indicate the s.e.m. derived from 2 independent experiments. *, significant at $p < 0.05$; **, significant at $p < 0.005$

3.2.3 TGN-to-PM transport of ts-O45-G was inhibited in RAB42-depleted HeLa cells

After ts-O45-G leaves the ER, it travels through the Golgi complex, gets sorted into the post-Golgi carrier and eventually arrives at the PM. We want

to examine where the inhibition of ts-O45-G transport occurred in RAB42-depleted HeLa cells. We adapted ts-O45-G transport assay by including a 20˚C incubation regimen, so as to accumulate ts-O45-G at the TGN (Griffiths et al., 1985). The block of ts-O45-G at the TGN at 20˚C is reversible. ts-O45-G can leave the TGN and reach the PM once the temperature is shifted to 32˚C. With this assay we can investigate the post-Golgi transport of ts-O45-G. In the control cells, arrival of ts-O45-G at the PM was normal as indicated by the strong PM-specific fluorescence. In the RAB6A siRNA transfected cells, PM-specific fluorescence was much weaker, indicating the transport of ts-O45-G from the Golgi to the PM was perturbed (Fig. 13A). The result is consistent with the report that depletion of RAB6A and RAB6A' delayed the secretion of ts-O45-G (Grigoriev et al., 2007). In RAB42 siRNA transfected cells, PM-specific fluorescence was weak and ts-O45-G was distributed in perinuclear region and cytoplasmic punctate structures (Fig. 13A). We didn't observe siginificant inhibition of ts-O45-G transport in the cells transfected with RAB42P1 siRNA. Cosistent with the previous result, the inhibition of ts-O45-G transport was not enhanced in the cells transfected with both RAB42 and RAB42P1 siRNAs (Fig. 13B). The result indicated the down-regulation of RAB42P1 didn't inhibit ts-O45-G transport from the Golgi, whereas the down-regulation of RAB42 did.

A

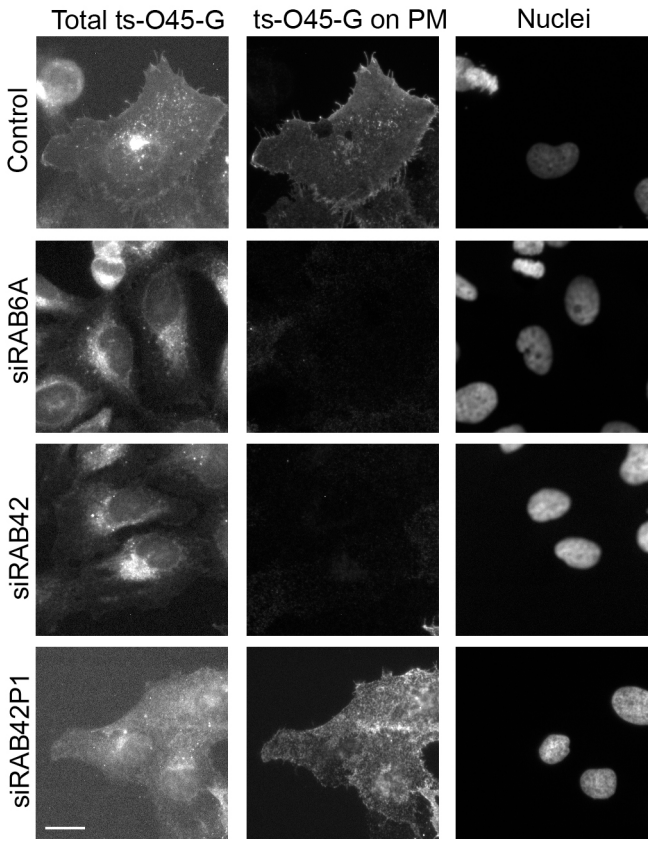

B

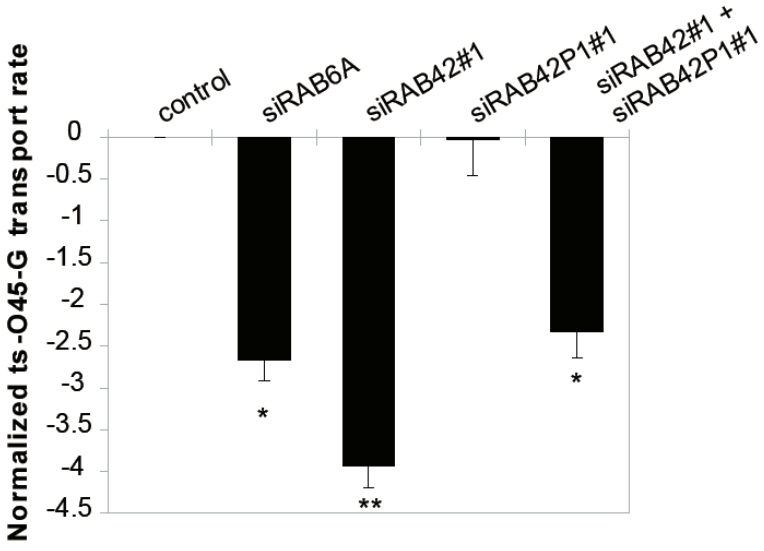

Figure 13 TGN-to-PM transport of ts-O45-G was inhibited in RAB42-depleted cells

(A) Post-TGN ts-O45-G transport assay was performed on the HeLa cells transfected with control, RAB42 and RAB42P1 siRNAs. After fixation, the

cells were immunostained with anti-VSVG. Images were acquired by wide-field microscopy. Scale bar, 20 μm (B) Effect of siRNAs on ts-O45-G secretion are summarized. Bars represent the ts-O45-G transport rate, and the error bars indicate the s.e.m. derived from 2 independent experiments. *, $p < 0.05$; **, $p < 0.005$

3.2.5 RAB42 is an unconventional Rab GTPase

RAB42 possesses all five consensus sequence motifs associated with GTP binding and hydrolysis (Bourne et al., 1991). However, RAB42 is unique in that the sequence of its G3 GTP-binding domain is WDTAGHE compared with the concensus WDTAGQE. This Gln-to-His substitution occurs in a position (histidine at position 73) that corresponds to the Gln_{61}-to-His mutation in H-*ras*, which is associated with potent transforming phenotype (Krengel et al., 1990). RAB42 is a conserved gene in primates. However, the conservation in histidine at position 73 varies in different species of primates. To investigate the function of G3 GTP-binding domain of RAB42, we generated His-to-Gln and His-to-Leu mutations in RAB42 (RAB42-H73Q, RAB42-H73L). His-to-Leu mutation is intended to render RAB42 constitutively GTP-bound, as WDTAGQE to WDTAGLE mutation is commonly used to generate constitutively active GTP-locked Rabs (Adari et al., 1988). ts-O45-G transport assay was performed on the HeLa cells transfected with FLAG-tagged RAB42, RAB42-H73Q, or RAB42-H73L. Preliminary result suggested over-expression of FLAG-tagged RAB42 and RAB42-H73Q didn't markedly inhibit the transport of ts-O45-G (Fig. 14).

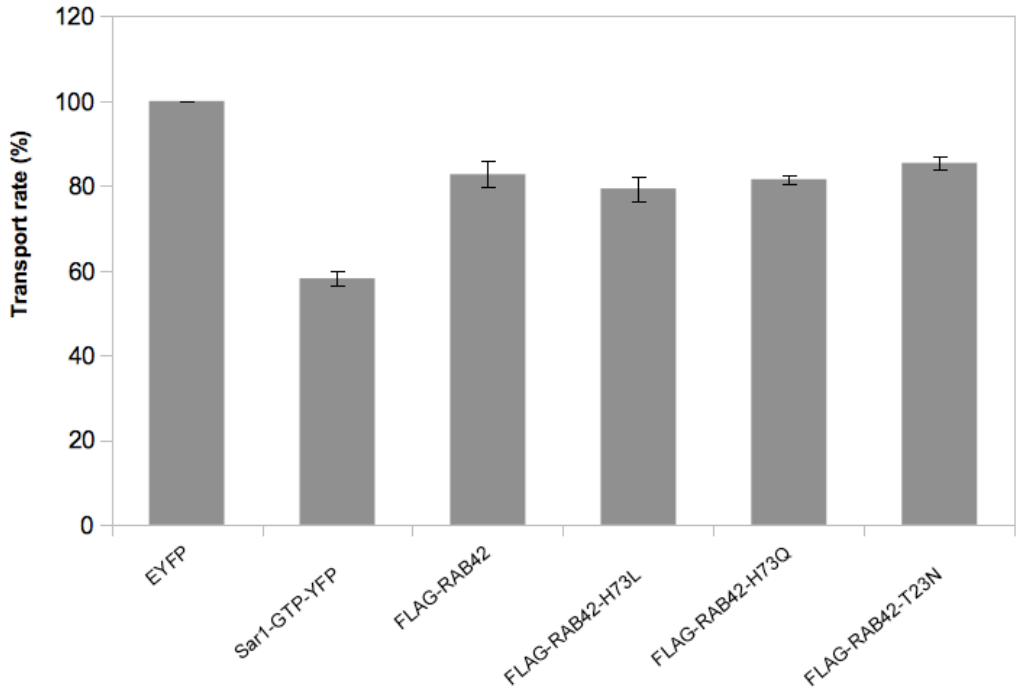

Figure 14 Over-expression of FLAG-tagged RAB42 and its mutants didn't markedly affect the transport of ts-O45-G

HeLa cells transfected with indicated plasmids. 24 hours following transfection, ts-O45-G transport assay was performed. The bars represent the relative transport rate compared to the control cells. The error bars indicate the s.e.m. from 3 replicates.

3.3 Characterization of a putative regulator of PC I secretion, Rab40c

Rab40c was identified as an inhibitory hit in the RNAi screen for procollagen secretion in NIH3T3 cells. Down-regulation of Rab40c inhibited the transport of PC I and ts-O45-G in the NIH3T3 cells. We went on to investigate where the transport inhibition of PC I and ts-O45-G-YFP occurs when Rab40c was down-regulated.

RAB40 is conserved in human, chimpanzee, mouse, rat, fruit fly and frog. In human cells there are three isoforms, RAB40A, RAB40B and RAB40C in RAB40 superfamily. RAB40C shares 88% and 91% protein sequence similarity with RAB40A and RAB40B, respectively. Two Rab40 isoforms, Rab40b and Rab40c, are expressed in mouse cells. Mouse Rab40c is closely related to human RAB40C (99% protein sequence similarity) and *Xenopus* Rab40 (96% protein sequence similarity). Rab40 might play an important role in biology, as it is highly conserved among phylogenetically distant species.

3.3.1 RNAi-mediated down-regulation of Rab40c

We sought to evaluate the efficiency of the siRNAs targeting Rab40c in down-regulation of Rab40c. qRT-PCR was performed to determine Rab40c mRNA level following 48 hours of RNAi. The result suggested a 60% reduction on Rab40c mRNAs in the NIH3T3 cells transfected with Rab40c siRNA (data not shown). We performed Western blot to quantify Rab40c protein level. Compared to the control cells, we observed a 30% reduction in Rab40c protein level in the cells transfected with the siRNAs targeting Rab40c (Sup. Fig. 2). The results confirmed siRNAs can mediate specific down-regulation of Rab40c in NHI3T3 cells.

3.3.2 PC I and ts-O45-G-YFP was blocked in the early secretory pathway when Rab40c is down-regulated in NIH3T3 cells

Secretion of PC I was inhibited in Rab40c-depleted NIH3T3 cells. To unravel the underlying mechanism, we investigate at which level the inhibition of PC I transport occurs. We performed PC I transport assay and examined the localization of PC I in the control and Rab40c-depleted NIH3T3 cells. In the control cells intracellular PC I-specific fluorescence is relatively dim, indicating PC I was secreted (Fig. 15). However, in the Rab40c-depleted cells a major fraction of PC I was retained in the intracellular structures colocalized with the ER markers, Hsp47 and over-expressed mRFP1-KDEL (Altan-Bonnet et al., 2006; Saga et al., 1987) (Fig. 15). The immunofluorescence analysis indicated down-regulation of Rab40c arrested PC I in the ER. Secretion of ts-O45-G-YFP was also examined in the control and Rab40c-depleted NIH3T3 cells. In the control cells, we observed a marked PM-specific fluorescence, indicating ts-O45-G was transported to the PM. Nevertheless, in Rab40c-depleted cells PM-specific fluorescence is markedly reduced and ts-O45-G-YFP was predominantly retained in the intracellular structures colocalized with the Golgi marker, GM130 (Nakamura et al., 1995) (Fig. 16). The data indicated down-regulation of Rab40c affected the transport of ts-O45-G-YFP from the Golgi apparatus. Taken together, our result indicated transport of PC I and ts-O45-G is blocked in the early secretory pathway when Rab40c is down-regulated in NIH3T3 cells.

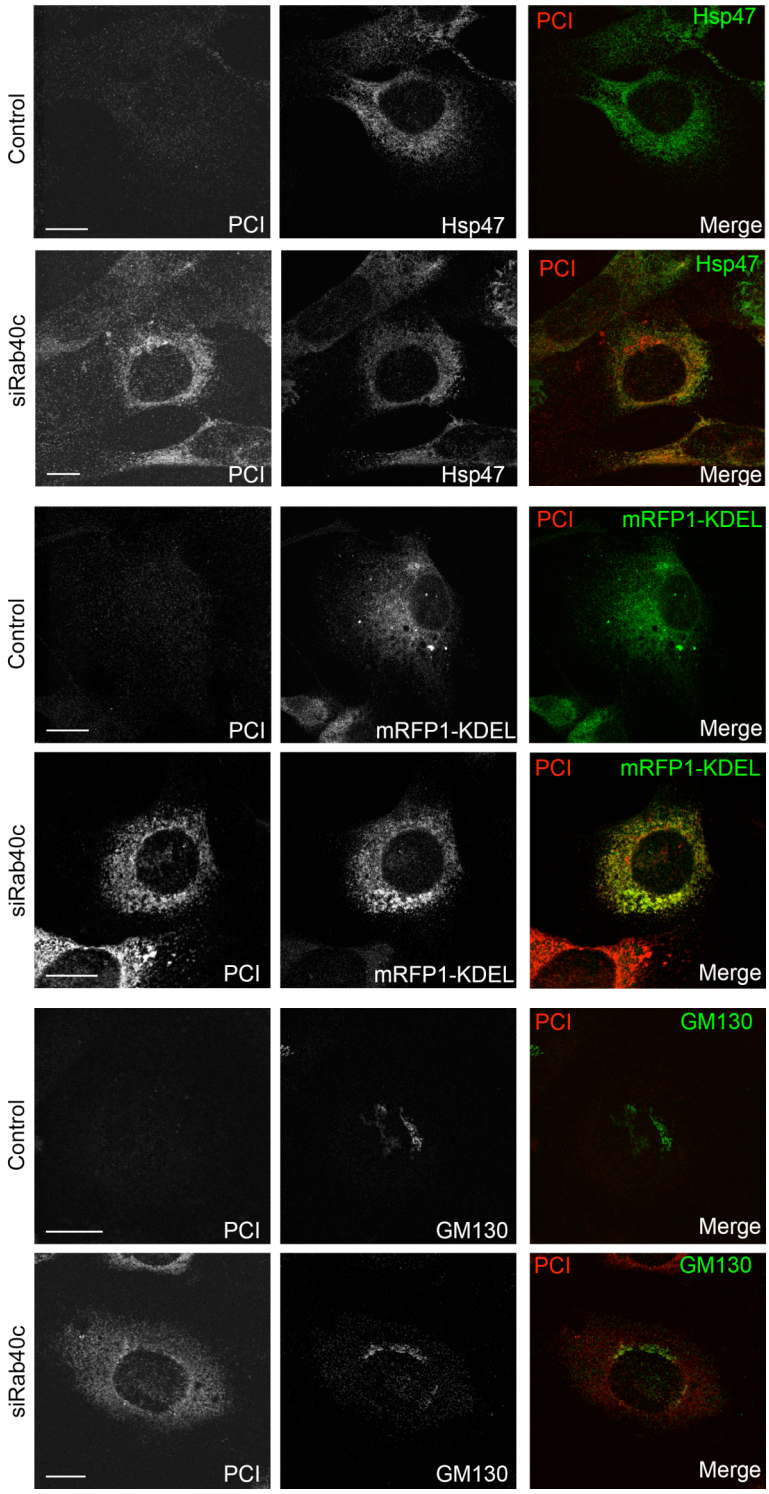

Figure 15 Down-regulation of Rab40c blocks the PC I secretion in the early secretory pathway

NIH3T3 cells were transfected with siRNA targeting Rab40c and negative control. Following 48 hours of incubation, PC I transport assay were performed. PC I colocalized with endogenous Hsp47, GM130 or over-

expressed mRFP1-KDEL. Images were acquired by confocal microscopy. Scale bars, 20 μm.

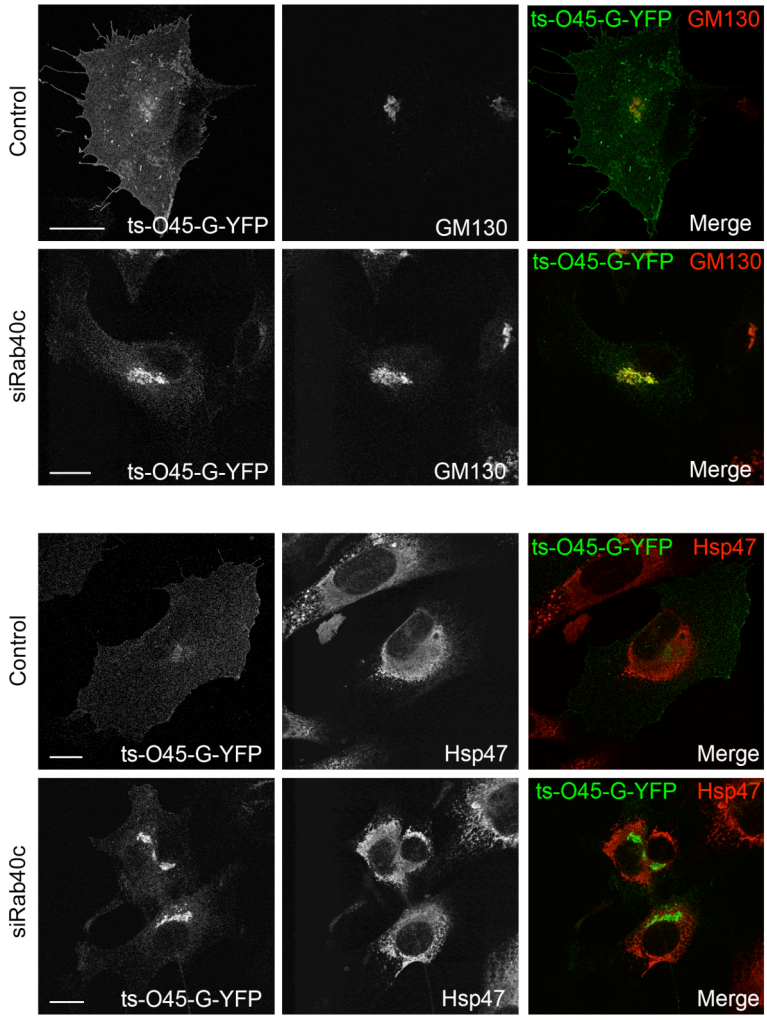

Figure 16 Down-regulation of Rab40c blocks the ts-O45-G secretion in the early secretory pathway

NIH3T3 cells were transfected with siRNA targeting Rab40c and negative control. Following 48 hours of incubation, ts-O45-G transport assay were performed. A major fraction of ts-O45-G-YFP co-localized with GM130. Images were acquired by confocal microscopy. Scale bars, 20 μm.

3.3.3 FLAG-Rab40c localized at the Golgi apparatus in NIH3T3 cells

EGFP-tagged *Xenopus* Rab40 was reported to localize at the Golgi apparatus (Allen and Seed, 1989; Lee et al., 2007). N-terminally EYFP-tagged rat Rab40c was reported to localize in perinuclear vesicular and tubulovesicular structures in HeLa cells (Rodriguez-Gabin et al., 2004). A recent study demonstrated Rab40c localized to lipid droplets (Tan et al., 2013). Since the reported localizations of Rab40c varied and the localization of Rab40c in NIH3T3 cells is unknown, we set out to investigate the localization of Rab40c in NIH3T3 cells.

Commerically available antibody against Rab40c cannot be used in immunofluorescence analysis. Therefore we use FLAG-tagged Rab40c (FLAG-Rab40c) for localization study. HeLa and NIH3T3 cells were transfected with FLAG-Rab40c and immunostained. Consistent with the previous report (Rodriguez-Gabin et al., 2004), FLAG-Rab40c is found to localize to perinuclear tubulovesicular structures and cytoplasmic vesicles in HeLa cells (Sup. Fig. 3). Interestingly, in NIH3T3 cells FLAG-Rab40c mainly localized to perinuclear tubulovesicular structures (Sup. Fig. 3). Localizations of FLAG-Rab40c in HeLa and NIH3T3 cells are different. Our data suggested cell type-specific localization of Rab40c.

We went on to determine the perinuclear tubulovesicular localization of FLAG-Rab40c. Localization of FLAG-Rab40c was compared with various organelle markers, including GM130 and over-expressed EGFP-tagged Rabs. EGFP-RAB1A served as *cis*-Golgi marker, EGFP-RAB6B and EGFP-RAB13 as *trans*-Golgi marker, and EGFP-RAB9A as late endosome marker (Goud et al., 1990; Lombardi et al., 1993; Plutner et al., 1991; Rodriguez-Gabin et al., 2001; Zahraoui et al., 1994). FLAG-Rab40c co-localized significantly with GM130 and over-expressed EGFP-RAB1A, EGFP-RAB6B and EGFP-RAB13, but not with EGFP-RAB9A (Fig. 17). Our result suggested FLAG-Rab40c localized to the Golgi complex in the NIH3T3 cells.

Rab40c is an interesting Rab GTPase in that it contains a GTPase domain and a SOCS (suppressors of cytokine signaling) box domain. It was reported that SOCS box domain is crucial for the localization and function of *Xenopus* Rab40 (Lee et al., 2007). To dissect the determinant for the localization of mouse Rab40c, we generated mutant constructs with deletion of the SOCS-box domain (ΔSOCS; 187-229 aa) or the GTPase domain (ΔRab; 1-177 aa). FLAG-ΔSOCS localizes to the PM and cytoplasm, and FLAG-ΔRab localizes at the Golgi apparatus (Fig. 18). Our result indicated SOCS-box domain is essential for the localization of Rab40c at the Golgi apparatus.

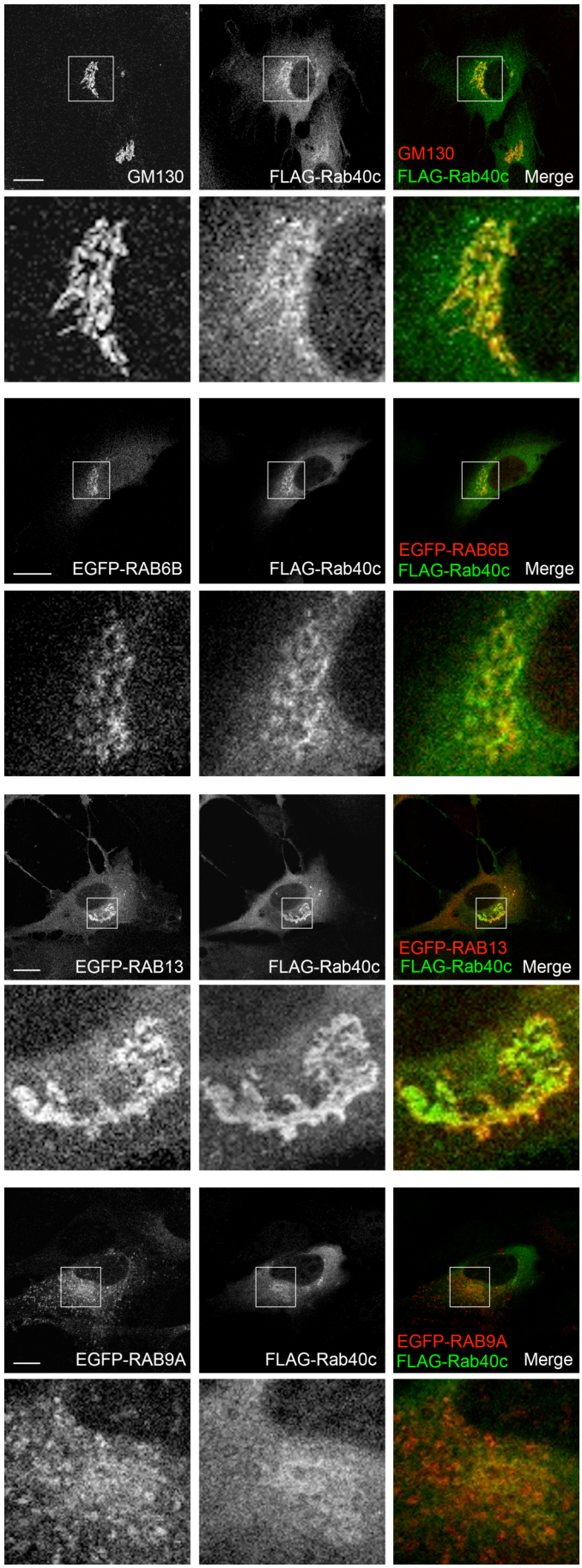
GM130
FLAG-Rab40c
GM130
FLAG-Rab40c
Merge
EGFP-RAB6B
FLAG-Rab40c
EGFP-RAB6B
FLAG-Rab40c
Merge
EGFP-RAB13
FLAG-Rab40c
EGFP-RAB13
FLAG-Rab40c
Merge
EGFP-RAB9A
FLAG-Rab40c
EGFP-RAB9A
FLAG-Rab40c
Merge

Figure 17 FLAG-Rab40c localizes to the Golgi apparatus in NIH3T3 cells

NIH3T3 cells were transfected with plasmid encoding FLAG-tagged Rab40c. Images were acquired by confocal microscopy. Co-localization of FLAG-Rab40c with GM130 and various EGFP-tagged Rabs were analysed. Scale bars, 20 μm.

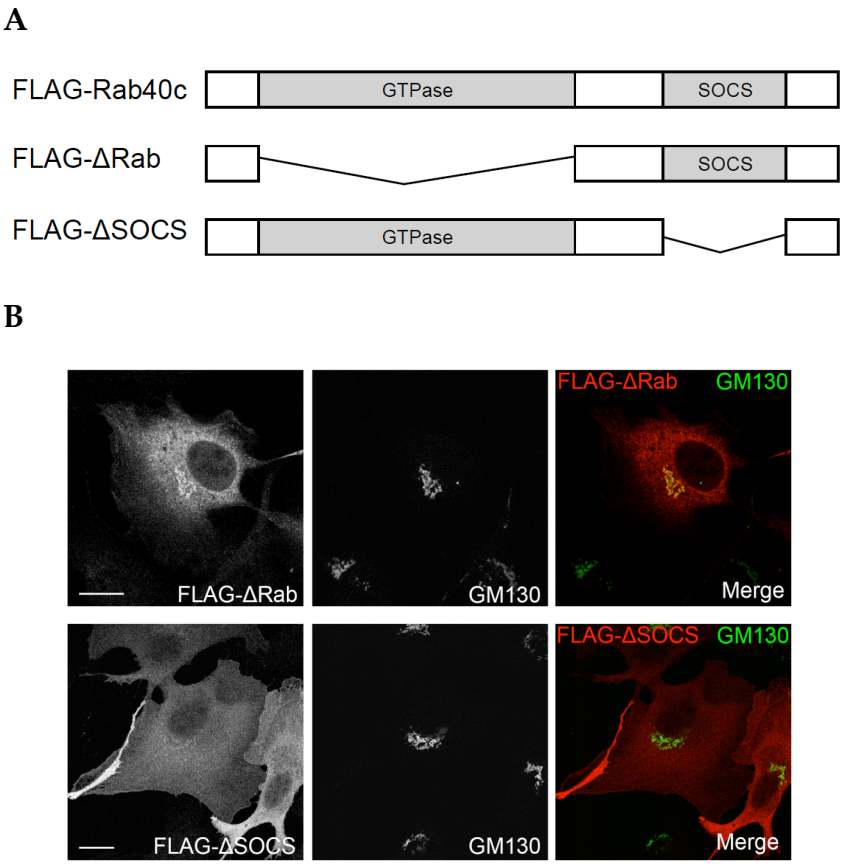

Figure 18 SOCS-box domain is crucial for the localization of Rab40c at the Golgi apparatus

(A) Schematical diagram of Rab40c deletion mutants (B) Localization of FLAG-tagged Rab40c deletion mutants in NIH3T3 cells. (Scale bars: 20 μm)

3.4 Secretion of GPI-anchored proteins

3.4.1 CFP-GL-GPI transport assay

We want to identify the role of Arf and Rab GTPases in the secretion of GPI-anchored proteins (GPI-APs) by applying microscopy-based RNAi screen. Therefore, we set out to develop a GPI-anchored protein transport assay, with which we can monitor the arrival of GPI-anchored proteins at the PM after their biosynthesis. We took CFP-GL-GPI as the GPI-anchored protein cargo (Keller et al., 2001), and performed a time-course analysis on the transport of CFP-GL-GPI to the PM. HeLa cells were infected with adenovirus for the expression of CFP-GL-GPI. 4 hours after the infection, the HeLa cells were incubated in the presence of cycloheximide to start the chase. The cells were fixed at various time points and immunostained with anti-GFP antibody to label the CFP-GL-GPI on the PM. Image acquisition was performed by an automated fluorescence microscope. Image analysis program measures the intensities of total CFP-GL-GPI fluorescence (total GPI) and PM-specific fluorescence (PM GPI). The ratio of total GPI and PM GPI was taken as the parameter to quantify the arrival of CFP-GL-GPI at the PM. We observed a gradually increase in PM GPI along the chase and it reaches the plateu between 70 and 80 minutes (Fig. 19). At 60 minutes most cargo proteins were transported to the PM and the transport process did not reach the plateau (Fig. 19). Therefore, 60 minutes was chosen as the time point to terminate the chase in CFP-GL-GPI transport assay. With this transport assay we should be able to identify the phenotypes in which CFP-GL-GPI transport is inhibited and facilitated.

Then, we included siRNAs in the experiment to test whether the transport assay can be applied in RNAi screen. Transport assay was performed on the HeLa cell that have been transfected with siRNA for 43

hours. For the positive control, we choose the siRNAs targeting COPI coat complex, α-COP and β'-COP. COPI coatomer is known to be involved in the retrograde transport from the Golgi to the ER. When the function of COPI coatomer is perturbed, some specific factors that are required for the anterograde transport of GPI-APs might not be retrieved from the Golgi to the ER. This hypothesis is supported by the report that the transport of GPI-APs is strongly inhibited in yeast mutants with defective α-COP (Sutterlin et al., 1997). In the cells transfected with negative control siRNA, PM-specific fluorescence is strong, indicating the cargo proteins are transported to the PM (Fig. 20). In the cells transfected with the β'-COP siRNA, the PM-specific fluorescence is relatively weak, indicating the defective transport of CFP-GL-GPI to the PM (Fig. 20). The assay allows us to evaluate the transport of CFP-GL-GPI and can be applied in RNAi screens.

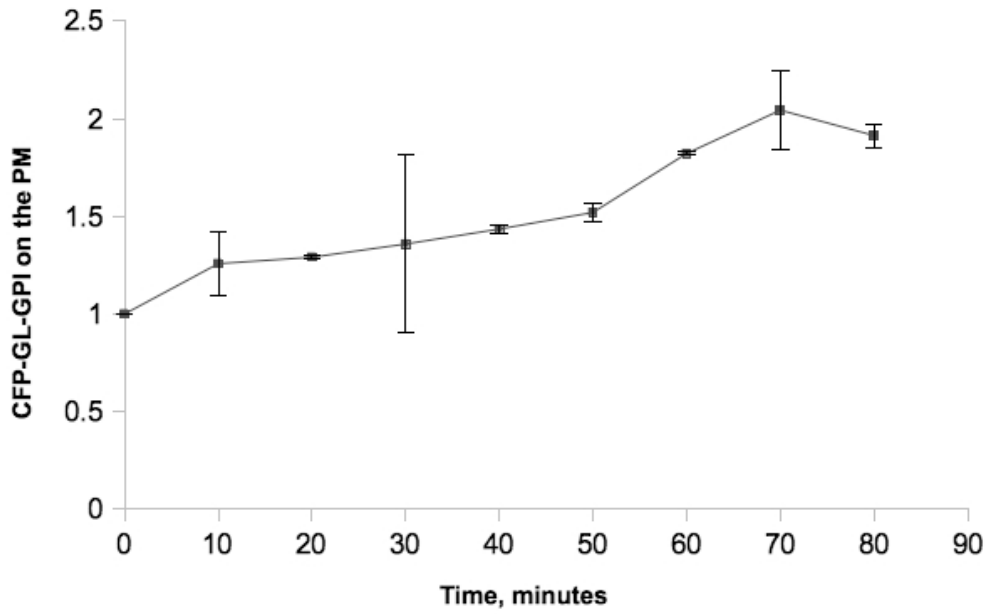

Figure 19 Time course analysis of CFP-GL-GPI transport

HeLa cells were infected with adenovirus for the expression of CFP-GL-GPI. 4 hours after the infection, the HeLa cells were incubated in the presence of cycloheximide to start the chase. The cells were fixed at the indicated time

points and immunostained with anti-GFP antibody to label the CFP-GL-GPI on the PM. Image acquisition was performed by an automated fluorescence microscope. The y-axis represents the amount of CFP-GL-GPI arrived on the PM, which is determined by the PM-specific fluorescence intensity. The error bars indicate the s.e.m. derived from 2 replicates.

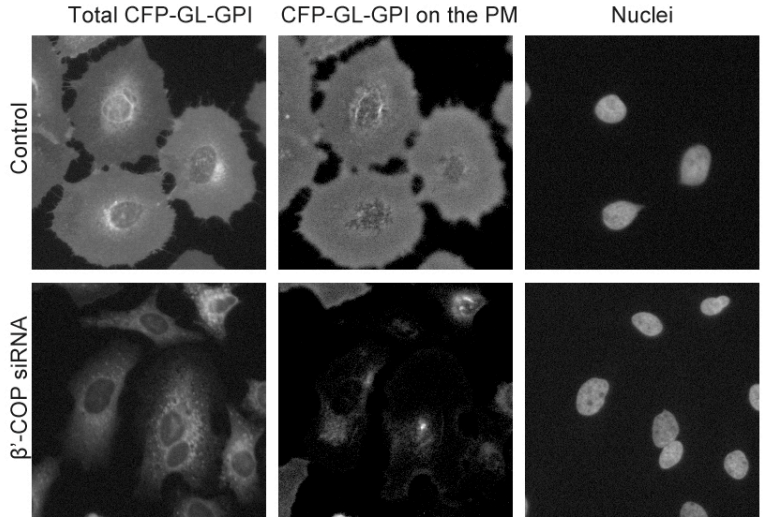

Figure 20 Images of CFP-GL-GPI transport assay

43 hours after the transfection of the indicated siRNAs, HeLa cells were infected with adenovirus for the expression of CFP-GL-GPI. 4 hours after the infection, the HeLa cells were incubated in the presence of cycloheximide to start the chase. The cells were fixed at 60 minutes after the chase and immunostained with anti-GFP antibody to label the CFP-GL-GPI on the PM. In the β'-COP siRNA-transfected cells, the PM-specific fluorescence is relatively weak compared to the cells transfected with control siRNA.

3.4.2 Targeted siRNA screens identify small GTPases that regulate the secretion of GPI-anchored protein

We went on to apply this assay to screen a library of ca. 200 siRNAs targeting 68 Rab GTPases and 25 Arf GTPases. 2 siRNAs were used to down-regulate each gene for 48 hours in primary screen. Solid-phase reverse transfection allows us to transfect HeLa cells with siRNAs simultaneously

(Erfle et al., 2007). The measurements of approximately 3200 cells for each siRNA from 4 replicate experiments were taken for statistical analysis. We normalized GPI-AP transport rate based on the median of ratios of all wells on the 96-well plate and summarized the effect of siRNA as z-score. The z-scores of positive control and negative control calculated from 4 independent experiments are -3.67 and -0.19, respectively. siRNA was considered as a hit when the z-score was either smaller than -1.5 (inhibitory hit) or larger than 1.5 (facilitating hit). 5 siRNAs with z-score smaller than -1.8 were regarded as strong inhibitors. Primary screen identified 5 Rabs and 3 Arfs as inhibitory hits, 6 Rabs and 1 Arf as facilitating hits (Fig. 21 and Sup. Table 4). All hit genes were obtained based on the effect of one of two siRNAs used in primary screen.

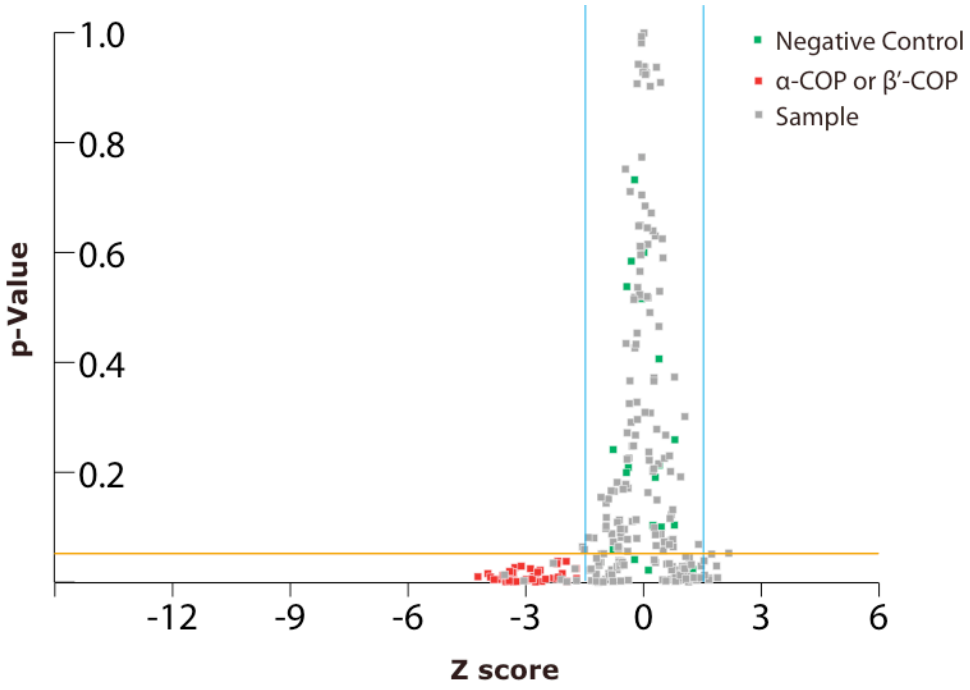

Figure 21 Result of GPI-AP primary screens

Result of GPI-anchored protein primary screens was shown. Z scores (normalized ratio) and p-values were calculated based on the data from 4 replicate experiments and the result of each siRNA is represented by a dot.

Thresholds for hit classification are indicated in blue (z score > 1.5 or < 1.5) and orange (p-value < 0.05) lines.

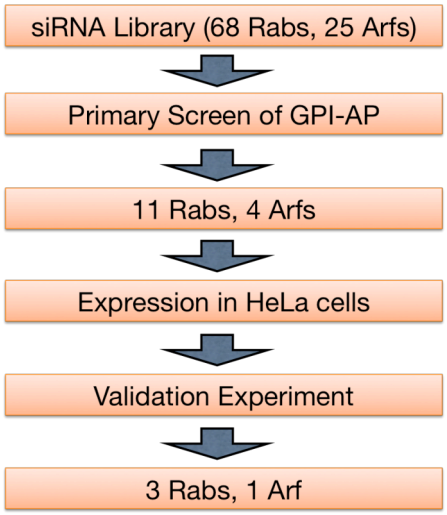

Figure 22 Overview of GPI-AP RNAi screens

3.4.3 Confirmation of the expression of small GTPases in HeLa by RT-PCR

To eliminate potential false positive hits, we looked into the expression of the genes in HeLa cells. Various hit genes are clearly expressed in the HeLa cells according to published studies and expression profile database, BioGPS (http://biogps.org/) (Wu et al., 2009a). However, expression profiles of some small GTPases in the HeLa cells were not available. Therefore we sought to probe their expression by RT-PCR using gene-specific primer pairs (Sup. Table 2). We didn't detect the expression of RAB39B in the HeLa cells by RT-PCR. The expression of this gene in the HeLa cells might be either absent or too low to be detected. The phenotypes of RNAi might be caused by the off-target effects of the siRNAs. Therefore, this gene was excluded in subsequent experiments.

3.4.4 Validation experiments of GPI-AP screen

We went on to further confirm the RNAi-mediated effect in validation experiments using the hit siRNA from the primary screen and a third siRNA. In contrast to primary screens, direct transfection of siRNAs was performed in validation experiments. The effect of siRNA-mediated inhibition on CFP-GL-GPI transport was summarized as z-score by normalization against negative control. The z-score for positive control and negative control are -5.6 and 0, respectively (Sup. Tab. 5). siRNA was considered as a hit when the z-score was either smaller than -1.0 (inhibitory hit) or larger than 1.0 (facilitating hit). 3 siRNAs with z-score smaller than -2.8 were regarded as strong inhibitors. 3 out of 5 strong inhibitors in primary screen came up as strong inhibitors in validation experiments. Genes were considered as validated hits when both the hit siRNA and the third siRNA caused the change in CFP-GL-GPI transport. RAB3D, RAB6A, RAB26 and ARF3 were identified as validated hits involved in the transport of CFP-GL-GPI (Sup. Table 5).

We examined the phenotypes of the cells in the validation experiments. In the α-COP siRNA transfected cell, we observed CFP-GL-GPI was blocked in the ER-like structure, suggesting the ER exit of CFP-GL-GPI in α-COP-depleted cells is defective (Fig. 23). By contrast, in the RAB6A and ARF3 siRNA transfected cells, we observed CFP-GL-GPI accumulated in the perinuclear region, probably the Golgi complex, and the PM-specific fluorescence is weak (Fig. 23). The phenotypes of these cells suggested that CFP-GL-GPI was able to leave the ER and proceed forward to the Golgi complex. The inhibition of CFP-GL-GPI secretion may not be occurred at the level of ER exit.

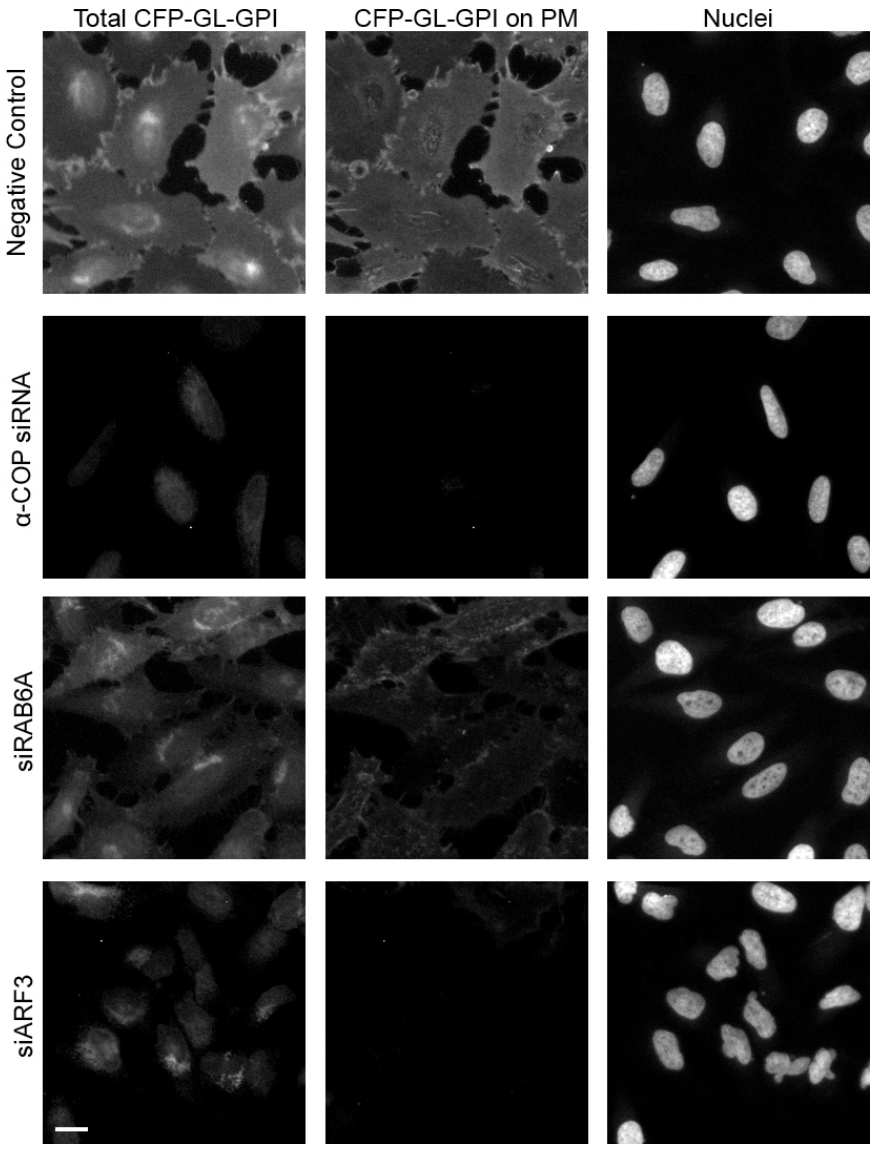

Figure 23 RNAi-mediated down-regulation of small GTPases inhibited CFP-GL-GPI secretion

CFP-GL-GPI transport assay was performed on the HeLa cells transfected with positive and negative control and siRNAs targeting various small GTPases. After fixation, the cells were immunostained with anti-GFP. Images were acquired by wide-field microscopy. CFP-GL-GPI secretion is inhibited when RAB6A and ARF3 were depleted. Scale bar, 20 μm.

3.4.5 Generation of stable cell-line that inducibly expresses the GPI-anchored reporter protein, CFP-GL-GPI

Since the reporter protein, CFP-GL-GPI, is not an endogenous protein in HeLa cells, we had to infect HeLa cells with adenovirus encoding CFP-GL-GPI for its expression. Infection with adenovirus can be avoided if we perform the assay with a stable cell-line that can inducibly express CFP-GL-GPI. With the aim to improve our assay, we set out to generate the stable cell-line.

The following steps were performed to generate stable cell-lines. HeLa cells were rendered susceptible to ecotropic retrovirus infection by transfection of the vector pcDNA3-zeo-mCAT1, which encodes the receptor for the envelope proteins of murine leukemia virus (Albritton et al., 1989; Davey et al., 1997). Cells were infected with an ecotropic retrovirus encoding a bicistronic construct containing doxycycline-sensitive transactivator rtTA2-M2 (Urlinger et al., 2000) and a truncated version of CD2 (Liu et al., 2000), which served as a cell surface marker. A pool of CD2-positive cells was isolated by FACS, and referred to hereafter as HeLaMT cells. We infected HeLaMT cells (kindly provided by Prof. Dr. Walter Nickel) with the ecotropic retrovirus encoding CFP-GL-GPI and doxycycline transactivator-dependent promoter. Three FAC sortings were performed to isolate the cells that can inducibly express CFP-GL-GPI (performed by Dr. Monika Langlotz at ZMBH Central Service Facility). The cells that constitutively express CFP-GL-GPI were excluded in the second FAC sorting, where the cells were incubated in the absence of doxycycline and CFP-negative cells were isolated. In the third FAC sorting, each of 96 isolated cells was collected as a single cell in 96-well plate, and some of them were propagated to obtain homogeneous stable cell-lines.

To test whether the stable cell-line can express CFP-GL-GPI inducibly, we added doxycycline in the culture medium. After the induction by doxycycline, cells were fixed and immunostained. CFP-GL-GPI on the PM were detected with anti-GFP antibody. Wide-field fluorescence microscopy

was used to image the cells. CFP-GL-GPI on the PM was only detected after the cells were treated with doxycycline (Fig. 24). The result revealed that the stable cell-line can express CFP-GL-GPI in a doxycycline-dependent manner.

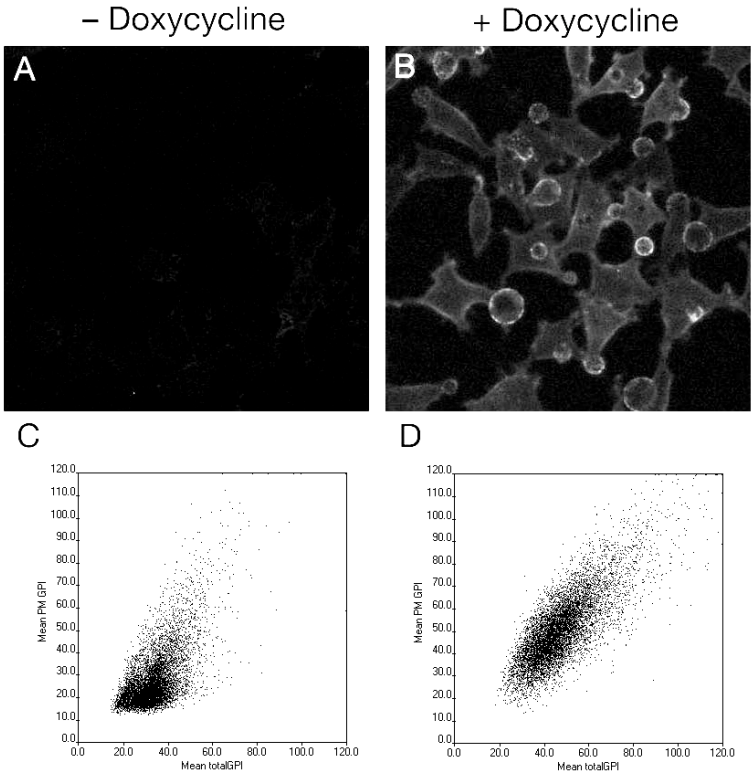

Figure 24 Inducible expression of CFP-GL-GPI in stable cell-line.

Panels A and B represent fluorescence microscopy analysis. Panels C and D are the results of image analysis. Cells were incubated in the absence of doxycycline (A, C); cells were incubated in the presence of doxycycline (B, D). CFP-GL-GPI on the PM were labelled with anti-GFP primary antibody and Cy5-conjugated secondary antibody.

3.4.6 Generation of temperature-sensitive GPI-anchored protein

Synchronization is an important step in ts-O45-G transport assay. Unlike ts-O45-G, GPI-anchored fluorescent protein (FP-GL-GPI) cannot be synchronized by temperature shift. Attaching the extracellular domain of ts-O45-G to the proteins can retain the proteins in the ER at restrictive temperature (Cole et al., 1998). This approach was applied to contruct a

chimeric GPI-anchored protein that can be synchronized by temperature shift (Takida et al., 2008). To synchronize the transport of GPI-anchored protein, we engineered two temperature-sensitive chimeric GPI-anchored proteins, VSVG464-FF-YFP-GL-GPI and VSVG464-YFP-GL-GPI. In VSVG464-FF-YFP-GL-GPI, we fused the extracellular domain of ts-O45-G, furin cleavage site and FLAG tag with YFP-GL-GPI (Fig. 25A). In VSVG464-YFP-GL-GPI, the furin cleavage site and FLAG tag were not included (Fig. 25A). Temperature-sensitivity and synchronized transport of the chimeric constructs were tested by immunofluorescence analysis. The chimeric constructs would accumulate in the ER at the restrictive temperature 39.5°C, and exit the ER, traverse the Golgi complex and eventually arrive at the PM upon shifting to permissive temperature. Because of the furin cleavage site in the VSVG464-FF-YFP-GL-GPI, in the TGN the furin proteases would cleave off its VSVG moiety, and this chimeric construct would arrive at the PM as FLAG-tagged YFP-GL-GPI.

To test the chimeric constructs, we transfected the HeLa cells with the plasmid encoding VSVG464-FF-YFP-GL-GPI, VSVG464-YFP-GL-GPI and VSVG-YFP. The cells were incubated at 39.5°C for 20 hours to accumulate the chimeric construct in the ER before the chase was initiated. By immunostaining using anti-GFP antibody we detected the arrival of chimeric construct at the PM after the chase (Fig. 25B). Before the chase, VSVG464-FF-YFP-GL-GPI, VSVG464-YFP-GL-GPI and VSVG-YFP were found in the intracelluar organelle resembles the ER, and the PM-specific fluorescence is weak. The PM-specific fluorescence can only be detected after the chase (Fig. 25B). After the chase, we can no longer observe intracellular VSVG-YFP in the ER-like organelle (Fig. 25B). By contrast, we noticed that most chimeric constructs (VSVG464-FF-YFP-GL-GPI and VSVG464-YFP-GL-GPI) were retained in the ER-like organelle after the chase (Fig. 25B). Furthermore, compared with the transport of VSVG-YFP, much less chimeric constructs were transported to the PM (Fig. 26). We also examined the functionality of

furin cleavage site of the chimeric construct by immunostaining using anti-VSVG antibody. VSVG-specific fluorescence is very weak (data not shown), consistent with the notion that VSVG moiety was cleaved off by the furin proteases in the TGN. The observation suggested the transport of the chimeric constructs is aberrant, and the defection of the transport might occur at the level of ER exit.

We also tested the RNAi-mediated effect on the transport of chimeric construct. For the controls, we chose the siRNAs targeting α-COP, RAB6A, RAB1A and RAB1B, as these siRNAs showed effects in the transport of ts-O45-G-YFP and CFP-GL-GPI. We observed the transport inhibition of the chimeric construct in α-COP, RAB6A, RAB1A and RAB1B siRNA transfected cells (Fig. 27). In the α-COP siRNA-transfected cells, the transport of ts-O45-G-YFP and CFP-GL-GPI was strongly inhibited. However, compared to the transport inhibition of ts-O45-G-YFP and CFP-GL-GPI, the transport inhibition of chimeric construct in α-COP siRNA-transfected cells was not very pronounced. The result suggested the CFP-GL-GPI transport assay we used is sensitive to detect the transport inhibition. It is unlikely that replacing CFP-GL-GPI with the chimeric construct in the transport assay would improve the sensitivity.

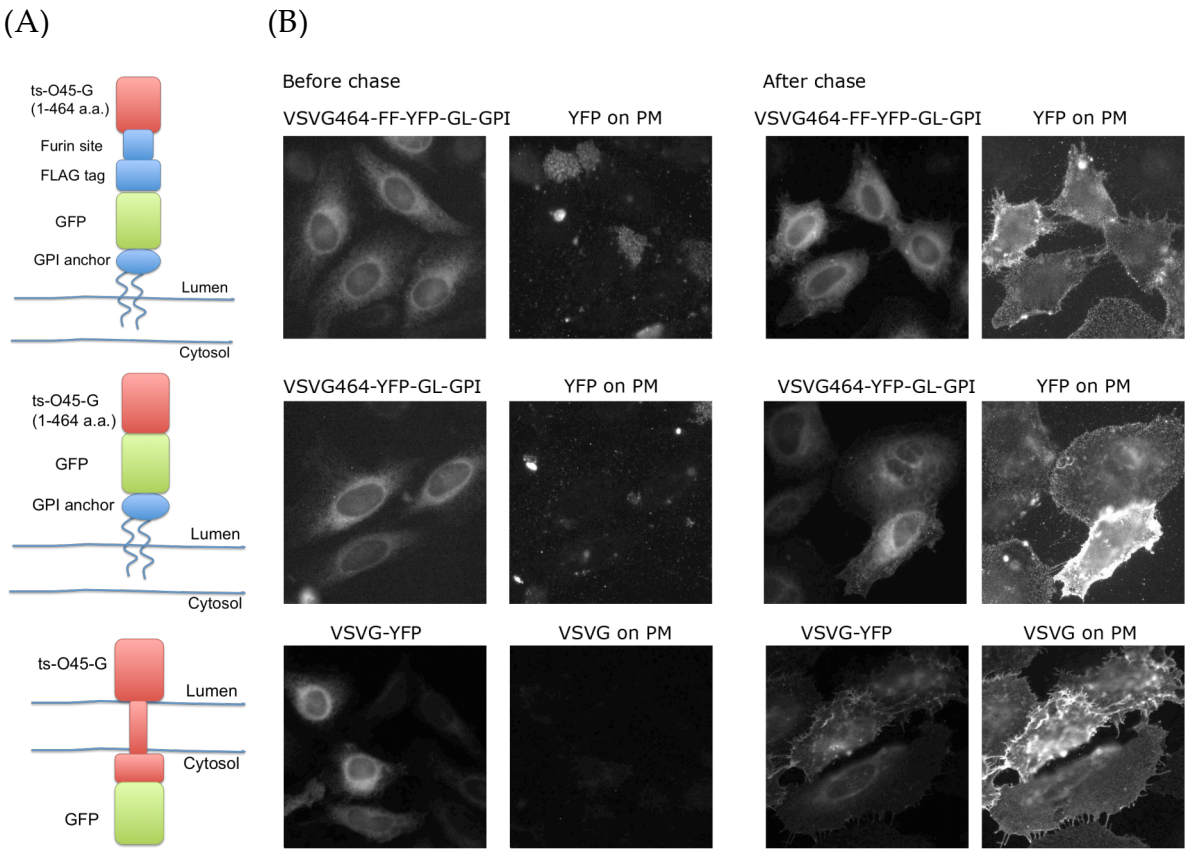

Figure 25 Temperature-sensitive chimeric GPI-anchored proteins

(A) Schematic presentation of the constructs. (B) Immunofluorescence analysis. HeLa cells were transfected with the plasmids encoding the indicated construct, and incubated at 39.5˚C for 20 hours before chase. Chase was initiated by incubation at 32˚C in the presence of cycloheximide. Cells were fixed 60 minutes after chase. The expressed proteins on the PM were labelled by anti-GFP or anti-VSVG antibodies.

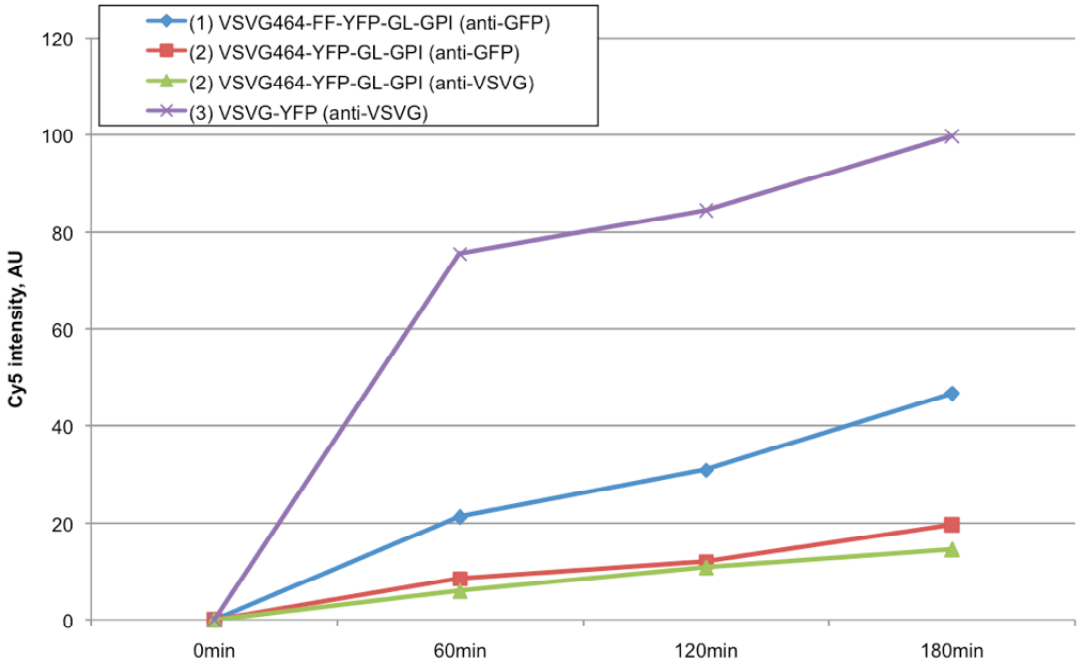

Figure 26 Time-course analysis of the transport of chimeric construct

HeLa cells were transfected with the plasmids encoding the indicated reporter construct, and incubated at 39.5˚C for 20 hours before chase. Chase was initiated by incubation at 32˚C in the presence of cycloheximide. Cells were fixed at the specified timepoint after chase. Fluorescence intensity represents the amount of the reporter proteins on the PM.

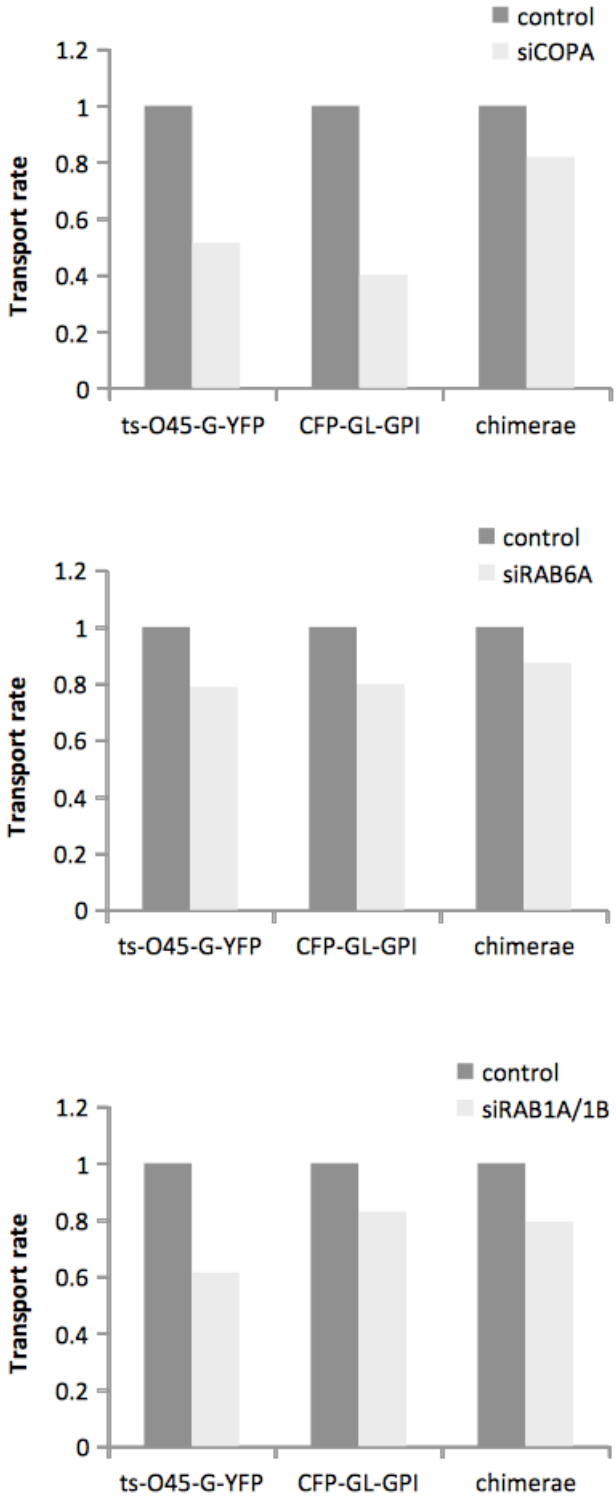

Figure 27 Comparison of the transport of chimeric construct, ts-O45-G and CFP-GL-GPI

The effect of the transfection of siRNAs on the transport of cargo proteins, ts-O45-G, CFP-GL-GPI, VSVG464-FF-YFP-GL-GPI (chimerae) are compared.

4 Discussion

4.1 Secretion of ts-O45-G

4.1.1 RNAi screen identified novel regulators for the transport of ts-O45-G

A number of small GTPases were identified as hit genes in genome-wide RNAi screens for secretory transport (Bard et al., 2006; Ostrowski et al., 2010; Simpson et al., 2012; Wendler et al., 2010). Two screens performed in *Drosophila* S2 cells took advantage of signal peptide-fused horseradish peroxidase and luciferase to investigate secretion. RAB1A, RAB11A and RAB21 were identified as hit genes from these two screens (Bard et al., 2006; Wendler et al., 2010). The effect of RNAi on the secretion of ts-O45-G in HeLa cells have been investigated. To our knowledge, down-regulation of RAB1A, RAB1B (Haas et al., 2007; Tisdale et al., 1992), RAB6A (Miserey-Lenkei et al., 2010), RAB34 (Goldenberg et al., 2007), RAB7B (Progida et al., 2010), RAB18 (Dejgaard et al., 2008), ARF1, ARF3, ARF4 (Volpicelli-Daley et al., 2005), and ARFRP1 (Nishimoto-Morita et al., 2009) inhibited the transport of ts-O45-G. We have performed RNAi screen with 68 Rab and 25 Arf GTPases and identified 18 regulators for the transport of ts-O45-G (Table 1). 14 of them are novel, since their roles in the ts-O45-G secretion are not characterized. Most of our hits localize to the organelles of early secretory pathway, such as the ER and the Golgi complex. Some of the hits, such as RAB4A/4B, , RAB8B, RAB11A, and RAB40C localize to recycling endosomes, suggesting protein recycling machinery might play a role in regulation of ts-O45-G secretion. Furthermore, some Rabs localize to secretory vesicles, such as RAB3B/3C/3D and RAB26, are identified, suggesting the mechanism of regulated secretion may be involved in coordinating ts-O45-G secretion. The result of our sceens provides a new perspective to understand ts-O45-G secretion.

4.2 Characterization of a putative regulator of ts-O45-G secretion, RAB42

4.2.1 RAB42 as a novel regulator for the transport of ts-O45-G

RAB42 is a validated hit in our RNAi screen. We demonstrated that down-regulation of RAB42 inhibited the transport of ts-O45-G. Subsequent experiments indicated TGN-to-PM transport of ts-O45-G was inhibited in RAB42-depleted HeLa cells (Fig. 13).

RAB42 has a unconventional G3 GTP-binding domain sequence, WDTAGHE. G3 GTP-binding domain is important for GTP-binding and GAP-stimulated GTPase activity (Bos et al., 2007). To functionally analyze the G3 GTP-binding domain of RAB42, we prepared various mutants of RAB42 by mutagenesis. We didn't obeserve markedly effect on ts-O45-G secretion in the cells over-expressing RAB42 mutants (Fig. 14). Biochemical assay to analyze the GTP-binding activity and GAP-stimulated GTPase activity of RAB42 and its mutants could be performed to extend our characterization of RAB42.

Another Rab GTPase that has unconventional amino acid sequence of G3 GTP-binding domain is RAB25. Its sequence of G3 GTP-binding domain is WDTAGLE. As Gln-to-Leu substitution is the common mutation that can be introduced in the G3 GTP-binding domain to render the small GTPases GTP-locked state, RAB25 was thought to have reduced GAP-stimulated GTPase activity. However, RAB25 was reported to exhibit normal GAP-stimulated GTPase activity (Wang et al., 2000). It was reported that mutation of the serine at position 21 of RAB25 to valine abolished the GAP-stimulated GTPase activity (Wang et al., 2000). Serine-21 of RAB25 corresponds to alanine-17 of RAB42. It might be of interest to introduce the alanine-to-valine mutation in RAB42 for subsequent analysis.

4.3 Characterization of a putative regulator of PC I secretion, Rab40c

4.3.1 Rab40c is a novel regulator of PC I secretion in NIH3T3 cells

Rab40c was identified as an inhibitory hit in our RNAi screen for procollagen secretion in NIH3T3 cells. We demonstrated that down-regulation of Rab40c inhibited procollagen secretion. In Rab40c-depleted NIH3T3 cells, PC I was blocked in the ER. Our immunofluorescence analysis indicated that Rab40c localized at the Golgi complex. Rab40c is an interesting Rab in that it contains a GTPase domain and a SOCS-box domain, which is associated with the formation of ubiquitin E3 ligase. We have analysed the localization of deletion mutants, and determined SOCS-box domain is essential for the localization of Rab40c at the Golgi complex (Fig. 18).

It was reported transport of fluorescently labeled procollagen (PC-FP) is dependent on the function of COPI and COPII complex (Stephens and Pepperkok, 2002). PC-FP were blocked in the ER in the cells over-expressing GTP-locked ARF1 (ARF1$^{(Q71L)}$) or SAR1 (SAR1a$^{(H79G)}$) (Stephens and Pepperkok, 2002). Since the phenotypes of defective transport of PC I upon down-regulation of Rab40c and upon over-expression of GTP-locked ARF1 or SAR1 are comparable: transport of PC I is blocked in the ER. Rab40c might play a role in maintenance of COPI or COPII function.

4.3.2 The role of Rab40c in regulating PC I secretion

Xenopus homolog of Rab40c is able to form a E3 ubiquitin ligase complex (Lee et al., 2007). It is plausible that Rab40c could form E3 ubiquitin ligase complex. An ubiquitin-dependent mechanism regulates the size of COPII vesicles has been proposed (Jin et al., 2012). Ubiquitination of the components

of COPII vesicles, SEC31, facilitates the formation of large COPII vesicles. Based on these studies, we hypothesized that Rab40c might regulate PC I secretion through the formation of a E3 ubiqutin ligase complex that can mediate the ubiquitination of SEC31. The hypothesis is consistent with the observation that PC I is blocked in the ER in Rab40c-depleted NIH3T3 cells. Subsequent experiments focused on the role of Rab40c in the context of ubiquitination would facilitate the characterization of Rab40c.

4.4 Secretion of GPI-anchored protein

4.4.1 RNAi screen identified novel regulators for the transport of CFP-GL-GPI

It has been demonstrated that GPI-anchored proteins are transported from the ER to the Golgi in distinct vesicles from non-GPI-anchored proteins (Muniz et al., 2001). The sorting of GPI-anchored proteins from non-GPI-anchored proteins occurs upon the ER exit and requires Rab GTPase Ypt1p and tethering factor Uso1, conserved oligomeric Golgi complex and ER v-SNAREs (Morsomme et al., 2003; Morsomme and Riezman, 2002). However, the regulation underlying the transport of GPI-anchored proteins is not fully understood. We perfromed RNAi screens to investigate the transport of a GPI-anchore protein CFP-GL-GPI and identified for the first time RAB3D, RAB6A, RAB26 and ARF3 as novel regulators. Interestingly RAB26 clusters with RAB3, RAB27 and RAB37 in the phylogenetic trees of human and mouse Rab GTPases (Fukuda, 2008; Pereira-Leal and Seabra, 2001). Expression and localization of RAB3D and RAB26 has been intensively investigated in secretory cells, such as pancreatic and parotid acinar cells (Millar et al., 2002; Wagner et al., 1995; Williams et al., 2009; Yoshie et al., 2000). They localize to secretory vesicles or granules that fuse with the plasma membrane by a

calcium-triggered mechanism (Takamori et al., 2006) and play a critical role in regulated secretion (Tian et al., 2010). Regulated secretion encompasses 4 distinct steps: recruitment of secretory vesicles to the release site, docking of secretory vesicles to the PM, priming, and stimulus-dependent fusion of secretory vesicles with the PM (Fukuda, 2008). That RAB3D and RAB26 regulated GPI-anchored protein secretion suggested the machinery of regulated secretion might also play a role in GPI-anchored protein secretion.

RAB6A and ARF3 localize to TGN (Manolea et al., 2010). That depletion of RAB6A and ARF3 inhibited GPI-anchored protein secretion might suggested sorting of GPI-anchored proteins at the TGN is critical for the transport of GPI-anchored proteins.

4.4.2 Transport of chimeric constructs is aberrant

As an attempt to synchronize the transport of GPI-anchored proteins, we engineered a temperature-sensitive chimeric GPI-anchored protein, VSVG464-FF-YFP-GL-GPI. We examined the transport of this chimeric construct, and found that the chimeric construct was not exported from the ER efficiently (Fig. 25B). The aberrant transport of chimeric construct could be explained by the mechanistic requirements of ts-O45-G transport: di-acidic signal and oligomerization. Di-acidic signal in the cytoplasmic domain of VSVG is required for the efficient transport of VSVG from the ER (Nishimura and Balch, 1997; Nishimura et al., 1999). The absence of the VSVG cytoplasmic domain in the chimeric construct could account for the decreased efficiency of ER exit. In addition to di-acidic signal, oligomerization is required for transport of ts-O45-G from the ER (Kreis and Lodish, 1986). The chimeric construct contains a signal peptide and the GFP variant, YFP. Secretory GFP fusion proteins were prone to form interchain disulfide bonds (Jain et al., 2001; Paladino et al., 2004). Presumably, the interchain disulfide bonds might

hinder the oligomerization of chimeric constructs, and thereby inhibits their ER exit.

Acknowledgement

I thank Dr. Vytaute Starkuviene for providing me an opportunity to work in her lab and to explore membrane trafficking. I thank Prof. Dr. Walter Nickel, Dr. Rainer Pepperkok, and Dr. Matthias Seedorf for their kind support and advice on my PhD thesis.

I thank all previous and present members in the lab of Dr. Starkuviene: Dr. Christoph Claas, Dr. Andrius Serva, Dr. Anastasia Eskova, Tautvydas Lisauskas, Susanne Reusing and Sanchari Roy. They are always very helpful to solve my problems and create a friendly and productive atmosphere in the lab.

Many people in BioQuant helped me during my PhD study. The projects would not move forward without their helps and advice. I thank Dr. Holger Erfle, Dr. Jürgen Reymann, Dr. Manuel Gunkel, Nina Beil, Jürgen Beneke and Benjamin Flottmann of RNAi screening facility in BioQaunt for their assistance in microscopy and RNAi technology.

I thank Sabine Wegehingel in the lab of Prof. Dr. Walter Nickel for her assistance in generating stable cell-lines. I thank Dr. Monika Langlotz for her expertise on cell sorting. I thank Dr. Bettina Knapp and Prof. Dr. Lars Kaderali for their help on statistical analysis. I thank Jan-Philip Bergeest and Dr. Karl Rohr for their expertise on image analysis. I thank Christina Jäger-Schmidt and Christian Lawerenz for the help on iCHIP data management system. I thank BioQuant IT team: Dr. Marc Hemberger, Peter Weyrich, Daniel Browne, Melinda Feucht. They provide a stable computing infrastructure and excellent poster printing service.

I thank Anny, Chia-Yi, Chen-Min, Kang, Yin-Yuin and Sing for their friendships and encouragement.

I am deeply grateful for the support from Heinz Götze Memorial Fellowship Program. I would like to express my most sincere gratitude to Prof. Dr. Dietrich Götze and Dr. Dietlind Wünsche for their generous support and guidance on my study and living in Germany.

Finally I thank my parents for supporting my study in Germany.

Appendix

NCBI Gene Symbol	Entrez Gene ID	Product ID[a]	Target Sequence	z-score[b]	p-value[c]
Negative control		SI03650318		-0.16	0.11
COPA	1314	SI00351491	CTGGCGCATGAATGAATCAAA	-6.67	**1.38e-15**
RAB1A	5861	SI00301560	GTCCAGCATGAATCCCGAATA	-0.03	**0.0314**
		SI02662716	AACTATAGAGTTAGACGGGAA	-1.28	**0.0303**
RAB1B	81876	SI02655604	ATGCCAGCGAGAACGTCAATA	-0.65	0.4332
		SI02662723	CGGTTCTGTCAGGGTCCCTAA	-0.91	0.1496
RAB2A	5862	SI00301567	GGCGACACAGGTGTTGGTAAA	0.12	0.2720
		SI02655023	CATGCTTATTGCTACAGTTTA	-0.7	0.3720
RAB2B	84932	SI02779217	AGGGTTCTTCTTATCCTCCTA	-5.18	**0.0348**
		SI02779224	CAGCGGAACTCTCGTGACATA	-0.68	0.3660
RAB3A	5864	SI00044800	CAAGATTCTCATCATCGGCAA	0.67	**0.0071**
		SI00044807	CACCAACGAGGAATCCTTCAA	1.37	**0.0019**
RAB3B	5865	SI00044828	CCGGACCATCACAACAGCCTA	-2.83	0.0575
		SI00044835	CAGAGAGCTCAGACTCTCTAA	-1.08	**0.0024**
RAB3C	115827	SI02779357	TACAAGATTGGTCAACTCAAA	-0.14	0.2472
		SI03106943	GTGGATATCATCTGCGACAAA	-1.71	0.1545
RAB3D	9545	SI00062181	CAGGCCCTGTTTAGCTGTTTA	-1	**0.0060**
		SI03052595	CAAACTGCTACTGATAGGCAA	1.88	**0.0296**
RAB4A	5867	SI00301581	AATGCAGGAACTGGCAAATCT	-1.38	0.4908
		SI02662786	AACCTACAATGCGCTTACTAA	2.21	0.9093
RAB4B	53916	SI02662793	CCGCACTATCCTCAACAAGAT	-0.76	0.0518
		SI03120670	TGGGAAGACTGTGAAGCTACA	-0.48	0.0979
RAB5A	5868	SI00301588	ATTCATGGAGACATCCGCTAA	-0.03	0.0735
		SI02655037	AACCCAAACTGTATGTCTTGA	0.36	0.0961
RAB5B	5869	SI02662233	CAGAATGCGACTGCTGATTTA	1.11	**0.0126**
		SI02662800	TAGGTACAAGACAGCGACTTA	-0.46	0.4655
RAB5C	5878	SI02663073	CACCATGATTTCTCCATATAA	0.97	0.0644
		SI02663080	CCCGACTGGAATCCACTCTAA	-0.51	0.2022
RAB6A	5870	SI02654036	CCCACTTATTGTCACCTTGTA	-6.18	**0.0244**
		SI02655044	CAGATTCATGTATGACAGTTT	-4.23	0.1139
RAB6B	51560	SI00116977	ATGGCCAGAGTGGGTCGTCAA	-0.25	0.1654
		SI02777705	CAGGGATCACATCACTCTTAA	0.43	0.9382
RAB6C	84084	SI03022754	TTCGAGTTACAGGTCAGGAAA	-0.81	0.2067
		SI03110947	TAGCAGAAATAACGATATCTA	0.58	**0.0042**
RAB7A	7879	SI02662240	CACGTAGGCCTTCAACACAAT	-0.73	0.0815
		SI03104255	GAGGTGGAGCTGTACAACGAA	-1	0.1024
RAB7B	338382	SI00160048	CAGCATCCTCTCCAAGATTAT	0.85	**0.0137**
		SI00160055	TCGAGGTACCAGAGCATCTTA	0.03	**0.0084**
RAB8A	4218	SI00076111	AAAGATGATACTCGGGAACAA	0.42	0.0667
		SI02662254	TCGCCAGAGATATCAAAGCAA	0.11	**0.0067**
RAB8B	51762	SI02662261	CAGCACAATCTTAGACTCATA	-0.57	**0.0438**
		SI02662814	CAGCAGAGGTTAATATACTAA	1.32	**0.0245**
RAB9A	9367	SI00061754	CACAGTCAATCTTCACCGAAA	0.52	0.2961
		SI02663234	CAGCAGTGTATCATCTACTAA	0.48	0.0969
RAB9B	51209	SI00115759	CTGGAGGTAGATGGACGCTTT	-0.08	0.1916
		SI00115766	CAGGGTCTTCGTGCTGTTAAA	0.14	**0.0080**
RAB10	10890	SI00301546	ACCTGCGTCCTTTTTCGTTTT	-0.48	0.6847
		SI03037076	AAGTGTGATATGGACGACAAA	-0.88	**0.0151**
RAB11A	8766	SI00301553	AAGAGTAATCTCCTGTCTCGA	-2.02	0.5901

NCBI Gene Symbol	Entrez Gene ID	Product ID[a]	Target Sequence	z-score[b]	p-value[c]
		SI02663206	AAGAGCGATATCGAGCTATAA	2.58	**0.0047**
RAB11B	9230	SI02662695	CCGCATCGTGTCACAGAAACA	-0.04	0.2783
		SI03649751	CGGCAAGACCATCAAGGCGCA	0.67	0.6114
RAB12	201475	SI04300534	ATGATTGATAAGTATGCTTCA	-0.22	0.5292
		SI04346447	ACCGTGGGTGTTGACTTCAAA	1.22	0.0689
RAB13	5872	SI02662149	CAGGGCAAACATAAATGTAAA	-0.2	0.0734
		SI02662702	ATGGTCTTTCTTGGTATTAAA	0.27	0.9024
RAB14	51552	SI00115346	CACGTTAATAGAGGTAGTACA	0.98	0.1694
		SI00115360	AACGGTTCACGTCTAGCCAAA	-0.16	0.0897
RAB15	376267	SI04271330	TGCAGCTACGCTCACCCTAAA	-7.26	**0.0135**
		SI04308346	CACTGCGTGGCTGCAGCCAAA	-0.13	0.5957
RAB17	64284	SI00133770	CAGCCTCTGGACAGAGAGGAA	0	**0.0075**
		SI03075569	CCAGGTGTCGGAGGTGTTCAA	1.68	0.9994
RAB18	22931	SI02662156	ACCAACTTGTACAGACTAATA	-0.77	0.1107
		SI02662709	CCAGGCCAATTTATAACTAAA	1.53	**0.0110**
RAB19	401409	SI04167667	TCGGCCAGTATTATCACCTTT	0.44	**0.0089**
		SI04183557	CTGGATTCATGAGATAGAGAA	0.53	0.4263
RAB20	55647	SI00119714	CAGTGGATATATCCAGTCATA	0.19	0.3014
		SI00119721	CAGCAGAATGTTGGAGTGGAA	-1.82	0.1439
RAB21	23011	SI02662177	CAGGCCCGTAACTGTCTACTA	0.28	0.1091
		SI02662730	CGAGAACAAGTTTAACGACAA	-0.7	0.5657
RAB22A	57403	SI02662184	CAGGTTTAATTTGATGGTCTA	0.43	0.0779
		SI02662737	AAGGCCTATCAGCCAATTAAA	-0.35	**0.0365**
RAB23	51715	SI03030391	AACTAACGCATTCAAGTAGTA	0.51	**0.0019**
		SI03103030	GAGCGACAAATTCAAGTTAAT	-0.17	0.0612
RAB24	53917	SI00149723	CCAGGTGATGACAGAGGACAA	0.37	0.7046
		SI03065713	CAGCAGCTTTGAGCGAGCAAA	-0.19	0.0780
RAB25	57111	SI02644089	AGCCTTTGAGACTGTCCTGAA	-1.72	**0.0023**
		SI03036544	AAGGTGGTGCTGATCGGCGAA	0.76	**0.0145**
RAB26	25837	SI02663262	TCCGGCTGCATGATTACGTTA	-0.41	**0.0117**
		SI02663269	CCGCAGTGTTACCCATGCCTA	1.83	**0.0126**
RAB27A	5873	SI02662744	AAGATAGATGTTCATATTGAA	0.07	0.2239
		SI03050075	ATGCCTCTACGGATCAGTTAA	1.43	0.3080
RAB27B	5874	SI00060424	ACCGAATGGATCTTCAGGGAA	-0.41	**0.0353**
		SI02662751	TAAGCTGTACTAGAATGAATA	0.47	0.6718
RAB28	9364	SI03024686	TTGGAGCATATGCGAACAATA	1.11	0.5203
		SI03082394	CCGGGAAGACCTCCTTAACTA	-2.97	0.1136
RAB30	27314	SI02655534	AAGGGAAAAGCATCAGCTATT	0.09	0.9267
		SI02662758	TCGGTCCATTACCCAGAGTTA	-0.02	0.1178
RAB31	11031	SI02638230	AAGGAATACGCTGAATCCATA	-0.66	**0.0364**
		SI03068520	CAGCTGTTATCGTGTATGATA	0.73	**0.0097**
RAB32	10981	SI02662198	CTCTGCAAAGGATAACATAAA	0.26	0.0883
		SI02662765	CACCAAAGCTTTCCTAATGAA	1.01	0.2911
RAB33A	9363	SI03086517	CGGCGTGGACTTCAGGGAGAA	1.38	0.0513
		SI03118521	TGCCGTGGTCTTCGTCTATGA	1.97	**0.0006**
RAB33B	83452	SI00301574	CTCCCGCATCTTCAAGATAAT	0.8	0.1321
		SI03037356	AATGACCATGTGGAAGCTATA	-0.21	0.5234
RAB34	83871	SI05138112	CACTGTGCCTTATGCATTAAA	0.3	**0.0147**
		SI05138126	CACTGACTTTATCCAGACCAA	-2.61	**0.0108**
RAB35	11021	SI02662205	CAGTTTCGTGCCGTTATTTAA	-0.97	0.0648
		SI03073105	CAGTGCCGAGTCCTTTGTCAA	0	**0.0284**

NCBI Gene Symbol	Entrez Gene ID	Product ID[a]	Target Sequence	z-score[b]	p-value[c]
RAB36	9609	SI00069965	GTGGCCATTCTTGTAGTTATA	-0.21	0.1516
		SI03071103	CAGGGAGATGCAGGCCGAGTA	0.35	**0.0044**
RAB37	326624	SI00159362	AAGGCGGATATGAGCAGCGAA	-2.02	0.1632
		SI03080084	CCGAGACTATGTAGAGTCCCA	0.67	**0.0225**
RAB38	23682	SI00133231	ACGAGGGTCTATTACCGAGAA	-1.6	**0.0028**
		SI02663255	ATGATTTGGACTCCAAGTTAA	0.82	0.6481
RAB39	54734	SI02663276	CAGGAGCGGTTCAGATCAATA	0.92	**0.0081**
		SI02663283	TAGCTTCACAACGTCAAGTTA	-1	**0.0312**
RAB39B	116442	SI00157143	TTGGATCAGTTCACAGCATTA	-0.32	0.0643
		SI00157157	TTGGATTAGATTGTCTCATAT	-0.92	0.7107
RAB40A	142684	SI00149450	TCGCATTGTAGATTCAAGAAA	1.62	**0.0287**
RAB40B	10966	SI02662212	CCGTCGGACTTCGAATTTCTA	1.12	0.9812
		SI02662772	TCGGCGAATGCTGCTTGCGAA	-0.66	0.2677
RAB40C	57799	SI02662219	TCCGGGAATCTTGGTCGGAAA	0.57	**0.0256**
		SI02662779	CAGTAACGGGATCGACTACAA	1.56	0.2300
RAB41	347517	SI00697431	AAGATTGATTTGGATAACAAA	0.85	0.9369
		SI00697445	ACGGTTGAAATCGAACTGGAA	-0.09	0.1162
RAB42	115273	SI00642467	AAGGGTTCATATAAACAGTAT	0.25	0.3081
		SI04320988	CCCAGTTACTCCAGAGGCTAA	1.9	0.0992
RAB43	339122	SI00697508	GCAGTACGATTTCCTGTTCAA	0.27	0.0563
		SI04023796	CAGGCCCACTCTGAAAGAGAA	-0.43	0.3093
RAB44	401258	SI04763570	AACCTTGCTGGTGGACAACAA	0.29	**0.0032**
		SI04763549	TCGGTTGAGGCTCACGGCCTA	0.72	0.2257
RABL2A	11159	SI02662268	CACAGCCACGGTAGATGGCAA	-0.68	0.4344
		SI04221721	TGCATCGTGGTGGCCAATAAA	1.51	0.9277
RABL2B	11158	SI03067015	CAGCGCAGTGGGCAAATCCAA	-0.64	**0.0337**
		SI03092663	CTCTTCAATGATGCAATTCGA	0.09	0.3278
RABL3	285282	SI02662275	TCCCTTAGCTATAATCAGAAA	1.56	**0.0391**
		SI02662821	CGGACTAATAGCCAGAGTTAA	0.88	0.0685
RABL4	11020	SI00092603	AGGAATGGATTTGGTGGTGAA	0.22	0.0597
		SI03092075	CTCGTCTATGATGTGACCAAT	-2.77	**0.0241**
RABL5	64792	SI02662282	CCGGATGGAATTCATAAAGTA	-1.54	**0.0006**
		SI02662828	CAGCCCAATGATACAACAGTA	0.15	**0.0321**
RAB7L1	8934	SI02662247	TAGGCACTTAGTCATAGGAAA	0.03	0.2482
		SI02662807	AACTTCTAACGTCATAATTAA	0.13	0.2219
RAB40AL	282808	SI04654811	TCGATGGATTAAGAAGATTGA	0.15	**0.0330**
		SI04193756	AGCAAGGTACTGAGCTTGCAA	-0.82	0.6100
ARF1	375	SI00299250	ACGTGGAAACCGTGGAGTACA	-1.22	0.6293
		SI02654470	CACCATAGGCTTCAACGTGGA	-3.10	**0.0258**
ARF3	377	SI02654477	CACCTATATGACCAATCCCTA	-4.97	0.0832
		SI04151210	AGGAAAGACCACCATCCTATA	0.41	0.0525
ARF4	378	SI04307142	CAAGACAACCATTCTGTATAA	-0.72	**0.0342**
		SI04313281	CTGCTTGTACCAGCCAGAGAA	-2.66	**0.0227**
ARF5	381	SI00300300	CACGAGCTGTCAAAGCGCTAA	0.12	0.8364
		SI03242351	TTCGCGGATCTTCGGGAAGAA	-2.87	**0.0174**
ARF6	382	SI02757286	CAACGTGGAGACGGTGACTTA	-0.44	0.3497
		SI04282488	TGCGACCACTATGATAATATT	0.35	0.2541
ARFRP1	10139	SI00301049	CACCACCACCGTGGGCCTAAA	-2.06	0.0540
		SI00301070	CGGCGTCATCTACGTCATTGA	0.70	0.1882
ARL1	400	SI04240236	AAGCTTGACTCATAAACTATA	-0.40	**0.0434**
		SI04282054	ATGGCAAATTCACTTGGGTTA	0.15	0.9062

NCBI Gene Symbol	Entrez Gene ID	Product ID[a]	Target Sequence	z-score[b]	p-value[c]
ARL2	402	SI00303415	TGGAAAGACAACCATCCTGAA	-0.07	0.2628
		SI04306232	AACGCTGGGCTTCAACATCAA	0.13	0.9018
ARL3	403	SI00062510	ACGGGTCAGGAACTAGCGGAA	0.14	0.9195
		SI02776914	ACCGATATTCTTATATATGTA	-0.02	0.8471
ARL4A	10124	SI04363513	ATGTGGAGCCTTCATATGTTA	0.15	0.9093
		SI04371675	CTGATGCGCTGTAGAATGAAA	0.61	0.2052
ARL4C	10123	SI04226530	AGCCCTGTGGTGTATCAACTA	0.19	0.4135
		SI04350829	CACCAATGTATCAATGGGTGA	0.56	0.2117
ARL5A	26225	SI04283650	CACGTTTCCTAATGTGGGATA	-0.08	0.9613
		SI04347126	CCACATCAGTTTAACACGATA	0.71	**0.0219**
ARL5B	221079	SI04181422	CTCCCGGATTGGTGTGAGATA	-4.32	**0.0102**
		SI04279632	AGGGAACGACTAGCTATTACA	-0.43	0.2170
ARL5C	390790	SI04843083	CACTCGGGAGGAGCTATATAA	0.94	0.2119
		SI04843090	CAGGATGCTTCAGTCCTGATA	0.34	0.4802
ARL6	84100	SI00303576	GACGATCATTAACAAACTTAA	-0.22	0.1762
		SI00303583	CACCGTCGAATTCCAATCTTA	-0.16	0.2972
ARL8A	127829	SI04183515	CACGCTGGTCGGGCTTCAGTA	0.81	**0.0499**
		SI00303261	CCCGGTCTTAGTCCTGGGTAA	0.24	0.4213
ARL9	132946	SI04305518	TCAGCAGATCACAGCCGATTA	0.40	0.4958
		SI04328639	CAGCCTATCACATTACAGATA	-0.68	0.1633
ARL10	285598	SI04171314	CTGACACTTATTATCGGTACA	0.35	0.3494
		SI04351816	CTGGGTCTACAGGCTATCGAT	-0.74	0.1355
ARL11	115761	SI00303324	AAGGTTGACCATAGCATCCTA	0.76	**0.0188**
		SI04164531	AGGCACAGATATCCTCGTGTA	-0.42	0.0557
ARL13A	392509	SI04329003	CAGCATCTAGAACAATGCTCA	-1.57	0.0765
		SI04656631	AAGAAGGTGAATGTTCTAGGA	0.10	0.4398
ARL13B	200894	SI04139996	TAGCGTTGTTCTTTAAGTGTA	1.01	**0.0235**
		SI04309697	CACCGGGTAGAACCACTTAAT	-0.02	0.5368
ARL14	80117	SI04152477	TAAATTCGTATTCCCTATTAA	0.41	0.2868
		SI04279709	ATGGGTTCGCTGGGTTCTAAA	0.73	0.0579
ARL15	54622	SI04160366	ATGCCTTCCTCTAGTAGTTAA	-0.96	0.2529
		SI04266682	AAGGATACATAGTGATTCGTA	0.08	0.4046
ARL16	339231	SI04137140	ACGGAGGAGATGAAGTCATTA	-0.51	0.0899
		SI04352201	CTGGTCCAGTTACTATGGAAA	1.21	0.0647

Sup. Table 1 Result of the VSVG primary screen

Genes are listed by NCBI gene symbol and the corresponding Entrez Gene ID. All siRNAs listed are purchased from Qiagen. Target sequence, normalized z-score and p-value are also given.

[a] Cat. No. for siRNAs from Qiagen

[b] The transport rate of VSVG was estimated by the ratio of PM VSVG intensity and total VSVG intensity. Median of the ratio was taken to summarize the effect of the siRNA. Z-score was computed by normalizing the median of ratio of the siRNA against the median of ratio of all siRNAs. Green (z-score>1.5); red (z-score<1.5).

[c] p-value was caluculated from 3 replicate experiments. Bold (p-value < 0.05)

Gene	Accession no. for mRNA sequence[a]	Forward Primer	Reverse Primer	PCR product size (bp)	Result
RAB25	NM_020387	5'-TCTACTCTCCCGATTCACGCGCAAT-3'	5'-TTGGTAGAGTCCAGGGCTGAGGTCT-3'	402	-
RAB28	NM_001017979	5'-AAATCGTCGTGCTGGGGGACGG-3'	5'-TATCTGCCTTCACCACCCTCTGTGA-3'	552	+
RAB28	NM_004249	5'-AGGAGAGCCAGGACCGGCAAC-3'	5'-TTCTGCCCTGACAATACGCTGTGAC-3'	575	+
RAB28	NM_001159601	5'-TCGGACTCTGAGGAGGAGAGCCA-3'	5'-TTAGAGCCACAAAGCACACTCGATT-3'	635	+
RAB37	NM_001006638	5'-CCTCACGGGCAAGGTGATGCTTCT-3'	5'-AGTCTCGGATCTGGAAGCTGGGC-3'	509	-
RAB37	NM_001163989	5'-CCCTCAGGGAACAGCAAGGTGAT-3'	5'-AGTCTCGGATCTGGAAGCTGGGC-3'	550	-
RAB37	NM_001163990	5'-CTACGACCTCACGGGCAAGAACAA-3'	5'-AGTCTCGGATCTGGAAGCTGGGC-3'	436	-
RAB37	NM_175738	5'-TCCTGGTGGGTGACAGTGGTGTG-3'	5'-AGTCTCGGATCTGGAAGCTGGGC-3'	527	-
RAB38	NM_022337	5'-GGCGTGGACTTCGCGCTCAA-3'	5'-GCTTCACGACGTCCGGCTCA-3'	457	+
RAB39B	NM_171998	5'-GAGGGTCGCTTTGCCCAGGTT-3'	5'-GCAGCAGCCAGTTTCTCGGCC-3'	344	-
RAB3B	NM_002867	5'-TTACCGTGGGGCCATGGGCTT-3'	5'-CCCAGCATCGACGGGTCTGT-3'	324	+
RAB3C	NM_138453	5'-TGAGACACGAAGCGCCCATG-3'	5'-TCGCTCAGTTGAGATGACCCGCT-3'	470	+
RAB42	NM_152304	5'-GGCCCGGACAAGGTCATCTTCCT-3'	5'-GCCTGCTGGATAGCATCAGCGAG-3'	188	+
RAB6A	NM_002869	5'-GGCCCGGACAAGGTCATCTTCCT-3'	5'-GTAAGGGGGCCAAAGCAGTGAGC-3'	437	+
RAB6A	NM_002869	5'-ACATCCGTGATTCTGCTGCAGC-3'	5'-AGCCTCCTTCACTGACTGGTTGCT-3'	372	+
RAB6A	NM_198896	5'-ACATTCGTGACTCCACTGTGGCA-3'	5'-AGCCTCCTTCACTGACTGGTTGCT-3'	349	+
RABL5	NM_022777	5'-CTCTTCGTGGGGCCTTGCGAGAG-3'	5'-CCAGGTGAAGGCTGGCTAGGTCA-3'	555	+
RABL5	NM_001130821	5'-GGGCCTTGCGAGCAAAGACCT-3'	5'-GTGAACGCCCTGTGTGACAGGTG-3'	719	+
RABL5	NM_001130822	5'-CGTGGGGCCTTGCGAGGATCCTA-3'	5'-GGGCTGCGACGGTTACAAGTCC-3'	776	+
ARF5	NM_001662	5'-CTCACCGTGTCCGCGCTCTTTT-3'	5'-GTGGCCTGGACATACCACGTGC-3'	467	+
ARL4C	NM_005737	5'-GATCAAGCTGAGCAACGGCACGG-3'	5'-CCGGCTGGACGTGATAGGTGGTG-3'	326	+
ARL5B	NM_178815	5'-CTTCGCCAAACTGTGGAGCCTCT-3'	5'-CCCTTCTCCTGTGAGAGCACAGC-3'	481	+
ARL13A	NM_001162490	5'-TGCCCATGCCGAGTAGAGCCA-3'	5'-GGTGGAGTTGTATGGGGAGTGTAGA-3'	624	-
ARL13A	NM_001012990	5'-TGCCCATGCCGAGTAGAGCCATG-3'	5'-AGCTTTGTCAGCAGCATCTCGGT-3'	585	-
ARL13A	NM_001162491	5'-TGCCCATGCCGAGTAGAGCCATG-3'	5'-AGCTTTGTCAGCAGCATCTCGGT-3'	404	-
ARL13A	NM_001012990	5'-TGTTCCGGCTTTTGTCCTCCTGC-3'	5'-GCGCAGTCCTTCAACTATGGGCT-3'	551	-

Sup. Table 2 Result of RT-PCR to probe the expression of small GTPases

[a] NCBI nucleotide database (http://www.ncbi.nlm.nih.gov/nuccore)

NCBI Gene Symbol	Product ID[a]	Target Sequence	z-score[b]	p-value[c]
Negative control			0	0.91
COPA	SI00351491	CTGGCGCATGAATGAATCAAA	-12.7	**0.0009**
RAB1A	SI04935805	AACTAAGGTATTCTAGACCTA	0.02	0.6410
	SI00301560	GTCCAGCATGAATCCCGAATA	-1.93	**0.0236**
RAB1B	SI02655604	ATGCCAGCGAGAACGTCAATA	-1.53	0.6504
	SI02662170	CTGCGGTGGGATCTGAGTATA	0.50	0.5882
RAB2B	SI00144739	CCCACTAAGAATTAGGGTCAA	1.6	0.3437
	SI02779217	AGGGTTCTTCTTATCCTCCTA	-10.05	**0.0358**
RAB3B	SI00044821	CGGGTGCAGAATCACTTTACA	-1.71	**0.1979**
	SI00044828	CCGGACCATCACAACAGCCTA	-5.44	0.3759
RAB3C	SI00150892	GTGGCAAATATGTGATCTTAA	-3.32	**0.0237**
	SI03106943	GTGGATATCATCTGCGACAAA	-3.93	0.0887
RAB3D	SI00062195	CTGGAACTATGGACCACATTA	-2.71	0.5164
	SI03052595	CAAACTGCTACTGATAGGCAA	5.66	0.4046
RAB4A	SI02655030	GACGGCCATGTCCGAAACCTA	-4.83	**0.0394**
	SI02662786	AACCTACAATGCGCTTACTAA	2.13	0.1252
RAB4B	SI02662793	CCGCACTATCCTCAACAAGAT	-3.84	0.1217
	SI03032547	AAGATTGACTCAGGCGAGCTA	-2	0.1896
RAB6A	SI02654036	CCCACTTATTGTCACCTTGTA	-9.25	0.0990
	SI02654120	TACGGTCTTCTTTGAGGTCAA	-10.79	**0.0016**
RAB7A	SI00066409	TAGATCAGCATTCTACTACAA	0.42	0.1426
	SI02662240	CACGTAGGCCTTCAACACAAT	0.2	0.9532
RAB7B	SI00160041	AACGAGCAGACTAAGGAGTAA	-5.2	0.0564
	SI00160055	TCGAGGTACCAGAGCATCTTA	-0.52	0.4597
RAB8B	SI02662814	CAGCAGAGGTTAATATACTAA	2.93	0.0827
	SI03023972	TTGCACGAGATATAATGACAA	-2.07	0.1900
RAB11A	SI00301553	AAGAGTAATCTCCTGTCTCGA	-8.61	0.3627
	SI02655247	CGAAATGAGTTTAATCTGGAA	-3	0.0754
	SI02663206	AAGAGCGATATCGAGCTATAA	5.14	0.3431
RAB15	SI04271330	TGCAGCTACGCTCACCCTAAA	-9.28	0.2052
	SI04350164	TGGCTCCTATGTATCAGGTTA	0.21	0.9208
RAB17	SI00133777	AAGTGAGATCCTGGAAGTGAA	1.76	**0.0024**
	SI03075569	CCAGGTGTCGGAGGTGTTCAA	-0.98	0.6500
RAB18	SI00130494	TGCATTTGTGTAGGAAGTATA	-0.01	0.8782
	SI02662709	CCAGGCCAATTTATAACTAAA	-0.13	0.6282
RAB20	SI00119707	CGACGTGTTCATTTATACAAA	0.21	0.8608
	SI00119721	CAGCAGAATGTTGGAGTGGAA	-4.6	**0.0320**
RAB22A	SI02662184	CAGGTTTAATTTGATGGTCTA	-1.15	0.3364
	SI03118584	TGCCTTAGCACCAATGTACTA	1.09	0.3677
RAB26	SI00105084	CACGCTCCACCTTGCACTCAA	-4.47	0.1512
	SI02663269	CCGCAGTGTTACCCATGCCTA	2.17	**0.0162**
RAB28	SI03037895	ACAGGGAGTCCTCTTGGTATA	1.25	0.2943
	SI03082394	CCGGGAAGACCTCCTTAACTA	-4.01	0.2041
RAB33A	SI00068516	AAGCATGGTCGAGCATTACTA	-0.88	0.3466
	SI03086517	CGGCGTGGACTTCAGGGAGAA	4.18	0.2651
	SI03118521	TGCCGTGGTCTTCGTCTATGA	4.62	0.3754
RAB34	SI05138119	TTCTTTGTTACGAGCACTTAA	1.24	0.1518
	SI05138126	CACTGACTTTATCCAGACCAA	-9.73	**0.0299**
RAB38	SI00133231	ACGAGGGTCTATTACCGAGAA	-4.49	0.1975
	SI03121013	TGGGATATCGCAGGTCAAGAA	-6.49	**0.0301**
RAB39	SI00118559	AAGGTTACAAACCCACACCAA	0.87	0.3870

NCBI Gene Symbol	Product ID[a]	Target Sequence	z-score[b]	p-value[c]
	SI02663276	CAGGAGCGGTTCAGATCAATA	1.42	0.5369
RAB40A	SI00149450	TCGCATTGTAGATTCAAGAAA	0.47	0.7550
	SI00149457	TAGGCTGAATAATCTCCTGTA	-0.92	0.7856
RAB40C	SI00129955	CTGGTTGGCCTTTCTTATTTA	-4.17	**0.0228**
	SI02662779	CAGTAACGGGATCGACTACAA	5.14	0.1691
RAB42	SI00642474	CAGGAAGTCCTTTGAACACAT	-2.49	0.1100
	SI04320988	CCCAGTTACTCCAGAGGCTAA	3.81	**0.0050**
RABL2A	SI02685683	CAGCGCAGTGGGCAAATCCAA	-2.97	0.2684
	SI04221721	TGCATCGTGGTGGCCAATAAA	-1.06	0.1291
RABL3	SI00158725	AAGCCTTGTGTAAATATGAGA	-0.37	0.5175
	SI02662275	TCCCTTAGCTATAATCAGAAA	0.3	0.8036
RABL4	SI00092596	TGGGAGAGTCCCAATGTCTTA	0.47	0.5226
	SI03092075	CTCGTCTATGATGTGACCAAT	-5.17	0.1720
RABL5	SI00134435	TGGAGTGGTGATCGTCTTCAA	-2.88	0.1272
	SI02662282	CCGGATGGAATTCATAAAGTA	-0.74	0.2481
ARF1	SI02757272	CACGATCCTCTACAAGCTTAA	0.47	**0.0498**
	SI02654470	CACCATAGGCTTCAACGTGGA	-7.08	0.1992
ARF3	SI02654477	CACCTATATGACCAATCCCTA	-12.80	0.1301
	SI04227041	CAGGATATGCTAAAGGACGAA	-4.40	0.5079
ARF4	SI04159029	AACGTTAAATGAAATTGGATA	-1.71	0.6474
	SI04313281	CTGCTTGTACCAGCCAGAGAA	-11.80	**0.0294**
ARF5	SI03242351	TTCGCGGATCTTCGGGAAGAA	-12.26	**0.0105**
	SI04363275	AGGGCTTCGGGTGGTGCTATA	0.00	0.8838
ARFRP1	SI00301049	CACCACCACCGTGGGCCTAAA	-8.68	0.0599
	SI04952080	ACCCGCTGTCTTCACAGCAAA	-2.57	0.2205
ARL5B	SI04181422	CTCCCGGATTGGTGTGAGATA	-8.25	**0.0223**
	SI04360209	TAGACGGTGCTGATTGGGAAA	-4.17	**0.0213**

Sup. Table 3 Result of VSVG validation experiments

Genes are listed by NCBI gene symbol. All siRNAs listed are purchased from Qiagen. Target sequence, normalized z-score and p-value are also given.

[a] Cat. No. for siRNAs from Qiagen

[b] The transport rate of VSVG was estimated by the ratio of PM VSVG intensity and total VSVG intensity. Median of the ratio was taken to summarize the effect of the siRNA. Z-score was computed by normalizing the median of ratio of the siRNA against the median of ratio of control siRNA. Green (z-score>1.5); red (z-score<1.5).

[c] p-value was caluculated from 3 replicate experiments. Bold (p-value < 0.05)

NCBI Gene Symbol	Entrez Gene ID	Product ID[a]	Target Sequence	z-score[b]	p-value[c]
Negative control		SI03650318		-0.19	**0.0412**
COPA	1314	SI00351491	CTGGCGCATGAATGAATCAAA	-3.67	**0.0055**
COPB2	9276	SI02664809	ACGATTCTTCAGAGTATGCAA	-3.54	**0.0122**
RAB1A	5861	SI00301560	GTCCAGCATGAATCCCGAATA	-0.59	**0.0314**
		SI02662716	AACTATAGAGTTAGACGGGAA	-0.57	**0.0303**
RAB1B	81876	SI02655604	ATGCCAGCGAGAACGTCAATA	-0.16	0.4332
		SI02662723	CGGTTCTGTCAGGGTCCCTAA	0.38	0.1496
RAB2A	5862	SI00301567	GGCGACACAGGTGTTGGTAAA	-0.38	0.2720
		SI02655023	CATGCTTATTGCTACAGTTTA	0.30	0.3720
RAB2B	84932	SI02779217	AGGGTTCTTCTTATCCTCCTA	-2.27	**0.0348**
		SI02779224	CAGCGGAACTCTCGTGACATA	0.29	0.3660
RAB3A	5864	SI00044800	CAAGATTCTCATCATCGGCAA	1.00	**0.0071**
		SI00044807	CACCAACGAGGAATCCTTCAA	0.85	**0.0019**
RAB3B	5865	SI00044828	CCGGACCATCACAACAGCCTA	0.53	0.0575
		SI00044835	CAGAGAGCTCAGACTCTCTAA	-0.55	**0.0024**
RAB3C	115827	SI02779357	TACAAGATTGGTCAACTCAAA	-0.26	0.2472
		SI03106943	GTGGATATCATCTGCGACAAA	-1.05	0.1545
RAB3D	9545	SI00062181	CAGGCCCTGTTTAGCTGTTTA	1.31	**0.0060**
		SI03052595	CAAACTGCTACTGATAGGCAA	1.89	**0.0296**
RAB4A	5867	SI00301581	AATGCAGGAACTGGCAAATCT	0.19	0.4908
		SI02662786	AACCTACAATGCGCTTACTAA	0.47	0.9093
RAB4B	53916	SI02662793	CCGCACTATCCTCAACAAGAT	-0.99	0.0518
		SI03120670	TGGGAAGACTGTGAAGCTACA	-0.93	0.0979
RAB5A	5868	SI00301588	ATTCATGGAGACATCCGCTAA	0.56	0.0735
		SI02655037	AACCCAAACTGTATGTCTTGA	-0.46	0.0961
RAB5B	5869	SI02662233	CAGAATGCGACTGCTGATTTA	0.97	**0.0126**
		SI02662800	TAGGTACAAGACAGCGACTTA	0.42	0.4655
RAB5C	5878	SI02663073	CACCATGATTTCTCCATATAA	0.79	0.0644
		SI02663080	CCCGACTGGAATCCACTCTAA	0.27	0.2022
RAB6A	5870	SI02654036	CCCACTTATTGTCACCTTGTA	-1.71	**0.0244**
		SI02655044	CAGATTCATGTATGACAGTTT	-0.16	0.1139
RAB6B	51560	SI00116977	ATGGCCAGAGTGGGTCGTCAA	-0.72	0.1654
		SI02777705	CAGGGATCACATCACTCTTAA	0.03	0.9382
RAB6C	84084	SI03022754	TTCGAGTTACAGGTCAGGAAA	0.29	0.2067
		SI03110947	TAGCAGAAATAACGATATCTA	1.38	**0.0042**
RAB7A	7879	SI02662240	CACGTAGGCCTTCAACACAAT	-1.37	0.0815
		SI03104255	GAGGTGGAGCTGTACAACGAA	-0.92	0.1024
RAB7B	338382	SI00160048	CAGCATCCTCTCCAAGATTAT	-0.78	**0.0137**
		SI00160055	TCGAGGTACCAGAGCATCTTA	1.32	**0.0084**
RAB8A	4218	SI00076111	AAAGATGATACTCGGGAACAA	0.35	0.0667
		SI02662254	TCGCCAGAGATATCAAAGCAA	1.11	**0.0067**
RAB8B	51762	SI02662261	CAGCACAATCTTAGACTCATA	-1.17	**0.0438**
		SI02662814	CAGCAGAGGTTAATATACTAA	1.08	**0.0245**
RAB9A	9367	SI00061754	CACAGTCAATCTTCACCGAAA	-0.12	0.2961
		SI02663234	CAGCAGTGTATCATCTACTAA	-0.56	0.0969
RAB9B	51209	SI00115759	CTGGAGGTAGATGGACGCTTT	0.98	0.1916
		SI00115766	CAGGGTCTTCGTGCTGTTAAA	1.49	**0.0080**
RAB10	10890	SI00301546	ACCTGCGTCCTTTTTCGTTTT	0.07	0.6847

NCBI Gene Symbol	Entrez Gene ID	Product ID[a]	Target Sequence	z-score[b]	p-value[c]
		SI03037076	AAGTGTGATATGGACGACAAA	1.12	**0.0151**
RAB11A	8766	SI00301553	AAGAGTAATCTCCTGTCTCGA	0.53	0.5901
		SI02663206	AAGAGCGATATCGAGCTATAA	1.69	**0.0047**
RAB11B	9230	SI02662695	CCGCATCGTGTCACAGAAACA	0.37	0.2783
		SI03649751	CGGCAAGACCATCAAGGCGCA	-0.06	0.6114
RAB12	201475	SI04300534	ATGATTGATAAGTATGCTTCA	0.44	0.5292
		SI04346447	ACCGTGGGTGTTGACTTCAAA	1.43	0.0689
RAB13	5872	SI02662149	CAGGGCAAACATAAATGTAAA	-0.74	0.0734
		SI02662702	ATGGTCTTTCTTGGTATTAAA	0.20	0.9024
RAB14	51552	SI00115346	CACGTTAATAGAGGTAGTACA	-0.49	0.1694
		SI00115360	AACGGTTCACGTCTAGCCAAA	-0.55	0.0897
RAB15	376267	SI04271330	TGCAGCTACGCTCACCCTAAA	-3.51	**0.0135**
		SI04308346	CACTGCGTGGCTGCAGCCAAA	-0.04	0.5957
RAB17	64284	SI00133770	CAGCCTCTGGACAGAGAGGAA	1.22	**0.0075**
		SI03075569	CCAGGTGTCGGAGGTGTTCAA	0.04	0.9994
RAB18	22931	SI02662156	ACCAACTTGTACAGACTAATA	-0.26	0.1107
		SI02662709	CCAGGCCAATTTATAACTAAA	1.25	**0.0110**
RAB19	401409	SI04167667	TCGGCCAGTATTATCACCTTT	1.42	**0.0089**
		SI04183557	CTGGATTCATGAGATAGAGAA	-0.19	0.4263
RAB20	55647	SI00119714	CAGTGGATATATCCAGTCATA	1.09	0.3014
		SI00119721	CAGCAGAATGTTGGAGTGGAA	-0.92	0.1439
RAB21	23011	SI02662177	CAGGCCCGTAACTGTCTACTA	-0.63	0.1091
		SI02662730	CGAGAACAAGTTTAACGACAA	-0.06	0.5657
RAB22A	57403	SI02662184	CAGGTTTAATTTGATGGTCTA	0.78	0.0779
		SI02662737	AAGGCCTATCAGCCAATTAAA	-1.06	**0.0365**
RAB23	51715	SI03030391	AACTAACGCATTCAAGTAGTA	-1.17	**0.0019**
		SI03103030	GAGCGACAAATTCAAGTTAAT	-0.60	0.0612
RAB24	53917	SI00149723	CCAGGTGATGACAGAGGACAA	-0.01	0.7046
		SI03065713	CAGCAGCTTTGAGCGAGCAAA	-0.38	0.0780
RAB25	57111	SI02644089	AGCCTTTGAGACTGTCCTGAA	0.60	**0.0023**
		SI03036544	AAGGTGGTGCTGATCGGCGAA	0.95	**0.0145**
RAB26	25837	SI02663262	TCCGGCTGCATGATTACGTTA	-0.85	**0.0117**
		SI02663269	CCGCAGTGTTACCCATGCCTA	1.58	**0.0126**
RAB27A	5873	SI02662744	AAGATAGATGTTCATATTGAA	-0.39	0.2239
		SI03050075	ATGCCTCTACGGATCAGTTAA	0.21	0.3080
RAB27B	5874	SI00060424	ACCGAATGGATCTTCAGGGAA	-1.11	**0.0353**
		SI02662751	TAAGCTGTACTAGAATGAATA	0.23	0.6718
RAB28	9364	SI03024686	TTGGAGCATATGCGAACAATA	-0.07	0.5203
		SI03082394	CCGGGAAGACCTCCTTAACTA	-0.15	0.1136
RAB30	27314	SI02655534	AAGGGAAAAGCATCAGCTATT	0.11	0.9267
		SI02662758	TCGGTCCATTACCCAGAGTTA	-0.92	0.1178
RAB31	11031	SI02638230	AAGGAATACGCTGAATCCATA	-0.50	**0.0364**
		SI03068520	CAGCTGTTATCGTGTATGATA	0.85	**0.0097**
RAB32	10981	SI02662198	CTCTGCAAAGGATAACATAAA	-0.78	0.0883
		SI02662765	CACCAAAGCTTTCCTAATGAA	-0.29	0.2911
RAB33A	9363	SI03086517	CGGCGTGGACTTCAGGGAGAA	1.77	0.0513
		SI03118521	TGCCGTGGTCTTCGTCTATGA	1.18	**0.0006**
RAB33B	83452	SI00301574	CTCCCGCATCTTCAAGATAAT	0.77	0.1321
		SI03037356	AATGACCATGTGGAAGCTATA	-0.07	0.5234
RAB34	83871	SI05138112	CACTGTGCCTTATGCATTAAA	-1.17	**0.0147**

NCBI Gene Symbol	Entrez Gene ID	Product ID[a]	Target Sequence	z-score[b]	p-value[c]
		SI05138126	CACTGACTTTATCCAGACCAA	-0.77	**0.0108**
RAB35	11021	SI02662205	CAGTTTCGTGCCGTTATTTAA	-0.61	0.0648
		SI03073105	CAGTGCCGAGTCCTTTGTCAA	0.76	**0.0284**
RAB36	9609	SI00069965	GTGGCCATTCTTGTAGTTATA	-0.86	0.1516
		SI03071103	CAGGGAGATGCAGGCCGAGTA	1.26	**0.0044**
RAB37	326624	SI00159362	AAGGCGGATATGAGCAGCGAA	0.15	0.1632
		SI03080084	CCGAGACTATGTAGAGTCCCA	0.75	**0.0225**
RAB38	23682	SI00133231	ACGAGGGTCTATTACCGAGAA	-1.68	**0.0028**
		SI02663255	ATGATTTGGACTCCAAGTTAA	-0.09	0.6481
RAB39	54734	SI02663276	CAGGAGCGGTTCAGATCAATA	1.92	**0.0081**
		SI02663283	TAGCTTCACAACGTCAAGTTA	-0.47	**0.0312**
RAB39B	116442	SI00157143	TTGGATCAGTTCACAGCATTA	-1.52	0.0643
		SI00157157	TTGGATTAGATTGTCTCATAT	-0.31	0.7107
RAB40A	142684	SI00149450	TCGCATTGTAGATTCAAGAAA	1.02	**0.0287**
RAB40B	10966	SI02662212	CCGTCGGACTTCGAATTTCTA	-0.02	0.9812
		SI02662772	TCGGCGAATGCTGCTTGCGAA	-0.17	0.2677
RAB40C	57799	SI02662219	TCCGGGAATCTTGGTCGGAAA	1.06	**0.0256**
		SI02662779	CAGTAACGGGATCGACTACAA	0.70	0.2300
RAB41	347517	SI00697431	AAGATTGATTTGGATAACAAA	0.36	0.9369
		SI00697445	ACGGTTGAAATCGAACTGGAA	0.71	0.1162
RAB42	115273	SI00642467	AAGGGTTCATATAAACAGTAT	0.06	0.3081
		SI04320988	CCCAGTTACTCCAGAGGCTAA	0.31	0.0992
RAB43	339122	SI00697508	GCAGTACGATTTCCTGTTCAA	-0.37	0.0563
		SI04023796	CAGGCCCACTCTGAAAGAGAA	0.07	0.3093
RAB44	401258	SI04763570	AACCTTGCTGGTGGACAACAA	0.92	**0.0032**
		SI04763549	TCGGTTGAGGCTCACGGCCTA	0.57	0.2257
RABL2A	11159	SI02662268	CACAGCCACGGTAGATGGCAA	-0.41	0.4344
		SI04221721	TGCATCGTGGTGGCCAATAAA	0.02	0.9277
RABL2B	11158	SI03067015	CAGCGCAGTGGGCAAATCCAA	0.68	**0.0337**
		SI03092663	CTCTTCAATGATGCAATTCGA	-0.14	0.3278
RABL3	285282	SI02662275	TCCCTTAGCTATAATCAGAAA	1.57	**0.0391**
		SI02662821	CGGACTAATAGCCAGAGTTAA	0.69	0.0685
RABL4	11020	SI00092603	AGGAATGGATTTGGTGGTGAA	-1.48	0.0597
		SI03092075	CTCGTCTATGATGTGACCAAT	-1.31	**0.0241**
RABL5	64792	SI02662282	CCGGATGGAATTCATAAAGTA	-1.00	**0.0006**
		SI02662828	CAGCCCAATGATACAACAGTA	1.25	**0.0321**
RAB7L1	8934	SI02662247	TAGGCACTTAGTCATAGGAAA	-0.22	0.2482
		SI02662807	AACTTCTAACGTCATAATTAA	0.18	0.2219
RAB40AL	282808	SI04654811	TCGATGGATTAAGAAGATTGA	0.62	**0.0330**
		SI04193756	AGCAAGGTACTGAGCTTGCAA	-0.02	0.6100
ARF1	375	SI00299250	ACGTGGAAACCGTGGAGTACA	0.17	0.2371
		SI02654470	CACCATAGGCTTCAACGTGGA	-1.30	**0.0030**
ARF3	377	SI02654477	CACCTATATGACCAATCCCTA	-3.01	**0.0025**
		SI04151210	AGGAAAGACCACCATCCTATA	1.20	**0.0446**
ARF4	378	SI04307142	CAAGACAACCATTCTGTATAA	-0.53	0.0818
		SI04313281	CTGCTTGTACCAGCCAGAGAA	-1.12	**0.0000**
ARF5	381	SI00300300	CACGAGCTGTCAAAGCGCTAA	1.02	**0.0163**
		SI03242351	TTCGCGGATCTTCGGGAAGAA	-2.07	**0.0050**
ARF6	382	SI02757286	CAACGTGGAGACGGTGACTTA	0.82	0.3733
		SI04282488	TGCGACCACTATGATAATATT	0.33	0.6300

NCBI Gene Symbol	Entrez Gene ID	Product ID[a]	Target Sequence	z-score[b]	p-value[c]
ARFRP1	10139	SI00301049	CACCACCACCGTGGGCCTAAA	-1.10	**0.0307**
		SI00301070	CGGCGTCATCTACGTCATTGA	0.12	0.5198
ARL1	400	SI04240236	AAGCTTGACTCATAAACTATA	-0.93	**0.0053**
		SI04282054	ATGGCAAATTCACTTGGGTTA	0.27	0.6395
ARL2	402	SI00303415	TGGAAAGACAACCATCCTGAA	-0.31	0.3663
		SI04306232	AACGCTGGGCTTCAACATCAA	0.72	0.2014
ARL3	403	SI00062510	ACGGGTCAGGAACTAGCGGAA	-0.36	**0.0037**
		SI02776914	ACCGATATTCTTATATATGTA	-0.13	0.4533
ARL4A	10124	SI04363513	ATGTGGAGCCTTCATATGTTA	-1.23	0.0805
		SI04371675	CTGATGCGCTGTAGAATGAAA	1.50	**0.0295**
ARL4C	10123	SI04226530	AGCCCTGTGGTGTATCAACTA	0.14	0.6149
		SI04350829	CACCAATGTATCAATGGGTGA	1.70	**0.0075**
ARL5A	26225	SI04283650	CACGTTTCCTAATGTGGGATA	0.13	0.6450
		SI04347126	CCACATCAGTTTAACACGATA	0.34	**0.0357**
ARL5B	221079	SI04181422	CTCCCGGATTGGTGTGAGATA	-1.92	**0.0008**
		SI04279632	AGGGAACGACTAGCTATTACA	0.73	**0.0050**
ARL5C	390790	SI04843083	CACTCGGGAGGAGCTATATAA	-0.42	0.1781
		SI04843090	CAGGATGCTTCAGTCCTGATA	0.07	0.9366
ARL6	84100	SI00303576	GACGATCATTAACAAACTTAA	-0.58	0.1133
		SI00303583	CACCGTCGAATTCCAATCTTA	-0.13	0.9071
ARL8A	127829	SI04183515	CACGCTGGTCGGGCTTCAGTA	-1.33	**0.0219**
		SI00303261	CCCGGTCTTAGTCCTGGGTAA	-0.64	0.1818
ARL9	132946	SI04305518	TCAGCAGATCACAGCCGATTA	-0.59	**0.0368**
		SI04328639	CAGCCTATCACATTACAGATA	0.82	**0.0068**
ARL10	285598	SI04171314	CTGACACTTATTATCGGTACA	0.81	**0.0071**
		SI04351816	CTGGGTCTACAGGCTATCGAT	0.51	0.6248
ARL11	115761	SI00303324	AAGGTTGACCATAGCATCCTA	0.60	0.2678
		SI04164531	AGGCACAGATATCCTCGTGTA	-0.78	**0.0227**
ARL13A	392509	SI04329003	CAGCATCTAGAACAATGCTCA	-0.59	0.0594
		SI04656631	AAGAAGGTGAATGTTCTAGGA	-0.01	0.7734
ARL13B	200894	SI04139996	TAGCGTTGTTCTTTAAGTGTA	1.11	**0.0470**
		SI04309697	CACCGGGTAGAACCACTTAAT	-0.43	0.7518
ARL14	80117	SI04152477	TAAATTCGTATTCCCTATTAA	0.38	0.0869
		SI04279709	ATGGGTTCGCTGGGTTCTAAA	-1.04	0.0516
ARL15	54622	SI04160366	ATGCCTTCCTCTAGTAGTTAA	-1.08	**0.0016**
		SI04266682	AAGGATACATAGTGATTCGTA	-0.05	0.6498
ARL16	339231	SI04137140	ACGGAGGAGATGAAGTCATTA	-0.64	**0.0231**
		SI04352201	CTGGTCCAGTTACTATGGAAA	1.14	**0.0297**

Sup. Table 4 Result of GPI-anchored protein primary screen

Genes are listed by NCBI gene symbol and the corresponding Entrez Gene ID. All siRNAs listed are purchased from Qiagen. Target sequence, normalized z-score and p-value are also given.

[a] Cat. No. for siRNAs from Qiagen

[b] The transport rate of CFP-GL-GPI was estimated by the ratio of PM GPI intensity and total GPI intensity. Median of the ratio was taken to summarize the effect of the siRNA. Z-score was computed by normalizing the median of

ratio of the siRNA against the median of ratio of all siRNAs. Green (z-score>1.5); red (z-score<1.5).

[c] p-value was caluculated from 4 replicate experiments. Bold (p-value < 0.05)

NCBI Gene Symbol	Product ID[a]	Target Sequence	z-score[b]	p-value[c]
Negative control			0	0.4561
COPA	SI00351491	CTGGCGCATGAATGAATCAAA	-5.60	**0.0100**
RAB2B	SI00144739	CCCACTAAGAATTAGGGTCAA	0.37	0.7529
	SI02779217	AGGGTTCTTCTTATCCTCCTA	-3.71	0.1300
RAB3D	SI00062195	CTGGAACTATGGACCACATTA	-1.96	0.3871
	SI03052595	CAAACTGCTACTGATAGGCAA	-1.42	**0.0098**
RAB6A	SI02654036	CCCACTTATTGTCACCTTGTA	-2.67	0.1553
	SI02654120	TACGGTCTTCTTTGAGGTCAA	-2.74	0.0608
RAB11A	SI00301553	AAGAGTAATCTCCTGTCTCGA	0.55	0.3693
	SI02655247	CGAAATGAGTTTAATCTGGAA	0.30	0.6805
	SI02663206	AAGAGCGATATCGAGCTATAA	1.64	0.4191
RAB15	SI04271330	TGCAGCTACGCTCACCCTAAA	-4.98	**0.0189**
	SI04350164	TGGCTCCTATGTATCAGGTTA	-0.22	0.3900
RAB26	SI00105084	CACGCTCCACCTTGCACTCAA	1.38	0.3328
	SI02663269	CCGCAGTGTTACCCATGCCTA	1.55	0.1368
RAB33A	SI00068516	AAGCATGGTCGAGCATTACTA	-1.38	**0.0454**
	SI03086517	CGGCGTGGACTTCAGGGAGAA	-0.45	0.7586
	SI03118521	TGCCGTGGTCTTCGTCTATGA	0.46	0.7066
RAB38	SI00133231	ACGAGGGTCTATTACCGAGAA	-0.86	0.6850
	SI03121013	TGGGATATCGCAGGTCAAGAA	-0.97	0.6200
RAB39	SI00118559	AAGGTTACAAACCCACACCAA	-0.74	0.2137
	SI02663276	CAGGAGCGGTTCAGATCAATA	-0.59	0.3908
RABL3	SI00158725	AAGCCTTGTGTAAATATGAGA	-1.16	0.1787
	SI02662275	TCCCTTAGCTATAATCAGAAA	0.09	0.7357
ARF3	SI02654477	CACCTATATGACCAATCCCTA	-5.04	**0.0256**
	SI04227041	CAGGATATGCTAAAGGACGAA	-1.23	**0.0323**
ARF5	SI03242351	TTCGCGGATCTTCGGGAAGAA	-0.94	0.0693
	SI04363275	AGGGCTTCGGGTGGTGCTATA	0.08	**0.0080**
ARL4C	SI04185293	AAGGATGAAGTCTTTCCGAAT	0.16	0.3925
	SI04350829	CACCAATGTATCAATGGGTGA	0.33	0.3544
ARL5B	SI04181422	CTCCCGGATTGGTGTGAGATA	-0.98	0.3755
	SI04360209	TAGACGGTGCTGATTGGGAAA	0.80	0.1988

Sup. Table 5 Result of GPI-AP validation experiments

Genes are listed by NCBI gene symbol. All siRNAs listed are purchased from Qiagen. Target sequence, normalized z-score and p-value are also given.

[a] Cat. No. for siRNAs from Qiagen

[b] The transport rate of CFP-GL-GPI was estimated by the ratio of PM GPI intensity and total GPI intensity. Median of the ratio was taken to summarize the effect of the siRNA. Z-score was computed by normalizing the median of ratio of the siRNA against the median of ratio of control siRNA. Green (z-score>1.0); red (z-score<1.0).

[c] p-value was caluculated from 2 replicate experiments. Bold (p-value < 0.05)

Name of primer	Sequence	Purpose
RAB42-F	5'-CATGGAGGCCGAGGGCTGCCGCTACCAATTTCG-3'	Cloning RAB42
RAB42-R	5'-ACCAGGTGGGCTAAGGCTGGGACTGCTTTAACC-3'	Cloning RAB42
RAB42-5-EcoRI-F	5'-CCGGAATTCCATGGAGGCCGAGGGC-3'	Subcloning RAB42
RAB42-3-BamHI-R	5'-GAACGCGGATCCTCAACACTGGCATGGGC-3'	Subcloning RAB42
42-5-EcoRI-ko-F	5'-CCGGAATTCCGCGGCCATGGAGGCCGAGGGC-3'	Subcloning RAB42
Flag-RAB42-5-EcoRI	5'-CCGGAATTCACCATGGACTACAAAGACGATGACGATAAAATGGAGGCCGAGGGC-3'	Subcloning FLAG-RAB42
42_T23_F	5'-CGGAGCTACGTGGCAGGCGC-3'	T23N mutagenesis
42T23N-R	5'-CAGCAGCGAGTTCTTGCCCAC-3'	T23N mutagenesis
42-H73L-F	5'-TCGAGCGCTTCAGGTGCATC-3'	H73L mutagenesis
42-H73-R2	5'-GGCCCGCGGTGTCC-3'	H73L mutagenesis
42-H73Q-F	5'-AGGAGCGCTTCAGGTGCATC-3'	H73Q mutagenesis

Sup. Table 6 Primers for cloning and mutagenesis of RAB42

A

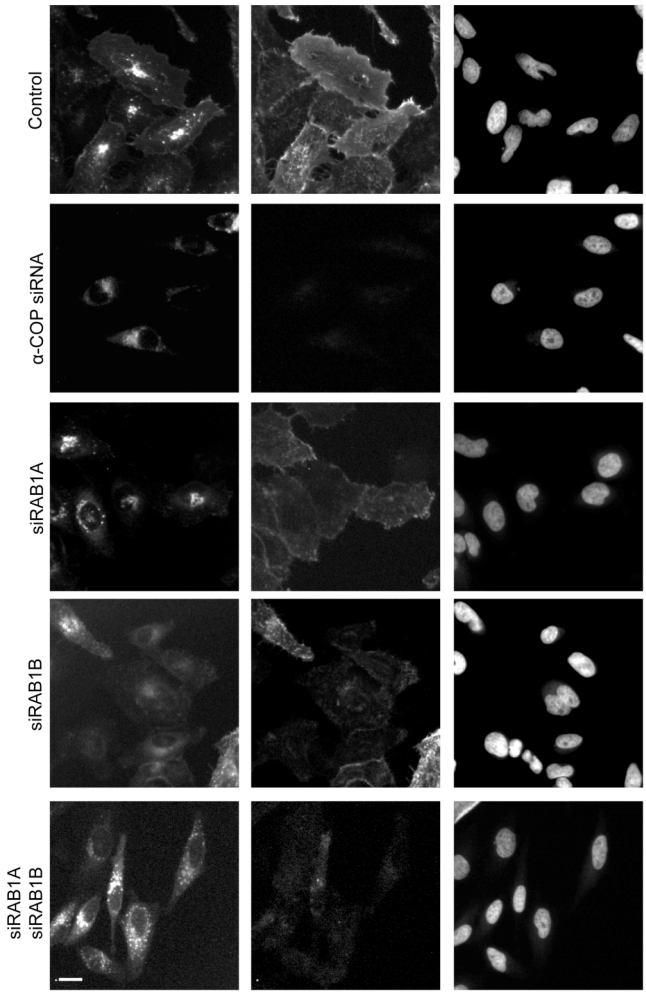

B

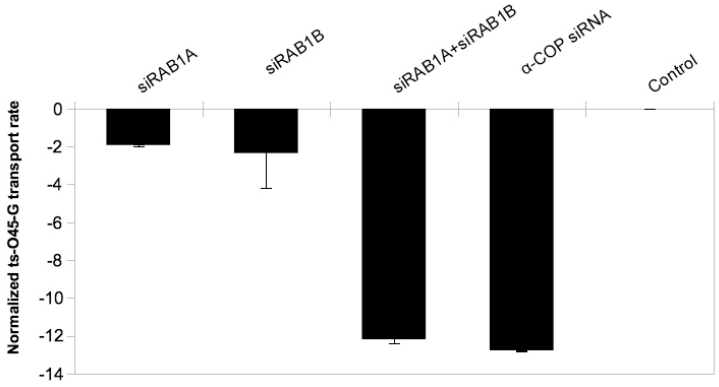

Sup. Figure 1 Functional redundancy of RAB1A and RAB1B

(A) ts-O45-G transport assay was performed on the HeLa cells transfected with control, RAB1A and RAB1B siRNAs. After fixation, the cells were immunostained with anti-VSVG. Images were acquired by wide-field microscopy. Scale bar, 20 μm (B) Effect of siRNAs on ts-O45-G secretion are summarized. Bars represent the ts-O45-G transport rate, and the error bars indicate the s.e.m. derived from 2 independent experiments.

A

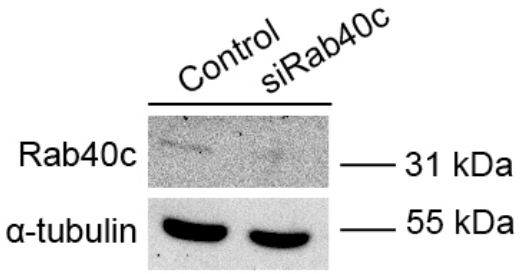

B

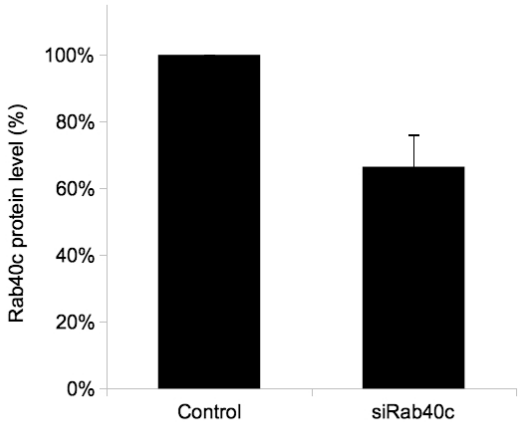

Sup. Figure 2 Rab40c is downregulated in NIH3T3 cells

NIH3T3 cells were transfected with siRNA targeting Rab40c for 48 hours. The expression of Rab40c were measured by Western blot (A) Western blotting with α-tubulin was used as loading control. (B) Quantification of Rab40c protein level. Bars represent the relative expression level, and the error bars indicate the s.e.m derived from 2 independent experiments.

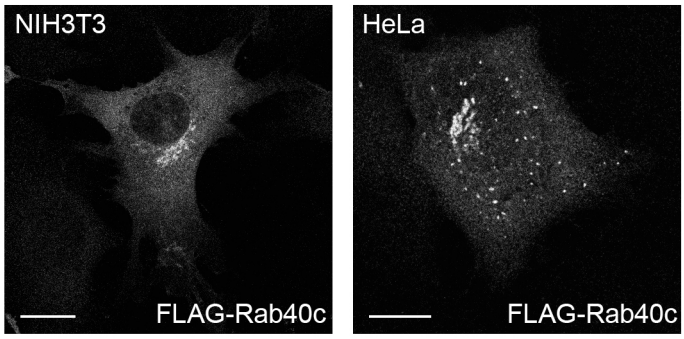

Sup. Figure 3 FLAG-tagged Rab40c localizes differently in NIH3T3 fibroblasts and HeLa

NIH3T3 cells or HeLa cells were transfected with the plasmid encoding FLAG-tagged Rab40c. In NIH3T3 cells FLAG-tagged Rab40c localized to perinuclear structures, whereas in HeLa cells FLAG-tagged Rab40c localized to perinuclear structures and vesicular structures. Images were acquired by confocal microscopy. Left panel: NIH3T3 cells, scale bar, 20 μm. Right panel: HeLa cells, scale bar, 10 μm.

References

Aboulaich, N., Vainonen, J. P., Stralfors, P. and Vener, A. V. (2004). Vectorial proteomics reveal targeting, phosphorylation and specific fragmentation of polymerase I and transcript release factor (PTRF) at the surface of caveolae in human adipocytes. *Biochem J* **383**, 237-48.

Adari, H., Lowy, D. R., Willumsen, B. M., Der, C. J. and McCormick, F. (1988). Guanosine triphosphatase activating protein (GAP) interacts with the p21 ras effector binding domain. *Science* **240**, 518-21.

Albritton, L. M., Tseng, L., Scadden, D. and Cunningham, J. M. (1989). A putative murine ecotropic retrovirus receptor gene encodes a multiple membrane-spanning protein and confers susceptibility to virus infection. *Cell* **57**, 659-66.

Allen, J. M. and Seed, B. (1989). Isolation and expression of functional high-affinity Fc receptor complementary DNAs. *Science* **243**, 378-81.

Altan-Bonnet, N., Sougrat, R., Liu, W., Snapp, E. L., Ward, T. and Lippincott-Schwartz, J. (2006). Golgi inheritance in mammalian cells is mediated through endoplasmic reticulum export activities. *Mol Biol Cell* **17**, 990-1005.

Amornphimoltham, P., Rechache, K., Thompson, J., Masedunskas, A., Leelahavanichkul, K., Patel, V., Molinolo, A., Gutkind, J. S. and Weigert, R. Rab25 regulates invasion and metastasis in head and neck cancer. *Clin Cancer Res*.

Antonny, B., Madden, D., Hamamoto, S., Orci, L. and Schekman, R. (2001). Dynamics of the COPII coat with GTP and stable analogues. *Nat Cell Biol* **3**, 531-7.

Barbacid, M. (1987). ras genes. *Annu Rev Biochem* **56**, 779-827.

Bard, F., Casano, L., Mallabiabarrena, A., Wallace, E., Saito, K., Kitayama, H., Guizzunti, G., Hu, Y., Wendler, F., Dasgupta, R. et al. (2006). Functional genomics reveals genes involved in protein secretion and Golgi organization. *Nature* **439**, 604-7.

Barrowman, J., Bhandari, D., Reinisch, K. and Ferro-Novick, S. (2010). TRAPP complexes in membrane traffic: convergence through a common Rab. *Nat Rev Mol Cell Biol* **11**, 759-63.

Bartz, F., Kern, L., Erz, D., Zhu, M., Gilbert, D., Meinhof, T., Wirkner, U., Erfle, H., Muckenthaler, M., Pepperkok, R. et al. (2009). Identification of cholesterol-regulating genes by targeted RNAi screening. *Cell Metab* **10**, 63-75.

Beck, R., Rawet, M., Wieland, F. T. and Cassel, D. (2009). The COPI system: molecular mechanisms and function. *FEBS Lett* **583**, 2701-9.

Bella, J., Brodsky, B. and Berman, H. M. (1995). Hydration structure of a collagen peptide. *Structure* **3**, 893-906.

Bergmann, J. E., Tokuyasu, K. T. and Singer, S. J. (1981). Passage of an integral membrane protein, the vesicular stomatitis virus glycoprotein, through the Golgi apparatus en route to the plasma membrane. *Proc Natl Acad Sci U S A* **78**, 1746-50.

Birk, J., Meyer, M., Aller, I., Hansen, H. G., Odermatt, A., Dick, T. P., Meyer, A. J. and Appenzeller-Herzog, C. (2013). Endoplasmic reticulum: Reduced and oxidized glutathione revisited. *J Cell Sci* **126**, 1604-1617.

Bishop, D. H., Repik, P., Obijeski, J. F., Moore, N. F. and Wagner, R. R. (1975). Restitution of infectivity to spikeless vesicular stomatitis virus by solubilized viral components. *J Virol* **16**, 75-84.

Bonfanti, L., Mironov, A. A., Jr., Martinez-Menarguez, J. A., Martella, O., Fusella, A., Baldassarre, M., Buccione, R., Geuze, H. J., Mironov, A. A. and Luini, A. (1998). Procollagen traverses the Golgi stack without leaving the lumen of cisternae: evidence for cisternal maturation. *Cell* **95**, 993-1003.

Bonifacino, J. S. (2004). The GGA proteins: adaptors on the move. *Nat Rev Mol Cell Biol* **5**, 23-32.

Bonifacino, J. S. and Glick, B. S. (2004). The mechanisms of vesicle budding and fusion. *Cell* **116**, 153-66.

Bos, J. L., Rehmann, H. and Wittinghofer, A. (2007). GEFs and GAPs: critical elements in the control of small G proteins. *Cell* **129**, 865-77.

Bourne, H. R., Sanders, D. A. and McCormick, F. (1991). The GTPase superfamily: conserved structure and molecular mechanism. *Nature* **349**, 117-27.

Brown, D. A. and Rose, J. K. (1992). Sorting of GPI-anchored proteins to glycolipid-enriched membrane subdomains during transport to the apical cell surface. *Cell* **68**, 533-44.

Brown, M. S. and Goldstein, J. L. (1986). A receptor-mediated pathway for cholesterol homeostasis. *Science* **232**, 34-47.

Cartwright, B., Smale, C. J. and Brown, F. (1969). Surface structure of vesicular stomatitis virus. *J Gen Virol* **5**, 1-10.

Castillon, G. A., Aguilera-Romero, A., Manzano-Lopez, J., Epstein, S., Kajiwara, K., Funato, K., Watanabe, R., Riezman, H. and Muniz, M. (2011). The yeast p24 complex regulates GPI-anchored protein transport and quality control by monitoring anchor remodeling. *Mol Biol Cell* **22**, 2924-36.

Chalfie, M., Tu, Y., Euskirchen, G., Ward, W. W. and Prasher, D. C. (1994). Green fluorescent protein as a marker for gene expression. *Science* **263**, 802-5.

Chatterjee, S. and Mayor, S. (2001). The GPI-anchor and protein sorting. *Cell Mol Life Sci* **58**, 1969-87.

Chen, W., Feng, Y., Chen, D. and Wandinger-Ness, A. (1998). Rab11 is required for trans-golgi network-to-plasma membrane transport and a preferential target for GDP dissociation inhibitor. *Mol Biol Cell* **9**, 3241-57.

Cole, N. B., Ellenberg, J., Song, J., DiEuliis, D. and Lippincott-Schwartz, J. (1998). Retrograde transport of Golgi-localized proteins to the ER. *J Cell Biol* **140**, 1-15.

Conner, S. D. and Schmid, S. L. (2003). Regulated portals of entry into the cell. *Nature* **422**, 37-44.

Conrad, C. and Gerlich, D. W. (2010). Automated microscopy for high-content RNAi screening. *J Cell Biol* **188**, 453-61.

Cook, A., Bono, F., Jinek, M. and Conti, E. (2007). Structural biology of nucleocytoplasmic transport. *Annu Rev Biochem* **76**, 647-71.

D'Souza-Schorey, C. and Chavrier, P. (2006). ARF proteins: roles in membrane traffic and beyond. *Nat Rev Mol Cell Biol* **7**, 347-58.

Damke, H., Baba, T., van der Bliek, A. M. and Schmid, S. L. (1995). Clathrin-independent pinocytosis is induced in cells overexpressing a temperature-sensitive mutant of dynamin. *J Cell Biol* **131**, 69-80.

Davey, R. A., Hamson, C. A., Healey, J. J. and Cunningham, J. M. (1997). In vitro binding of purified murine ecotropic retrovirus envelope surface protein to its receptor, MCAT-1. *J Virol* **71**, 8096-102.

De Matteis, M. A. and Godi, A. (2004). PI-loting membrane traffic. *Nat Cell Biol* **6**, 487-92.

De Matteis, M. A. and Luini, A. (2008). Exiting the Golgi complex. *Nat Rev Mol Cell Biol* **9**, 273-84.

Dejgaard, S. Y., Murshid, A., Erman, A., Kizilay, O., Verbich, D., Lodge, R., Dejgaard, K., Ly-Hartig, T. B., Pepperkok, R., Simpson, J. C. et al. (2008). Rab18 and Rab43 have key roles in ER-Golgi trafficking. *J Cell Sci* **121**, 2768-81.

Derby, M. C., Lieu, Z. Z., Brown, D., Stow, J. L., Goud, B. and Gleeson, P. A. (2007). The trans-Golgi network golgin, GCC185, is required for endosome-to-Golgi transport and maintenance of Golgi structure. *Traffic* **8**, 758-73.

Doherty, G. J. and McMahon, H. T. (2009). Mechanisms of endocytosis. *Annu Rev Biochem* **78**, 857-902.

Dunphy, W. G. and Rothman, J. E. (1985). Compartmental organization of the Golgi stack. *Cell* **42**, 13-21.

Elbashir, S. M., Harborth, J., Lendeckel, W., Yalcin, A., Weber, K. and Tuschl, T. (2001). Duplexes of 21-nucleotide RNAs mediate RNA interference in cultured mammalian cells. *Nature* **411**, 494-8.

Enomoto, K. and Gill, D. M. (1980). Cholera toxin activation of adenylate cyclase. Roles of nucleoside triphosphates and a macromolecular factor in the ADP ribosylation of the GTP-dependent regulatory component. *J Biol Chem* **255**, 1252-8.

Erfle, H., Neumann, B., Liebel, U., Rogers, P., Held, M., Walter, T., Ellenberg, J. and Pepperkok, R. (2007). Reverse transfection on cell arrays for high content screening microscopy. *Nat Protoc* **2**, 392-9.

Erfle, H., Neumann, B., Rogers, P., Bulkescher, J., Ellenberg, J. and Pepperkok, R. (2008). Work flow for multiplexing siRNA assays by solid-phase reverse transfection in multiwell plates. *J Biomol Screen* **13**, 575-80.

Etchison, J. R., Robertson, J. S. and Summers, D. F. (1977). Partial structural analysis of the oligosaccharide moieties of the vesicular stomatitis virus glycoprotein by sequential chemical and enzymatic degradation. *Virology* **78**, 375-92.

Farquhar, M. G. (1985). Progress in unraveling pathways of Golgi traffic. *Annu Rev Cell Biol* **1**, 447-88.

Fath, S., Mancias, J. D., Bi, X. and Goldberg, J. (2007). Structure and organization of coat proteins in the COPII cage. *Cell* **129**, 1325-36.

Ferguson, M. A., Haldar, K. and Cross, G. A. (1985). Trypanosoma brucei variant surface glycoprotein has a sn-1,2-dimyristyl glycerol membrane anchor at its COOH terminus. *J Biol Chem* **260**, 4963-8.

Ferguson, M. A., Homans, S. W., Dwek, R. A. and Rademacher, T. W. (1988). Glycosyl-phosphatidylinositol moiety that anchors Trypanosoma brucei variant surface glycoprotein to the membrane. *Science* **239**, 753-9.

Fessler, J. H. and Fessler, L. I. (1978). Biosynthesis of procollagen. *Annu Rev Biochem* **47**, 129-62.

Fire, A., Xu, S., Montgomery, M. K., Kostas, S. A., Driver, S. E. and Mello, C. C. (1998). Potent and specific genetic interference by double-stranded RNA in Caenorhabditis elegans. *Nature* **391**, 806-11.

Flamand, A. (1970). [Genetic study of vesicular stomatitis virus: classification of spontaneous thermosensitive mutants into complementation groups]. *J Gen Virol* **8**, 187-95.

Fridmann-Sirkis, Y., Siniossoglou, S. and Pelham, H. R. (2004). TMF is a golgin that binds Rab6 and influences Golgi morphology. *BMC Cell Biol* **5**, 18.

Fujita, M. and Kinoshita, T. (2010). Structural remodeling of GPI anchors during biosynthesis and after attachment to proteins. *FEBS Lett* **584**, 1670-7.

Fujita, M. and Kinoshita, T. (2012). GPI-anchor remodeling: potential functions of GPI-anchors in intracellular trafficking and membrane dynamics. *Biochim Biophys Acta* **1821**, 1050-8.

Fujita, M., Watanabe, R., Jaensch, N., Romanova-Michaelides, M., Satoh, T., Kato, M., Riezman, H., Yamaguchi, Y., Maeda, Y. and Kinoshita, T. (2011). Sorting of GPI-anchored proteins into ER exit sites by p24 proteins is dependent on remodeled GPI. *J Cell Biol* **194**, 61-75.

Fukuda, M. (2008). Regulation of secretory vesicle traffic by Rab small GTPases. *Cell Mol Life Sci* **65**, 2801-13.

Fukuda, M., Kanno, E., Ishibashi, K. and Itoh, T. (2008). Large scale screening for novel rab effectors reveals unexpected broad Rab binding specificity. *Mol Cell Proteomics* **7**, 1031-42.

Futerman, A. H., Low, M. G., Ackermann, K. E., Sherman, W. R. and Silman, I. (1985). Identification of covalently bound inositol in the hydrophobic membrane-anchoring domain of Torpedo acetylcholinesterase. *Biochem Biophys Res Commun* **129**, 312-7.

Gallione, C. J. and Rose, J. K. (1985). A single amino acid substitution in a hydrophobic domain causes temperature-sensitive cell-surface transport of a mutant viral glycoprotein. *J Virol* **54**, 374-82.

Gedeon, A. K., Colley, A., Jamieson, R., Thompson, E. M., Rogers, J., Sillence, D., Tiller, G. E., Mulley, J. C. and Gecz, J. (1999). Identification of the gene (SEDL) causing X-linked spondyloepiphyseal dysplasia tarda. *Nat Genet* **22**, 400-4.

Giepmans, B. N., Adams, S. R., Ellisman, M. H. and Tsien, R. Y. (2006). The fluorescent toolbox for assessing protein location and function. *Science* **312**, 217-24.

Glick, B. S. and Malhotra, V. (1998). The curious status of the Golgi apparatus. *Cell* **95**, 883-9.

Glick, B. S. and Nakano, A. (2009). Membrane traffic within the Golgi apparatus. *Annu Rev Cell Dev Biol* **25**, 113-32.

Goldberg, J. (1998). Structural basis for activation of ARF GTPase: mechanisms of guanine nucleotide exchange and GTP-myristoyl switching. *Cell* **95**, 237-48.

Goldenberg, N. M., Grinstein, S. and Silverman, M. (2007). Golgi-bound Rab34 is a novel member of the secretory pathway. *Mol Biol Cell* **18**, 4762-71.

Goud, B., Zahraoui, A., Tavitian, A. and Saraste, J. (1990). Small GTP-binding protein associated with Golgi cisternae. *Nature* **345**, 553-6.

Grant, B. D. and Donaldson, J. G. (2009). Pathways and mechanisms of endocytic recycling. *Nat Rev Mol Cell Biol* **10**, 597-608.

Griffiths, G., Pfeiffer, S., Simons, K. and Matlin, K. (1985). Exit of newly synthesized membrane proteins from the trans cisterna of the Golgi complex to the plasma membrane. *J Cell Biol* **101**, 949-64.

Griffiths, G. and Simons, K. (1986). The trans Golgi network: sorting at the exit site of the Golgi complex. *Science* **234**, 438-43.

Grigoriev, I., Splinter, D., Keijzer, N., Wulf, P. S., Demmers, J., Ohtsuka, T., Modesti, M., Maly, I. V., Grosveld, F., Hoogenraad, C. C. et al. (2007). Rab6 regulates transport and targeting of exocytotic carriers. *Dev Cell* **13**, 305-14.

Haas, A. K., Yoshimura, S., Stephens, D. J., Preisinger, C., Fuchs, E. and Barr, F. A. (2007). Analysis of GTPase-activating proteins: Rab1 and Rab43 are key Rabs required to maintain a functional Golgi complex in human cells. *J Cell Sci* **120**, 2997-3010.

Hayes, G. L., Brown, F. C., Haas, A. K., Nottingham, R. M., Barr, F. A. and Pfeffer, S. R. (2009). Multiple Rab GTPase binding sites in GCC185 suggest a model for vesicle tethering at the trans-Golgi. *Mol Biol Cell* **20**, 209-17.

Hofmann, I., Thompson, A., Sanderson, C. M. and Munro, S. (2007). The Arl4 family of small G proteins can recruit the cytohesin Arf6 exchange factors to the plasma membrane. *Curr Biol* **17**, 711-6.

Hutagalung, A. H. and Novick, P. J. (2011). Role of Rab GTPases in membrane traffic and cell physiology. *Physiol Rev* **91**, 119-49.

Ikezawa, H., Yamanegi, M., Taguchi, R., Miyashita, T. and Ohyabu, T. (1976). Studies on phosphatidylinositol phosphodiesterase (phospholipase C type) of Bacillus cereus. I. purification, properties and phosphatase-releasing activity. *Biochim Biophys Acta* **450**, 154-64.

Itzen, A. and Goody, R. S. (2011). GTPases involved in vesicular trafficking: structures and mechanisms. *Semin Cell Dev Biol* **22**, 48-56.

Jacobs, S., Schilf, C., Fliegert, F., Koling, S., Weber, Y., Schurmann, A. and Joost, H. G. (1999). ADP-ribosylation factor (ARF)-like 4, 6, and 7 represent a subgroup of the ARF family characterization by rapid nucleotide exchange and a nuclear localization signal. *FEBS Lett* **456**, 384-8.

Jain, R. K., Joyce, P. B., Molinete, M., Halban, P. A. and Gorr, S. U. (2001). Oligomerization of green fluorescent protein in the secretory pathway of endocrine cells. *Biochem J* **360**, 645-9.

Jensen, D. and Schekman, R. (2011). COPII-mediated vesicle formation at a glance. *J Cell Sci* **124**, 1-4.

Jin, L., Pahuja, K. B., Wickliffe, K. E., Gorur, A., Baumgartel, C., Schekman, R. and Rape, M. (2012). Ubiquitin-dependent regulation of COPII coat size and function. *Nature* **482**, 495-500.

Kadler, K. E., Baldock, C., Bella, J. and Boot-Handford, R. P. (2007). Collagens at a glance. *J Cell Sci* **120**, 1955-8.

Kahn, R. A., Cherfils, J., Elias, M., Lovering, R. C., Munro, S. and Schurmann, A. (2006). Nomenclature for the human Arf family of GTP-binding proteins: ARF, ARL, and SAR proteins. *J Cell Biol* **172**, 645-50.

Kahn, R. A. and Gilman, A. G. (1984). Purification of a protein cofactor required for ADP-ribosylation of the stimulatory regulatory component of adenylate cyclase by cholera toxin. *J Biol Chem* **259**, 6228-34.

Kahn, R. A. and Gilman, A. G. (1986). The protein cofactor necessary for ADP-ribosylation of Gs by cholera toxin is itself a GTP binding protein. *J Biol Chem* **261**, 7906-11.

Kakinuma, T., Ichikawa, H., Tsukada, Y., Nakamura, T. and Toh, B. H. (2004). Interaction between p230 and MACF1 is associated with transport of a glycosyl phosphatidyl inositol-anchored protein from the Golgi to the cell periphery. *Exp Cell Res* **298**, 388-98.

Kanno, E., Ishibashi, K., Kobayashi, H., Matsui, T., Ohbayashi, N. and Fukuda, M. (2010). Comprehensive screening for novel rab-binding proteins by GST pull-down assay using 60 different mammalian Rabs. *Traffic* **11**, 491-507.

Keller, P. and Simons, K. (1997). Post-Golgi biosynthetic trafficking. *J Cell Sci* **110 (Pt 24)**, 3001-9.

Keller, P., Toomre, D., Diaz, E., White, J. and Simons, K. (2001). Multicolour imaging of post-Golgi sorting and trafficking in live cells. *Nat Cell Biol* **3**, 140-9.

Kinoshita, T., Fujita, M. and Maeda, Y. (2008). Biosynthesis, remodelling and functions of mammalian GPI-anchored proteins: recent progress. *J Biochem* **144**, 287-94.

Kirchhausen, T. (2000). Three ways to make a vesicle. *Nat Rev Mol Cell Biol* **1**, 187-98.

Kitching, R., Qi, S., Li, V., Raouf, A., Vary, C. P. and Seth, A. (2002). Coordinate gene expression patterns during osteoblast maturation and retinoic acid treatment of MC3T3-E1 cells. *J Bone Miner Metab* **20**, 269-80.

Krauss, M., Kinuta, M., Wenk, M. R., De Camilli, P., Takei, K. and Haucke, V. (2003). ARF6 stimulates clathrin/AP-2 recruitment to synaptic membranes by activating phosphatidylinositol phosphate kinase type Igamma. *J Cell Biol* **162**, 113-24.

Kreis, T. E. and Lodish, H. F. (1986). Oligomerization is essential for transport of vesicular stomatitis viral glycoprotein to the cell surface. *Cell* **46**, 929-37.

Krengel, U., Schlichting, I., Scherer, A., Schumann, R., Frech, M., John, J., Kabsch, W., Pai, E. F. and Wittinghofer, A. (1990). Three-dimensional structures of H-ras p21 mutants: molecular basis for their inability to function as signal switch molecules. *Cell* **62**, 539-48.

Laemmli, U. K. (1970). Cleavage of structural proteins during the assembly of the head of bacteriophage T4. *Nature* **227**, 680-5.

Lafay, F. (1974). Envelope proteins of vesicular stomatitis virus: effect of temperature-sensitive mutations in complementation groups III and V. *J Virol* **14**, 1220-8.

Lamaze, C., Dujeancourt, A., Baba, T., Lo, C. G., Benmerah, A. and Dautry-Varsat, A. (2001). Interleukin 2 receptors and detergent-resistant membrane domains define a clathrin-independent endocytic pathway. *Mol Cell* **7**, 661-71.

Lanzetti, L. and Di Fiore, P. P. (2008). Endocytosis and Cancer: an 'Insider' Network with Dangerous Liaisons. *Traffic*.

Lee, M. C., Orci, L., Hamamoto, S., Futai, E., Ravazzola, M. and Schekman, R. (2005). Sar1p N-terminal helix initiates membrane curvature and completes the fission of a COPII vesicle. *Cell* **122**, 605-17.

Lee, R. H., Iioka, H., Ohashi, M., Iemura, S., Natsume, T. and Kinoshita, N. (2007). XRab40 and XCullin5 form a ubiquitin ligase complex essential for the noncanonical Wnt pathway. *EMBO J* **26**, 3592-606.

Lemaitre, G., Gonnet, F., Vaigot, P., Gidrol, X., Martin, M. T., Tortajada, J. and Waksman, G. (2005). CD98, a novel marker of transient amplifying human keratinocytes. *Proteomics* **5**, 3637-45.

Li, Y., Kelly, W. G., Logsdon, J. M., Jr., Schurko, A. M., Harfe, B. D., Hill-Harfe, K. L. and Kahn, R. A. (2004). Functional genomic analysis of the ADP-ribosylation factor family of GTPases: phylogeny among diverse eukaryotes and function in C. elegans. *FASEB J* **18**, 1834-50.

Lieu, Z. Z., Derby, M. C., Teasdale, R. D., Hart, C., Gunn, P. and Gleeson, P. A. (2007). The golgin GCC88 is required for efficient retrograde transport of cargo from the early endosomes to the trans-Golgi network. *Mol Biol Cell* **18**, 4979-91.

Lieu, Z. Z., Lock, J. G., Hammond, L. A., La Gruta, N. L., Stow, J. L. and Gleeson, P. A. (2008). A trans-Golgi network golgin is required for the regulated secretion of TNF in activated macrophages in vivo. *Proc Natl Acad Sci U S A* **105**, 3351-6.

Lin, C. Y., Huang, P. H., Liao, W. L., Cheng, H. J., Huang, C. F., Kuo, J. C., Patton, W. A., Massenburg, D., Moss, J. and Lee, F. J. (2000). ARL4, an ARF-like protein that is developmentally regulated and localized to nuclei and nucleoli. *J Biol Chem* **275**, 37815-23.

Lingappa, V. R., Katz, F. N., Lodish, H. F. and Blobel, G. (1978). A signal sequence for the insertion of a transmembrane glycoprotein. Similarities to the signals of secretory proteins in primary structure and function. *J Biol Chem* **253**, 8667-70.

Lippincott-Schwartz, J., Altan-Bonnet, N. and Patterson, G. H. (2003). Photobleaching and photoactivation: following protein dynamics in living cells. *Nat Cell Biol* **Suppl**, S7-14.

Lisanti, M. P., Caras, I. W., Davitz, M. A. and Rodriguez-Boulan, E. (1989). A glycophospholipid membrane anchor acts as an apical targeting signal in polarized epithelial cells. *J Cell Biol* **109**, 2145-56.

Liu, X., Constantinescu, S. N., Sun, Y., Bogan, J. S., Hirsch, D., Weinberg, R. A. and Lodish, H. F. (2000). Generation of mammalian cells stably expressing multiple genes at predetermined levels. *Anal Biochem* **280**, 20-8.

Liu, Y. W., Lee, S. W. and Lee, F. J. (2006). Arl1p is involved in transport of the GPI-anchored protein Gas1p from the late Golgi to the plasma membrane. *J Cell Sci* **119**, 3845-55.

Lock, J. G., Hammond, L. A., Houghton, F., Gleeson, P. A. and Stow, J. L. (2005). E-cadherin transport from the trans-Golgi network in tubulovesicular carriers is selectively regulated by golgin-97. *Traffic* **6**, 1142-56.

Lodish, H. F. and Weiss, R. A. (1979). Selective isolation of mutants of vesicular stomatitis virus defective in production of the viral glycoprotein. *J Virol* **30**, 177-89.

Lodish, H. F., Wirth, D. and Porter, M. (1980). Synthesis and assembly of viral membrane proteins. *Ann N Y Acad Sci* **343**, 319-37.

Lombardi, D., Soldati, T., Riederer, M. A., Goda, Y., Zerial, M. and Pfeffer, S. R. (1993). Rab9 functions in transport between late endosomes and the trans Golgi network. *EMBO J* **12**, 677-82.

Loo, L. H., Wu, L. F. and Altschuler, S. J. (2007). Image-based multivariate profiling of drug responses from single cells. *Nat Methods* **4**, 445-53.

Losev, E., Reinke, C. A., Jellen, J., Strongin, D. E., Bevis, B. J. and Glick, B. S. (2006). Golgi maturation visualized in living yeast. *Nature* **441**, 1002-6.

Low, M. G. and Finean, J. B. (1977). Release of alkaline phosphatase from membranes by a phosphatidylinositol-specific phospholipase C. *Biochem J* **167**, 281-4.

Low, M. G. and Finean, J. B. (1978). Specific release of plasma membrane enzymes by a phosphatidylinositol-specific phospholipase C. *Biochim Biophys Acta* **508**, 565-70.

Lu, L., Tai, G. and Hong, W. (2004). Autoantigen Golgin-97, an effector of Arl1 GTPase, participates in traffic from the endosome to the trans-golgi network. *Mol Biol Cell* **15**, 4426-43.

Macia, E., Ehrlich, M., Massol, R., Boucrot, E., Brunner, C. and Kirchhausen, T. (2006). Dynasore, a cell-permeable inhibitor of dynamin. *Dev Cell* **10**, 839-50.

Manolea, F., Chun, J., Chen, D. W., Clarke, I., Summerfeldt, N., Dacks, J. B. and Melancon, P. (2010). Arf3 is activated uniquely at the trans-Golgi network by brefeldin A-inhibited guanine nucleotide exchange factors. *Mol Biol Cell* **21**, 1836-49.

Matanis, T., Akhmanova, A., Wulf, P., Del Nery, E., Weide, T., Stepanova, T., Galjart, N., Grosveld, F., Goud, B., De Zeeuw, C. I. et al. (2002). Bicaudal-D regulates COPI-independent Golgi-ER transport by recruiting the dynein-dynactin motor complex. *Nat Cell Biol* **4**, 986-92.

Matsuura-Tokita, K., Takeuchi, M., Ichihara, A., Mikuriya, K. and Nakano, A. (2006). Live imaging of yeast Golgi cisternal maturation. *Nature* **441**, 1007-10.

Maxfield, F. R. and McGraw, T. E. (2004). Endocytic recycling. *Nat Rev Mol Cell Biol* **5**, 121-32.

Mayor, S. and Pagano, R. E. (2007). Pathways of clathrin-independent endocytosis. *Nat Rev Mol Cell Biol* **8**, 603-12.

McBride, H. M., Rybin, V., Murphy, C., Giner, A., Teasdale, R. and Zerial, M. (1999). Oligomeric complexes link Rab5 effectors with NSF and drive membrane fusion via interactions between EEA1 and syntaxin 13. *Cell* **98**, 377-86.

Meister, G. and Tuschl, T. (2004). Mechanisms of gene silencing by double-stranded RNA. *Nature* **431**, 343-9.

Mellman, I. and Simons, K. (1992). The Golgi complex: in vitro veritas? *Cell* **68**, 829-40.

Meyer, A. J. and Dick, T. P. (2010). Fluorescent protein-based redox probes. *Antioxid Redox Signal* **13**, 621-50.

Millar, A. L., Pavios, N. J., Xu, J. and Zheng, M. H. (2002). Rab3D: a regulator of exocytosis in non-neuronal cells. *Histol Histopathol* **17**, 929-36.

Miller, E., Antonny, B., Hamamoto, S. and Schekman, R. (2002). Cargo selection into COPII vesicles is driven by the Sec24p subunit. *EMBO J* **21**, 6105-13.

Mills, I. G. (2007). The interplay between clathrin-coated vesicles and cell signalling. *Semin Cell Dev Biol* **18**, 459-70.

Mironov, A. A., Beznoussenko, G. V., Nicoziani, P., Martella, O., Trucco, A., Kweon, H. S., Di Giandomenico, D., Polishchuk, R. S., Fusella, A., Lupetti, P. et al. (2001). Small cargo proteins and large aggregates can traverse the Golgi by a common mechanism without leaving the lumen of cisternae. *J Cell Biol* **155**, 1225-38.

Miserey-Lenkei, S., Chalancon, G., Bardin, S., Formstecher, E., Goud, B. and Echard, A. (2010). Rab and actomyosin-dependent fission of transport vesicles at the Golgi complex. *Nat Cell Biol* **12**, 645-54.

Miyawaki, A. (2005). Innovations in the imaging of brain functions using fluorescent proteins. *Neuron* **48**, 189-99.

Miyawaki, A., Nagai, T. and Mizuno, H. (2005). Engineering fluorescent proteins. *Adv Biochem Eng Biotechnol* **95**, 1-15.

Mollenhauer, H. H. and Morre, D. J. (1991). Perspectives on Golgi apparatus form and function. *J Electron Microsc Tech* **17**, 2-14.

Morsomme, P., Prescianotto-Baschong, C. and Riezman, H. (2003). The ER v-SNAREs are required for GPI-anchored protein sorting from other secretory proteins upon exit from the ER. *J Cell Biol* **162**, 403-12.

Morsomme, P. and Riezman, H. (2002). The Rab GTPase Ypt1p and tethering factors couple protein sorting at the ER to vesicle targeting to the Golgi apparatus. *Dev Cell* **2**, 307-17.

Muniz, M., Morsomme, P. and Riezman, H. (2001). Protein sorting upon exit from the endoplasmic reticulum. *Cell* **104**, 313-20.

Munro, S. (2011). The Golgin Coiled-Coil Proteins of the Golgi Apparatus. *Cold Spring Harb Perspect Biol*.

Myllyharju, J. and Kivirikko, K. I. (2004). Collagens, modifying enzymes and their mutations in humans, flies and worms. *Trends Genet* **20**, 33-43.

Nabavi, N., Pustylnik, S. and Harrison, R. E. (2012). Rab GTPase mediated procollagen trafficking in ascorbic acid stimulated osteoblasts. *PLoS One* **7**, e46265.

Nakamura, N., Rabouille, C., Watson, R., Nilsson, T., Hui, N., Slusarewicz, P., Kreis, T. E. and Warren, G. (1995). Characterization of a cis-Golgi matrix protein, GM130. *J Cell Biol* **131**, 1715-26.

Nakano, A. and Muramatsu, M. (1989). A novel GTP-binding protein, Sar1p, is involved in transport from the endoplasmic reticulum to the Golgi apparatus. *J Cell Biol* **109**, 2677-91.

Naslavsky, N., Weigert, R. and Donaldson, J. G. (2004). Characterization of a nonclathrin endocytic pathway: membrane cargo and lipid requirements. *Mol Biol Cell* **15**, 3542-52.

Ng, E. L., Ng, J. J., Liang, F. and Tang, B. L. (2009). Rab22B is expressed in the CNS astroglia lineage and plays a role in epidermal growth factor receptor trafficking in A431 cells. *J Cell Physiol* **221**, 716-28.

Nie, Z., Hirsch, D. S. and Randazzo, P. A. (2003). Arf and its many interactors. *Curr Opin Cell Biol* **15**, 396-404.

Nishimoto-Morita, K., Shin, H. W., Mitsuhashi, H., Kitamura, M., Zhang, Q., Johannes, L. and Nakayama, K. (2009). Differential effects of depletion of ARL1 and ARFRP1 on membrane trafficking between the trans-Golgi network and endosomes. *J Biol Chem* **284**, 10583-92.

Nishimura, N. and Balch, W. E. (1997). A di-acidic signal required for selective export from the endoplasmic reticulum. *Science* **277**, 556-8.

Nishimura, N., Bannykh, S., Slabough, S., Matteson, J., Altschuler, Y., Hahn, K. and Balch, W. E. (1999). A di-acidic (DXE) code directs concentration of cargo during export from the endoplasmic reticulum. *J Biol Chem* **274**, 15937-46.

Nuoffer, C., Davidson, H. W., Matteson, J., Meinkoth, J. and Balch, W. E. (1994). A GDP-bound of rab1 inhibits protein export from the endoplasmic reticulum and transport between Golgi compartments. *J Cell Biol* **125**, 225-37.

Orci, L., Glick, B. S. and Rothman, J. E. (1986). A new type of coated vesicular carrier that appears not to contain clathrin: its possible role in protein transport within the Golgi stack. *Cell* **46**, 171-84.

Orlean, P. and Menon, A. K. (2007). Thematic review series: lipid posttranslational modifications. GPI anchoring of protein in yeast and mammalian cells, or: how we learned to stop worrying and love glycophospholipids. *J Lipid Res* **48**, 993-1011.

Osborne, A. R., Rapoport, T. A. and van den Berg, B. (2005). Protein translocation by the Sec61/SecY channel. *Annu Rev Cell Dev Biol* **21**, 529-50.

Ostrowski, M., Carmo, N. B., Krumeich, S., Fanget, I., Raposo, G., Savina, A., Moita, C. F., Schauer, K., Hume, A. N., Freitas, R. P. et al. (2010). Rab27a and Rab27b control different steps of the exosome secretion pathway. *Nat Cell Biol* **12**, 19-30; sup pp 1-13.

Palade, G. (1975). Intracellular aspects of the process of protein synthesis. *Science* **189**, 347-58.

Paladino, S., Pocard, T., Catino, M. A. and Zurzolo, C. (2006). GPI-anchored proteins are directly targeted to the apical surface in fully polarized MDCK cells. *J Cell Biol* **172**, 1023-34.

Paladino, S., Sarnataro, D., Pillich, R., Tivodar, S., Nitsch, L. and Zurzolo, C. (2004). Protein oligomerization modulates raft partitioning and apical sorting of GPI-anchored proteins. *J Cell Biol* **167**, 699-709.

Palmiter, R. D., Davidson, J. M., Gagnon, J., Rowe, D. W. and Bornstein, P. (1979). NH2-terminal sequence of the chick proalpha1(I) chain synthesized in the reticulocyte lysate system. Evidence for a transient hydrophobic leader sequence. *J Biol Chem* **254**, 1433-6.

Panic, B., Perisic, O., Veprintsev, D. B., Williams, R. L. and Munro, S. (2003). Structural basis for Arl1-dependent targeting of homodimeric GRIP domains to the Golgi apparatus. *Mol Cell* **12**, 863-74.

Pasqualato, S., Renault, L. and Cherfils, J. (2002). Arf, Arl, Arp and Sar proteins: a family of GTP-binding proteins with a structural device for 'front-back' communication. *EMBO Rep* **3**, 1035-41.

Pelham, H. R. (1998). Getting through the Golgi complex. *Trends Cell Biol* **8**, 45-9.

Pelkmans, L., Fava, E., Grabner, H., Hannus, M., Habermann, B., Krausz, E. and Zerial, M. (2005). Genome-wide analysis of human kinases in clathrin- and caveolae/raft-mediated endocytosis. *Nature* **436**, 78-86.

Pepperkok, R. and Ellenberg, J. (2006). High-throughput fluorescence microscopy for systems biology. *Nat Rev Mol Cell Biol* **7**, 690-6.

Pepperkok, R., Scheel, J., Horstmann, H., Hauri, H. P., Griffiths, G. and Kreis, T. E. (1993). Beta-COP is essential for biosynthetic membrane transport from the endoplasmic reticulum to the Golgi complex in vivo. *Cell* **74**, 71-82.

Pereira-Leal, J. B., Hume, A. N. and Seabra, M. C. (2001). Prenylation of Rab GTPases: molecular mechanisms and involvement in genetic disease. *FEBS Lett* **498**, 197-200.

Pereira-Leal, J. B. and Seabra, M. C. (2001). Evolution of the Rab family of small GTP-binding proteins. *J Mol Biol* **313**, 889-901.

Peterkofsky, B. (1991). Ascorbate requirement for hydroxylation and secretion of procollagen: relationship to inhibition of collagen synthesis in scurvy. *Am J Clin Nutr* **54**, 1135S-1140S.

Pfeffer, S. R. (2001). Rab GTPases: specifying and deciphering organelle identity and function. *Trends Cell Biol* **11**, 487-91.

Phizicky, E., Bastiaens, P. I., Zhu, H., Snyder, M. and Fields, S. (2003). Protein analysis on a proteomic scale. *Nature* **422**, 208-15.

Plutner, H., Cox, A. D., Pind, S., Khosravi-Far, R., Bourne, J. R., Schwaninger, R., Der, C. J. and Balch, W. E. (1991). Rab1b regulates vesicular transport between the endoplasmic reticulum and successive Golgi compartments. *J Cell Biol* **115**, 31-43.

Prasher, D. C., Eckenrode, V. K., Ward, W. W., Prendergast, F. G. and Cormier, M. J. (1992). Primary structure of the Aequorea victoria green-fluorescent protein. *Gene* **111**, 229-33.

Presley, J. F., Cole, N. B., Schroer, T. A., Hirschberg, K., Zaal, K. J. and Lippincott-Schwartz, J. (1997). ER-to-Golgi transport visualized in living cells. *Nature* **389**, 81-5.

Price, H. P., Panethymitaki, C., Goulding, D. and Smith, D. F. (2005). Functional analysis of TbARL1, an N-myristoylated Golgi protein essential for viability in bloodstream trypanosomes. *J Cell Sci* **118**, 831-41.

Prockop, D. J. and Kivirikko, K. I. (1995). Collagens: molecular biology, diseases, and potentials for therapy. *Annu Rev Biochem* **64**, 403-34.

Progida, C., Cogli, L., Piro, F., De Luca, A., Bakke, O. and Bucci, C. (2010). Rab7b controls trafficking from endosomes to the TGN. *J Cell Sci* **123**, 1480-91.

Rabouille, C. and Klumperman, J. (2005). Opinion: The maturing role of COPI vesicles in intra-Golgi transport. *Nat Rev Mol Cell Biol* **6**, 812-7.

Reading, C. L., Penhoet, E. E. and Ballou, C. E. (1978). Carbohydrate structure of vesicular stomatitis virus glycoprotein. *J Biol Chem* **253**, 5600-12.

Reddy, J. V., Burguete, A. S., Sridevi, K., Ganley, I. G., Nottingham, R. M. and Pfeffer, S. R. (2006). A functional role for the GCC185 golgin in mannose 6-phosphate receptor recycling. *Mol Biol Cell* **17**, 4353-63.

Ren, M., Xu, G., Zeng, J., De Lemos-Chiarandini, C., Adesnik, M. and Sabatini, D. D. (1998). Hydrolysis of GTP on rab11 is required for the direct delivery of transferrin from the pericentriolar recycling compartment to the cell surface but not from sorting endosomes. *Proc Natl Acad Sci U S A* **95**, 6187-92.

Robert, C. H., Cherfils, J., Mouawad, L. and Perahia, D. (2004). Integrating three views of Arf1 activation dynamics. *J Mol Biol* **337**, 969-83.

Roberts, W. L. and Rosenberry, T. L. (1985). Identification of covalently attached fatty acids in the hydrophobic membrane-binding domain of human erythrocyte acetylcholinesterase. *Biochem Biophys Res Commun* **133**, 621-7.

Robinson, M. S. (2004). Adaptable adaptors for coated vesicles. *Trends Cell Biol* **14**, 167-74.

Rodriguez-Boulan, E., Kreitzer, G. and Musch, A. (2005). Organization of vesicular trafficking in epithelia. *Nat Rev Mol Cell Biol* **6**, 233-47.

Rodriguez-Gabin, A. G., Almazan, G. and Larocca, J. N. (2004). Vesicle transport in oligodendrocytes: probable role of Rab40c protein. *J Neurosci Res* **76**, 758-70.

Rodriguez-Gabin, A. G., Cammer, M., Almazan, G., Charron, M. and Larocca, J. N. (2001). Role of rRAB22b, an oligodendrocyte protein, in regulation of transport of vesicles from trans Golgi to endocytic compartments. *J Neurosci Res* **66**, 1149-60.

Rose, J. K., Welch, W. J., Sefton, B. M., Esch, F. S. and Ling, N. C. (1980). Vesicular stomatitis virus glycoprotein is anchored in the viral membrane by a hydrophobic domain near the COOH terminus. *Proc Natl Acad Sci U S A* **77**, 3884-8.

Rothman, J. E. (1994). Mechanisms of intracellular protein transport. *Nature* **372**, 55-63.

Rothman, J. E. and Lodish, H. F. (1977). Synchronised transmembrane insertion and glycosylation of a nascent membrane protein. *Nature* **269**, 775-80.

Rothman, J. E. and Wieland, F. T. (1996). Protein sorting by transport vesicles. *Science* **272**, 227-34.

Saga, S., Nagata, K., Chen, W. T. and Yamada, K. M. (1987). pH-dependent function, purification, and intracellular location of a major collagen-binding glycoprotein. *J Cell Biol* **105**, 517-27.

Sahin, O., Lobke, C., Korf, U., Appelhans, H., Sultmann, H., Poustka, A., Wiemann, S. and Arlt, D. (2007). Combinatorial RNAi for quantitative protein network analysis. *Proc Natl Acad Sci U S A* **104**, 6579-84.

Saito, K., Chen, M., Bard, F., Chen, S., Zhou, H., Woodley, D., Polischuk, R., Schekman, R. and Malhotra, V. (2009). TANGO1 facilitates cargo loading at endoplasmic reticulum exit sites. *Cell* **136**, 891-902.

Sandvig, K., Torgersen, M. L., Raa, H. A. and van Deurs, B. (2008). Clathrin-independent endocytosis: from nonexisting to an extreme degree of complexity. *Histochem Cell Biol* **129**, 267-76.

Saraste, M., Sibbald, P. R. and Wittinghofer, A. (1990). The P-loop--a common motif in ATP- and GTP-binding proteins. *Trends Biochem Sci* **15**, 430-4.

Schekman, R. and Orci, L. (1996). Coat proteins and vesicle budding. *Science* **271**, 1526-33.

Schloemer, R. H. and Wagner, R. R. (1975). Association of vesicular stomatitis virus glycoprotein with virion membrane: characterization of the lipophilic tail fragment. *J Virol* **16**, 237-40.

Shimomura, O., Johnson, F. H. and Saiga, Y. (1962). Extraction, purification and properties of aequorin, a bioluminescent protein from the luminous hydromedusan, Aequorea. *J Cell Comp Physiol* **59**, 223-39.

Shin, H. W. and Nakayama, K. (2004). Dual control of membrane targeting by PtdIns(4)P and ARF. *Trends Biochem Sci* **29**, 513-5.

Short, B., Preisinger, C., Schaletzky, J., Kopajtich, R. and Barr, F. A. (2002). The Rab6 GTPase regulates recruitment of the dynactin complex to Golgi membranes. *Curr Biol* **12**, 1792-5.

Shukla, S. D., Coleman, R., Finean, J. B. and Michell, R. H. (1980). Selective release of plasma-membrane enzymes from rat hepatocytes by a phosphatidylinositol-specific phospholipase C. *Biochem J* **187**, 277-80.

Simons, K. and Ikonen, E. (1997). Functional rafts in cell membranes. *Nature* **387**, 569-72.

Simonsen, A., Lippe, R., Christoforidis, S., Gaullier, J. M., Brech, A., Callaghan, J., Toh, B. H., Murphy, C., Zerial, M. and Stenmark, H. (1998). EEA1 links PI(3)K function to Rab5 regulation of endosome fusion. *Nature* **394**, 494-8.

Simpson, J. C., Joggerst, B., Laketa, V., Verissimo, F., Cetin, C., Erfle, H., Bexiga, M. G., Singan, V. R., Heriche, J. K., Neumann, B. et al. (2012). Genome-wide RNAi screening identifies human proteins with a regulatory function in the early secretory pathway. *Nat Cell Biol*.

Sprenger, R. R., Speijer, D., Back, J. W., De Koster, C. G., Pannekoek, H. and Horrevoets, A. J. (2004). Comparative proteomics of human endothelial cell caveolae and rafts using two-dimensional gel electrophoresis and mass spectrometry. *Electrophoresis* **25**, 156-72.

Starkuviene, V., Seitz, A., Erfle, H. and Pepperkok, R. (2008). Measuring secretory membrane traffic: a quantitative fluorescence microscopy approach. *Methods Mol Biol* **457**, 193-201.

Stenmark, H. (2009). Rab GTPases as coordinators of vesicle traffic. *Nat Rev Mol Cell Biol*.

Stephens, D. J. and Pepperkok, R. (2002). Imaging of procollagen transport reveals COPI-dependent cargo sorting during ER-to-Golgi transport in mammalian cells. *J Cell Sci* **115**, 1149-60.

Sutterlin, C., Doering, T. L., Schimmoller, F., Schroder, S. and Riezman, H. (1997). Specific requirements for the ER to Golgi transport of GPI-anchored proteins in yeast. *J Cell Sci* **110 (Pt 21)**, 2703-14.

Takamori, S., Holt, M., Stenius, K., Lemke, E. A., Gronborg, M., Riedel, D., Urlaub, H., Schenck, S., Brugger, B., Ringler, P. et al. (2006). Molecular anatomy of a trafficking organelle. *Cell* **127**, 831-46.

Takida, S., Maeda, Y. and Kinoshita, T. (2008). Mammalian GPI-anchored proteins require p24 proteins for their efficient transport from the ER to the plasma membrane. *Biochem J* **409**, 555-62.

Tan, R., Wang, W., Wang, S., Wang, Z., Sun, L., He, W., Fan, R., Zhou, Y., Xu, X., Hong, W. et al. (2013). Small GTPase Rab40c Associates with Lipid Droplets and Modulates the Biogenesis of Lipid Droplets. *PLoS One* **8**, e63213.

Tian, X., Jin, R. U., Bredemeyer, A. J., Oates, E. J., Blazewska, K. M., McKenna, C. E. and Mills, J. C. (2010). RAB26 and RAB3D are direct transcriptional targets of MIST1 that regulate exocrine granule maturation. *Mol Cell Biol* **30**, 1269-84.

Tiller, G. E., Hannig, V. L., Dozier, D., Carrel, L., Trevarthen, K. C., Wilcox, W. R., Mundlos, S., Haines, J. L., Gedeon, A. K. and Gecz, J. (2001). A recurrent RNA-splicing mutation in the SEDL gene causes X-linked spondyloepiphyseal dysplasia tarda. *Am J Hum Genet* **68**, 1398-407.

Tisdale, E. J., Bourne, J. R., Khosravi-Far, R., Der, C. J. and Balch, W. E. (1992). GTP-binding mutants of rab1 and rab2 are potent inhibitors of vesicular transport from the endoplasmic reticulum to the Golgi complex. *J Cell Biol* **119**, 749-61.

Toomre, D., Keller, P., White, J., Olivo, J. C. and Simons, K. (1999). Dual-color visualization of trans-Golgi network to plasma membrane traffic along microtubules in living cells. *J Cell Sci* **112 (Pt 1)**, 21-33.

Townley, A. K., Feng, Y., Schmidt, K., Carter, D. A., Porter, R., Verkade, P. and Stephens, D. J. (2008). Efficient coupling of Sec23-Sec24 to Sec13-Sec31 drives COPII-dependent collagen secretion and is essential for normal craniofacial development. *J Cell Sci* **121**, 3025-34.

Tromp, G., Kuivaniemi, H., Stacey, A., Shikata, H., Baldwin, C. T., Jaenisch, R. and Prockop, D. J. (1988). Structure of a full-length cDNA clone for the prepro alpha 1(I) chain of human type I procollagen. *Biochem J* **253**, 919-22.

Tse, A. G., Barclay, A. N., Watts, A. and Williams, A. F. (1985). A glycophospholipid tail at the carboxyl terminus of the Thy-1 glycoprotein of neurons and thymocytes. *Science* **230**, 1003-8.

Tsien, R. Y. (1998). The green fluorescent protein. *Annu Rev Biochem* **67**, 509-44.

Udenfriend, S. and Kodukula, K. (1995). How glycosylphosphatidylinositol-anchored membrane proteins are made. *Annu Rev Biochem* **64**, 563-91.

Urlinger, S., Baron, U., Thellmann, M., Hasan, M. T., Bujard, H. and Hillen, W. (2000). Exploring the sequence space for tetracycline-dependent transcriptional activators: novel mutations yield expanded range and sensitivity. *Proc Natl Acad Sci U S A* **97**, 7963-8.

van der Sluijs, P., Hull, M., Webster, P., Male, P., Goud, B. and Mellman, I. (1992). The small GTP-binding protein rab4 controls an early sorting event on the endocytic pathway. *Cell* **70**, 729-40.

Venditti, R., Scanu, T., Santoro, M., Di Tullio, G., Spaar, A., Gaibisso, R., Beznoussenko, G. V., Mironov, A. A., Mironov, A., Jr., Zelante, L. et al. (2012). Sedlin controls the ER export of procollagen by regulating the Sar1 cycle. *Science* **337**, 1668-72.

Vetter, I. R. and Wittinghofer, A. (2001). The guanine nucleotide-binding switch in three dimensions. *Science* **294**, 1299-304.

Volpicelli-Daley, L. A., Li, Y., Zhang, C. J. and Kahn, R. A. (2005). Isoform-selective effects of the depletion of ADP-ribosylation factors 1-5 on membrane traffic. *Mol Biol Cell* **16**, 4495-508.

Wagner, A. C., Strowski, M. Z., Goke, B. and Williams, J. A. (1995). Molecular cloning of a new member of the Rab protein family, Rab 26, from rat pancreas. *Biochem Biophys Res Commun* **207**, 950-6.

Wang, J., Sun, H. Q., Macia, E., Kirchhausen, T., Watson, H., Bonifacino, J. S. and Yin, H. L. (2007). PI4P promotes the recruitment of the GGA adaptor proteins to the trans-Golgi network and regulates their recognition of the ubiquitin sorting signal. *Mol Biol Cell* **18**, 2646-55.

Wang, X., Kumar, R., Navarre, J., Casanova, J. E. and Goldenring, J. R. (2000). Regulation of vesicle trafficking in madin-darby canine kidney cells by Rab11a and Rab25. *J Biol Chem* **275**, 29138-46.

Wang, Y. J., Wang, J., Sun, H. Q., Martinez, M., Sun, Y. X., Macia, E., Kirchhausen, T., Albanesi, J. P., Roth, M. G. and Yin, H. L. (2003). Phosphatidylinositol 4 phosphate regulates targeting of clathrin adaptor AP-1 complexes to the Golgi. *Cell* **114**, 299-310.

Wendler, F., Gillingham, A. K., Sinka, R., Rosa-Ferreira, C., Gordon, D. E., Franch-Marro, X., Peden, A. A., Vincent, J. P. and Munro, S. (2010). A genome-wide RNA interference screen identifies two novel components of the metazoan secretory pathway. *EMBO J* **29**, 304-14.

Wennerberg, K., Rossman, K. L. and Der, C. J. (2005). The Ras superfamily at a glance. *J Cell Sci* **118**, 843-6.

Williams, J. A., Chen, X. and Sabbatini, M. E. (2009). Small G proteins as key regulators of pancreatic digestive enzyme secretion. *Am J Physiol Endocrinol Metab* **296**, E405-14.

Wittinghofer, A. and Vetter, I. R. (2011). Structure-function relationships of the G domain, a canonical switch motif. *Annu Rev Biochem* **80**, 943-71.

Wouters, F. S., Verveer, P. J. and Bastiaens, P. I. (2001). Imaging biochemistry inside cells. *Trends Cell Biol* **11**, 203-11.

Wu, C., Orozco, C., Boyer, J., Leglise, M., Goodale, J., Batalov, S., Hodge, C. L., Haase, J., Janes, J., Huss, J. W., 3rd et al. (2009a). BioGPS: an extensible and customizable portal for querying and organizing gene annotation resources. *Genome Biol* **10**, R130.

Wu, C. Y., Tseng, R. C., Hsu, H. S., Wang, Y. C. and Hsu, M. T. (2009b). Frequent down-regulation of hRAB37 in metastatic tumor by genetic and epigenetic mechanisms in lung cancer. *Lung Cancer* **63**, 360-7.

Yoshie, S., Imai, A., Nashida, T. and Shimomura, H. (2000). Expression, characterization, and localization of Rab26, a low molecular weight GTP-binding protein, in the rat parotid gland. *Histochem Cell Biol* **113**, 259-63.

Yoshino, A., Setty, S. R., Poynton, C., Whiteman, E. L., Saint-Pol, A., Burd, C. G., Johannes, L., Holzbaur, E. L., Koval, M., McCaffery, J. M. et al. (2005). tGolgin-1 (p230, golgin-245) modulates Shiga-toxin transport to the Golgi and Golgi motility towards the microtubule-organizing centre. *J Cell Sci* **118**, 2279-93.

Zahraoui, A., Joberty, G., Arpin, M., Fontaine, J. J., Hellio, R., Tavitian, A. and Louvard, D. (1994). A small rab GTPase is distributed in cytoplasmic vesicles in non polarized cells but colocalizes with the tight junction marker ZO-1 in polarized epithelial cells. *J Cell Biol* **124**, 101-15.

Zerial, M. and McBride, H. (2001). Rab proteins as membrane organizers. *Nat Rev Mol Cell Biol* **2**, 107-17.

Zhou, C., Cunningham, L., Marcus, A. I., Li, Y. and Kahn, R. A. (2006). Arl2 and Arl3 regulate different microtubule-dependent processes. *Mol Biol Cell* **17**, 2476-87.

Ziauddin, J. and Sabatini, D. M. (2001). Microarrays of cells expressing defined cDNAs. *Nature* **411**, 107-10.

Zilberstein, A., Snider, M. D., Porter, M. and Lodish, H. F. (1980). Mutants of vesicular stomatitis virus blocked at different stages in maturation of the viral glycoprotein. *Cell* **21**, 417-27.